Ultrastructural analysis of synaptic inputs to dopamine neurons in the substantia nigra pars compacta and the ventral tegmental area

by

Charlotte Copas

B.Sc. University of Waterloo, 2020

A Thesis Submitted in Partial Fulfillment
of the Requirements for the Degree of

MASTER OF SCIENCE

In the Division of Medical Sciences

Supervisory Committee

Ultrastructural analysis of synaptic inputs to dopamine neurons in the substantia nigra pars compacta and the ventral tegmental area

by

Charlotte Copas

B.Sc. University of Waterloo, 2020

Supervisory Committee

Dr. Patrick C. Nahirney, Division of Medical Sciences
Supervisor

Dr. Brian R. Christie, Division of Medical Sciences
Committee Member

Dr. Raad Nashmi, Division of Medical Sciences
Committee Member

Abstract

Dopaminergic (DA) neurons in the substantia nigra pars compacta (SNc) form the foundation of the nigrostriatal pathway and are most notably discussed in the context of Parkinson's disease (PD) pathology. The ventral tegmental area (VTA) which resides just medial to the SNc is a second influential DA output center and is the relay station for the mesocortical and mesolimbic pathways. Despite an ever-growing body of literature investigating the broad effects of their outputs due to their influential roles in movement execution and reinforcement learning, respectively, one question that remains unanswered is how these DA neurons are modulated by their afferent inputs. Previous research shows that glutamate (Glut), acetylcholine (ACh), and γ-aminobutyric acid (GABA) are a few of the major neurotransmitters that modulate the activity of midbrain DA neurons. Interestingly, these findings also suggest that there is a population of terminals that co-localize both ACh and GABA vesicles, implying that DA neurons are under extremely fine-tuned afferent control. The aims of this study were to describe the morphology of putative Glut, ACh, and GABA vesicles, determine if ACh and GABA are indeed packaged in the same terminals, determine the frequency of co-transmission, and finally investigate whether there is heterogeneity in the prevalence of these inputs between the medial and lateral adult mouse SNc and VTA. Immunohistochemical staining for tyrosine hydroxylase (TH), vesicular GABA transporter (VGAT), vesicular acetylcholine transporter (VAChT), and vesicular glutamate transporter 2 (VGLUT2) was employed to visualize synaptic terminals at the confocal level. Here, we show that there is in fact overlap between VGAT and VAChT in terminals on DA dendrites, however this occurs much less frequently than ACh or GABA only inputs. Using electron microscopy (EM), several distinct types of synapses are observed in these regions. Putative cholinergic synapses are filled with large uniform-sized round vesicles ~50-60 nm diameter, GABAergic type terminals with small oblong vesicles that vary greatly in size but average at ~50-80 nm in length and ~20-30 nm in width, and glutamate (Glut) terminals with small-sized round vesicles (~30-45 nm diameter). Some terminals showed a mixture of oblong vesicles and large round vesicles, and to our surprise, terminals mixed with oblong, and small round vesicles whose diameter was consistent with that of Glut vesicles were also present, prompting us at add a fifth category of synapse, putative Glut/GABA. In total 613 synapses were categorized, on average 200 per region, using the criteria above. At the EM level we found that across all regions pure GABA terminals rarely appeared and were often were co-localized with

either large or small round vesicles. In addition, glutamate was the most common neurotransmitter found opposing DA dendrites in the VTA and was observed at a higher frequency compared to the medial SNc. Similarly, the lateral SNc has a significantly higher incidence of mixed ACh/GABA terminals compared to the VTA. The results of this study offer a glimpse into the regulation of these essential modulatory neurons, adding a small piece of the puzzle to the ongoing investigation concerning basic ultrastructure and normal functioning of the SNc and VTA.

Table of contents

Supervisory Committee ii
Abstract iii
Table of contents v
List of figures vii
List of tables ix
List of abbreviations x
Acknowledgements xii

Chapter 1 – Introduction 1
1.1 Background 1
1.2 Midbrain dopaminergic centers 4
1.2.1 The substantia nigra 6
1.2.2 The ventral tegmental area 8
1.3 Synapses & their neurotransmitters 10
1.3.1 Glutamate 11
1.3.2 Acetylcholine 13
1.3.3 GABA 14
1.4 Synapse classification 16
1.5 Co-transmission/co-localization of neurotransmitters in the CNS 18
1.6 Objectives & Hypotheses 20
Chapter 2 - Materials and Methods 21
2.1 Tissue processing for confocal microscopy 21
2.1.1 Confocal image acquisition 22
2.2 Tissue processing and collection for immuno-electron microscopy 22
2.2.1 Transmission electron micrograph acquisition and analysis 24
2.2.2 3D electron-tomography 27
2.3 Statistical analysis 28
Chapter 3 – Results 29
3.1 General histology 29
3.2 Confocal microscopy 39
3.3 Qualitative assessment of TH-DAB stained sections 45
3.4 Heterogeneous neurotransmitter distribution between and within regions 48
3.5 Correlation between vesicle shape and size 51

Chapter 4 – Discussion 57
4.1 General discussion 57
4.2 The SNcL receives more co-localization than the VTA 60
4.3 Increased glutamatergic transmission to the VTA 61
4.4 Limitations & Future Directions 62
References 64
Appendix 77

List of figures

Figure 1. Major input and output pathways of the substantia nigra pars compacta (SNc) and ventral tegmental area (VTA). 5

Figure 2. Schematic illustration of a variety of synapse types in the CNS based on EM ultrastructure. 18

Figure 3. Flowchart for tissue collection, imaging and morphometric analysis of presynaptic terminals. 26

Figure 4. Morphometric analysis of vesicles within presynaptic terminals on DA dendrites using ImageJ (FIJI). 27

Figure 5. Low (above) and high (below) magnification LM views of a toluidine blue-stained coronal section of the mouse midbrain. 31

Figure 6. Low magnification EM of the SNcL in proximity to the IIIrd nerve. 32

Figure 7. Medium magnification EM view of a DA neuron and surrounding neuropil in the SNcL. 33

Figure 8. Detailed view of a glutamatergic synapse on a proximal DA neuron dendrite in the SNcM. 34

Figure 9. Examples of ACh, mixed ACh/GABA, and Glut terminals in the SNcM. 35

Figure 10. Fifty degree tilts of ACh, Glut, and ACh/GABA terminals. 36

Figure 11. Other cellular constituents are also present within the midbrain neuropil. 37

Figure 12. Low mag survey view of the SNc showing a portion of a DA neuron and its dendrite abutting a capillary (Cap) and astrocytic end feet (AEF) near the capillary. 38

Figure 13. Low magnification confocal images of TH (magenta) and VGLUT2 (cyan) labeling in a sagittal section of the mouse midbrain. 40

Figure 14. High magnification confocal images of TH (magenta) and VGLUT2 (cyan) labeling in the VTA. 41

Figure 15. Confocal images of TH, VGAT, and VAChT labeling in a coronal section of the midbrain. 42

Figure 16. High magnification confocal views of VAChT (green) and VGAT (red) labeling in the SNcM, SNcL and VTA. 43

Figure 17. High magnification triple labeling of TH (magenta), VAChT (green), VGAT (red) in the SNcL. 44

Figure 18. Low and high magnification brightfield images of TH expression in the mouse midbrain. 46

Figure 19. Immuno-EM of a TH-positive neuron labeled with DAB (dark precipitate). 47

Figure 20. Examples of each terminal type opposing TH-DAB dendrites. 49

Figure 21. Percentage of each NT groups within the SNcM, SNcL, and VTA.. 50

Figure 22. Differences in NT groups between regions. 51

Figure 23. Correlations between vesicle size and shape of each neurotransmitter group in the SNcM. 53

Figure 24.Correlations between size and shape of vesicles of each neurotransmitter group in the SNcL. 54

Figure 25. Correlations between size and shape of each neurotransmitter group in the VTA. 55

Figure 26. High magnification EM of a mixed ACh/GABA terminal (yellow) on a DA dendrite (magenta) in the SNcM. 56

Figure 27. Visual summary 59

Figure 28. Lower magnification confocal images of VAChT (green) and VGAT (red) labeling in the SNcM, SNcL and VTA from figure 17. 77

Figure 29. EM of a neuromuscular junction in a diaphragm muscle of a rat showing the size and shape of ACh vesicles. 78

List of tables

Table 1. Summary of total number of terminals and vesicles contacting TH+ dendrites within each region. 27

Table 2. Results from correlation tests comparing vesicle roundness and diameter length. 36

Table 3. Antibody list 76

List of abbreviations

6-OHDA	6-hydroxydopamine
ACh	Acetylcholine
AIS	Axon initial segment
AMPA	a-amino-3-hydroxy-5-methyl-4-isoxazolepropionic acid
BSA	Bovine serum albumin
CNS	Central nervous system
DA	Dopamine
DAB	3,3'-diaminobenzidine
DBS	Deep brain stimulation
EM	Electron microscopy
GABA	γ-aminobutyric acid
GAD	Glutamate decarboxylase
Glut	Glutamate
L-DOPA	Levo-3,4-dihydroxy-phenylalanine
LDT	Laterodorsal tegmental nucleus
LHb	Lateral habenula
mAChR	Muscarinic acetylcholine receptor
mPFC	Medial prefrontal cortex
MSN	Medium spiny neurons
nAChR	Nicotinic acetylcholine receptor
NDS	Normal donkey serum
NMDA	N-methyl-D-aspartate
PBP	Parabrachial pigmented nucleus
PBS	Phosphate buffered saline
PD	Parkinson's disease
PFA	Paraformaldehyde
PN	Paranigral nucleus
PNS	Peripheral nervous system
PPT	Pedunculopontine tegmental nucleus

PSD	Post synaptic density
PTSD	Post-traumatic stress disorder
SNc	Substantia nigra pars compacta
SNr	Substantia nigra pars reticulata
STN	Subthalamic nucleus
TEM	Transmission electron microscope
TH	Tyrosine hydroxylase
UPRDRS	Unified Parkinson's Disease Rating Scale
VAChT	Vesicular acetylcholine transporter
V-ATPase	Vacuolar ATPase
VGAT	Vesicular GABA transporter
VGLUT1	Vesicular glutamate transporter 1
VGLUT2	Vesicular glutamate transporter 2
VIAAT	Vesicular inhibitory amino acid transporter
VTA	Ventral tegmental area

Acknowledgements

I first want to thank Dr. Patrick Nahirney for trusting me with your microscope, pushing me to go big or go home, and for re-writing all of my figure legends. I'll figure it out one day. I also would like to extend my gratitude to my committee members Dr. Brian Christie and Dr. Raad Nashmi and external examiner Dr. Susan Sesack for your support and advice throughout the progression of this degree. Committee meetings and hallway chats were always something to look forward to.

Irene Shkolnikov, without you this thesis would never have come to be. We may become doctors before we ever learn how to ollie, but which is more impressive anyway?

To Dr. Jenessa Johnston, Dr. Luis Bettio, Dr. Josh Allen, Kaylene Scheil, Alejandra Raudales, Carla Liria Sanchez-Lafuente, Mat Hammerstrom, and Ciara Halvorson, thank you for matching my weird and making my time in Victoria the best it could have ever possibly been. You all have taught me how to work hard and play harder and I wouldn't have chosen to spend the past two (and some) years with a different group of people. Thank you for adopting me as one of your surrogate lab members, I can't wait to have places to crash all around the world. To my NGSA co-executives Eva Šimončičvá and Elisa Gonçalves de Andrade, I would like to think we have made the NGP a better place and I'm so thankful we got to do it together.

This body of work also would not have been possible without support from back home. Amie, for making me cry-laugh during times when I didn't think it was even close to possible. Your unconditional friendship and sisterhood mean more to me than I could ever express. Grant, for keeping my feet on the ground and my delusional thoughts in line, you are the definition of tough love. Last but certainly not least, Aaron, Hal, and John for being my roots back home and always picking up right where we left off, as if I had never even moved across the country.

To my parents, your encouragement and unwavering belief in me is what pushed me to pursue this degree in the first place. I am eternally grateful. And to Rachel, for always reminding me that I am not, in fact, the cooler sister. I'm not sure where the intersection between beer and brains is, but I think we balance it out pretty well.

Chapter 1 – Introduction

1.1 Background

Independence is one of the main determinants that can predict a high quality of life. Being able to navigate your environment efficiently and integrate seamlessly within your community are components of life that are seemingly so ubiquitous that the skills and dexterity that are required to fulfill these tasks are often overlooked. Consider not being able to carry out basic life-fulfilling tasks such as eating, practicing basic hygiene, or spending quality time with loved ones. This is often the reality for individuals living with the debilitating neurodegenerative disease known as paralysis agitans, or Parkinson's disease (PD). It is currently defined as:

A movement disorder which causes the normally very dense population of dopaminergic (DA) neurons of the substantia nigra pars compacta (SNc) to degenerate (E. Hirsch et al., 1988).

Despite PD being the second most common neurodegenerative disease and most common movement disorder in the world (Tysnes & Storstein, 2017; McGregor & Nelson, 2019) there are extremely limited treatment options for those suffering from this disease. Moreover, the options that are available can often only alleviate symptoms rather than re-establish DA neurons back into the SNc. Oral administration of levo-3,4-dihydroxy-phenylalanine (L-Dopa) is the most common pharmacological intervention for managing PD and is currently considered the gold standard therapy for this disease (Lewitt, 2015). L-Dopa is the precursor for DA and is given to patients instead of DA itself due to its ability to cross the blood-brain barrier, a key ability that its successor does not have (Nagatsua & Sawadab, 2009). Once in the brain, L-Dopa is synthesized by the enzyme aromatic L-amino acid decarboxylase into DA and acts as a surrogate for the depleted endogenous striatal DA caused by the death of midbrain DA neurons (Nagatsua & Sawadab, 2009). Relief from motor disturbances is relatively short lived however, as brief as 2 years, since prolonged administration of L-Dopa leads to impairments that present similarly to PD symptomology such as L-Dopa-induced dyskinesia and dystonia, and shorter time windows during which the drug is effective (Nagatsua & Sawadab, 2009; Lewitt, 2015; Lipski et al., 2011). A second common treatment method is deep brain stimulation (DBS) of the subthalamic

nucleus (STN), with more than 70 000 patients having undergone this procedure since its approval by the Food and Drug Administration in 2002 (Bronstein et al., 2011). In a study done by Limousin and colleagues, it was discovered that patients who underwent DBS surgery and were taken off all previous PD medications increased their daily living and motor examination scores in the Unified Parkinson's Disease Rating Scale (UPDRS) (parts II and III, respectively) by 60% after their first year with the implant (Limousin et al., 1998). Despite the fact that this procedure is relatively safe considering the significant number of quality-of-life years regained, there are profound economic barriers to entry. In the United States, the cost of DBS implantation ranges from $70 000 - $100 000, not including the charge for battery replacement which is an additional $17 000 - $27 000 (Cabrera et al., 2018). Additionally, after a 5-year follow-up post DBS implant, patient scores on the UPDRS were lower than baseline, most likely since DBS does not halt degeneration of the SNc but rather temporarily quells the motor symptoms that result from it (Limousin & Foltynie, 2019).

Due to the fact that PD is so prevalent in the world population, that there is still no known cure for the disease, and because as previously described the treatments we currently have are sometimes not easily accessible and only manage symptoms, the majority of research that delves into the inner workings of the SNc are either trying to find out how to model PD in mouse and rat populations or how to regrow DA neurons with a seemingly never ending pool of potential drugs or medications. While these are obviously important questions to answer, there is seemingly a lack of research that is concerned with the normal, non-diseased functioning of the SNc. The SNc has been recognized as an important structure in the basal ganglia for some time, with seminal research showing how important DA neurons are in fine-tuning volitional movement through modulating basal ganglia circuits (Guatteo et al., 2009).

Despite this ever-growing body of literature investigating the broad effects of their outputs, one question that remains unanswered is how are DA neurons modulated by afferent inputs?

Through previous research by many groups over the decades, it has been demonstrated that three neurotransmitters play a particularly important role in presynaptic connections onto DA SNc neurons – glutamate, acetylcholine (ACh), and γ-aminobutyric acid (GABA) (Kitai et

al., 1999; Misgeld, 2004; Tepper & Lee, 2007). Intriguingly, emerging new research provides evidence of a recently discovered fourth synaptic terminal input: co-transmission of ACh and GABA from the same synaptic terminal, whose mechanisms have yet to be fully elucidated despite their probable crucial role in movement refinement. (Estakhr et al., 2017; Gratiet et al., 2022; Li & Spitzer, 2020)

The neighbouring ventral tegmental area (VTA) is a second dopaminergic hub in the midbrain, sending long range projections to the nucleus accumbens (NAc) and the medial pre-frontal cortex. Despite being so physically and seemingly morphologically similar to the SNc, the VTA participates in the mesolimbic and mesocortical pathways, the circuitry responsible for feelings of reward, reinforcement learning, and is speculated to drive organisms to partake in basic life-sustaining activities and avoid harm (Alcaro et al., 2007). Intriguingly, the DA neurons of the VTA are seemingly spared when the cells of the bordering SNc start to die off during the onset of PD and remain less affected throughout the progression of the disease. The reason behind this phenomenon is unknown, however recent studies in flies, rodents, and humans have hinted that the most resilient DA neurons are the ones that co-transmit dopamine and glutamate to their output targets (Buck et al., 2022; Steinkellner et al., 2022). By surveying the synaptic landscape of the VTA, we are able to gain insights into how these neurons are modulated and if there are any significant differences compared to the SNc.

With the use of confocal and electron microscopy, my goals for this study are to offer a glimpse into the regulation of these essential modulatory DA neurons, providing unique insights concerning the basic ultrastructure and normal functioning of the SNc and VTA. By quantifying and categorizing the diverse range of synaptic inputs onto DA cells in these regions, we pave the way for future research that could lead to life changing therapeutics for those suffering from PD. Our aims are to determine if there is co-localization of putative ACh and GABA vesicles in the same terminals, determine the frequency of glutamatergic, cholinergic, GABAergic, and mixed terminals, and finally investigate whether there is heterogeneity in the prevalence of these inputs between the medial and lateral SNc, and the VTA.

1.2 Midbrain dopaminergic centers

Dopamine is an extremely important and powerful molecule in the brain. It has a constellation of functions such as modulating movement, learning, sleep, stress, motivation, reward, and involved with the onset of psychiatric disturbances, with the loss of DA neurons being implicated in a myriad of disorders, some often fatal (Calabresi et al., 2007; Juárez Olguín et al., 2016; van Hooijdonk et al., 2023; Welberg, 2008). There are three areas of the brain where large clusters of DA neurons are found - the retrorubral field, the SNc, and the VTA - which coincide with the A8, A9, and A10 cell grouping nomenclature, respectively (Gantz et al., 2018). In humans, there is an estimated 400,000 – 600,000 DA neurons divided between these three regions (Baik, 2013). The retrorubal field (A8) manages a measly 5% of these clusters, whereas the SNc (A9) accounts for ~70% of the remaining population split with the VTA (A8) (Baik, 2013; Björklund & Dunnett, 2007). In adult C57BL/6 mice, the SNc and VTA contain ~8000 – 12,000 DA neurons bilaterally (Fu et al., 2016; Nelson et al., 1996). The sprawled connections of these brain areas and their functional connectedness with several different neuromodulatory systems lends them to be involved in the integration of our default mode network (Zhang et al., 2017). Indeed, the functions of these SNc and VTA DA neurons play such a fundamental role in our most basic responses to the environment, subsequently laying the foundation for our behaviour, that they form the basis of three separate pathways that have been teased apart from the rich network of neuronal highways in the brain (Fig 1.) The VTA is a central relay station for two out of the three systems, the mesolimbic and mesocortical pathways, which project to the limbic system and cortex, respectively (Morales & Margolis, 2017). The limbic connections make it so that the VTA plays a role in behavioural and emotional responses such as reward and motivation, and there is strong evidence that suggests that dysregulation of this system can increase the risk of depression and drug seeking behaviours in susceptible individuals (Alcaro et al., 2007; Baik, 2013; Tye et al., 2012). Projections to the dorsomedial prefrontal cortex (mPFC) from the VTA make up the mesocortical pathway which encodes effort learning rather than the more emotional reward learning of the mesolimbic system (Hauser et al., 2017). The third and final dopaminergic pathway is the mesostriatal pathway, also referred to as the nigrostriatal pathway. It is composed of projections from the SNc to the dorsal striatum and is infamous for

causing the severe motor complications in PD that occur when the neuronal system breaks down (Zecca et al., 2001).

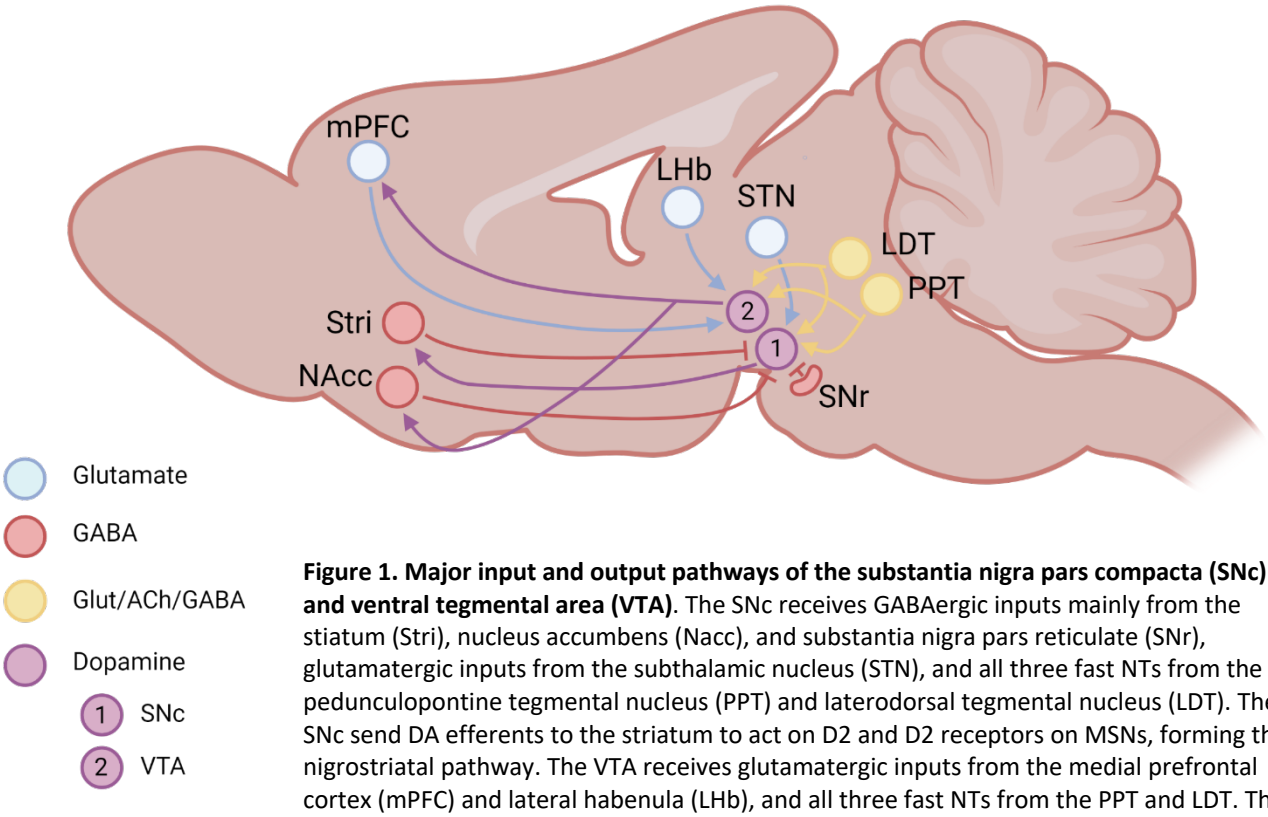

Figure 1. Major input and output pathways of the substantia nigra pars compacta (SNc) and ventral tegmental area (VTA). The SNc receives GABAergic inputs mainly from the stiatum (Stri), nucleus accumbens (Nacc), and substantia nigra pars reticulate (SNr), glutamatergic inputs from the subthalamic nucleus (STN), and all three fast NTs from the pedunculopontine tegmental nucleus (PPT) and laterodorsal tegmental nucleus (LDT). The SNc send DA efferents to the striatum to act on D2 and D2 receptors on MSNs, forming the nigrostriatal pathway. The VTA receives glutamatergic inputs from the medial prefrontal cortex (mPFC) and lateral habenula (LHb), and all three fast NTs from the PPT and LDT. The VTA sends DA projections to the mPFC to form the mesocortical pathway, and to the NAcc of the limbic system to form the mesolimbic pathway.

Electrophysiological studies show that DA neurons exhibit a unique firing pattern of slow, tonic activity intermingled with spontaneous bursts of increased activity (Grace & Bunney, 1984a, 1984b). Shultz had deciphered this pattern of continuous activity with phasic excitatory or inhibitory periods to be responses tied to expected rewards (Schultz, 1998). If an animal receives an unexpected reward after a behaviour or stimulus, a sharp increase in activity is elicited. Conversely, if an animal does not receive a reward after a conditioned behaviour or stimulus, predicting reward tonic firing is shunted. As more and more studies were published exploring the intricacies of this phenomena, the role of midbrain DA neurons was pigeon-holed into encoding reward prediction errors. This is obviously an important function as this promotes reinforcement-dependent learning (Schultz, 1998), however, this stable outflow of dopamine may also play a role in the autoregulation of DA neurons themselves.

DA neurons of the murine SNc do not display the phenotypical dark colouration found in human samples. Therefore, the tagging of TH, the rate limiting enzyme for dopamine synthesis, is necessary in histological experiments to identify the DA neuron population from the otherwise monochromatic neural tissue. By adding this method to the arsenal of other techniques used to uncover the inner workings of midbrain DA neurons, it is now evident that the SNc and VTA have unique morphological and electrophysiological profiles (Holly & Miczek, 2015; Lammel et al., 2008). The key to understanding how and why VTA DA neurons are for the most part spared during the progression of PD could lay in these differences.

1.2.1 The substantia nigra

The SN is a midbrain DA nucleus which has functions in sleep, reward and motivation, addiction, and most notably, execution of volitional movement (Chinta & Andersen, 2005; Wise, 2009). This modulatory hub can be divided into two morphologically and functionally distinct regions: the substantia nigra pars compacta (SNc) and the substantia nigra pars reticulata (SNr) (Paladini & Tepper, 2016). The SNr is comprised of mainly GABAergic projection neurons that synapse somewhat locally onto DA neurons of the SNc and act as an output center of the basal ganglia (Deniau et al., 2007; C. R. Lee & Tepper, 2007). The SNc houses a densely-packed population of DA neurons, which in humans look black to the naked eye due to the accumulation of neuromelanin, giving rise to the regions name “black substance” in Latin (Sonne et al., 2022). Degeneration of these neurons, whether it be due to genetic or environmental factors, manifests the motor complications associated with PD (Zecca et al., 2001).

SNc DA neurons are the main effectors of the nigrostriatal pathway, the bilateral circuit that innervates the striatum, a forebrain structure belonging to the basal ganglia and composed of the caudate and putamen. The striatum is the diverging point for the two opposing but synergistic pathways of the basal ganglia: the direct pathway and indirect pathway. Here, DA acts on GABAergic medium spiny neurons (MSNs) in the striatum which express either D1 or D2 receptors (Young et al., 2022). Both of these targets are G protein-coupled receptors that respond to DA, however act in conflicting manners (Verharen et al., 2019). The population of MSNs that express D1 receptors are preferentially expressed in the striatum, and when activated trigger the cascade of inhibition and excitation of basal ganglia nuclei involved in the direct pathway (Nishi

et al., 2011). Broadly, the direct pathway endorses movement starting with the cortex exciting D1 receptors on MSNs in the striatum which in turn inhibits GABAergic neurons of the globus pallidus internus (GPi) and SNr that project to the thalamus, allowing the thalamus to excite the cortex and permit movement (Nishi et al., 2011). D2 receptors on the other hand dampen the inhibitory signal of the striatum to the GPi and SNr, subsequently inhibiting the thalamus and therefore the motor cortex, blocking the execution of movement. Without sufficient DA signaling, the balance between the two pathways is tipped in favour of the indirect pathway, resulting in the bradykinesia that PD patients often face as the disease progresses (MgGregor & Nelson, 2019).

The complex connections between midbrain DA neurons and the striatum greatly overshadows all other networks the SNc is involved in. Not only do DA neurons receive inputs from the striatum but also from the cortex, lateral habenula (LHb), pedunculopontine tegmental nucleus (PPT), and laterodorsal tegmental nucleus (LDT) (Galtieri et al., 2017; Grillner & Robertson, 2016). To further its complexity, recent studies have shown that the SNc itself can be divided into four distinct heterogenous subpopulations, the dorsal, ventral, lateral, and medial regions, all with their own unique inputs, outputs, functions, and morphology (Estakhr et al., 2017; Fu et al., 2012, 2016; Gratiet et al., 2022; Grillner & Robertson, 2016; Hong & Hikosaka, 2014; Lerner et al., 2015; Y. Zhang et al., 2017). For example, DA neuron cell bodies in the lateral SNc are small and round whereas dorsal DA neurons are larger and oval-shaped (Fu et al., 2012). In the medial SNc, DA neurons have far reaching dendrites that extend into the SNr and express a higher concentration of K-ATP channels, the targets that are responsible for burst firing, than the lateral SNc (Lerner et al., 2015). This suggests that the area of striatal output innervated by the medial SNc would receive a higher instance of dopaminergic signaling after the animal experiences an unexpected reward or novel stimuli (Lerner et al., 2015; Schiemann et al, 2012). We can look to the PPT for evidence of heterogeneous innervation, as this midbrain nucleus stimulates either the medial or lateral region of the SNc depending on expected outcome of rewards and environment. If the animal receives a better-than-expected reward, a signal is sent to the medial SNc, whereas the lateral SNc is stimulated after an unpredicted reward (Hong & Hikosaka, 2014).

1.2.2 The ventral tegmental area

Like the SNc, the VTA is an extremely heterogeneous structure of the midbrain. It is most commonly recognized as a dopamine output center, however an estimated 30-35% of the cell population is GABAergic, and a small portion (2-3%) glutamatergic (Baik, 2020; Holly & Miczek, 2015; Sesack & Grace, 2010; Nair-Roberts et al, 2008). Despite having no clear distinctive borders, the VTA can roughly be divided into four sub regions along both its rostral/caudal and medial/lateral axis each with their own unique cytoarchitectonic features (Holly & Miczek, 2015; Trutti et al., 2019). The two subregions that bookend the VTA are the parafasiculus retroflexus area and the ventral tegmental tail, both of which display very fair TH staining. The parafasiculus retroflexus area is most rostral and has been described as an extension of the posterior hypothalamus area (Holly & Miczek, 2015; Ikemoto, 2007). The ventral tegmental tail, also known as the rostromedial tegmental nucleus (RMTg), is located at the most caudal end, and has been described as "a major break for dopamine systems," as it is rich in GABAergic neurons that send efferents into other VTA subregions as well as the SNc (Bourdy & Barrot, 2012; Ikemoto, 2007; Sánchez-Catalán et al., 2017). The more ventromedial posteriorly placed paranigral nucleus (PN) and parabrachial pigmented area (PBP) are rich in DA neurons and occupy the middle two thirds of the VTA (Holly & Miczek, 2015). The PN is a high throughput area, extending projections to several targets such as the shell of NAc, mPFC, and medial olfactory tubule (Lammel et al., 2011; Morales & Margolis, 2017). Lastly, the PBP is thought to be a continuation of the anterior SNc and is involved in homeostatic regulation and relaying sensory information to the forebrain (Palmiter, 2018).

The rich connections that VTA DA neurons make throughout the brain are divided into the mesolimbic and mesocortical pathways, sending projections to the NAc, a segment of the limbic system in the striatum, and prefrontal cortex, respectively (Morales & Margolis, 2017; Trutti et al., 2019). Presence of dopamine in these areas is what allows an individual to find pleasure in life sustaining activities, rewarding and reinforcing the act of seeking out food, drink, and sex (Feltenstein et al., 2021). The connection with the NAc is the driver for reward learning and motivation and has been highly implicated in the reinforcement of pleasurable behaviours (Salamone et al., 2003). Projections to the mPFC are involved with more logical rather than emotional cognition, such as emotion regulation and executive functioning (Feltenstein et al.,

1993). Interestingly, recent studies have found that DA neurons in the mesocortical pathway also respond to aversive stimuli, broadening the scope of function for this neuronal population (Lammel et al., 2011).

The regulation of VTA activity is mediated by cholinergic, glutamatergic, and GABAergic projections from a variety of brain regions, similarly to the neighbouring SNc (Morales & Margolis, 2017; Yoo et al., 2017). Cholinergic innervation to the VTA arrives mainly from the PPT and LDT, with each region preferentially synapsing onto DA neurons involved in either the mesocortical or mesolimbic pathways (Dautan et al., 2016; Omelchenko & Sesack, 2006). The PPT contributes to mesocortical DA neurons within the VTA, whereas the LDT is functionally connected to VTA DA neurons in the mesolimbic pathway (Dautan et al., 2016). The role of ACh mediated excitation is important for the regulation of the reward and pleasure-seeking behaviours controlled by the VTA, evidenced by the extremely addictive qualities of nicotine, a consequence stemming from the activation of VTA DA neurons upon binding to their nicotinic acetylcholine receptors (Liu et al., 2012; Mao et al., 2011). Glutamatergic projections from the mPFC, PPT, LDT, LHb, periaqueductal grey, and dorsal raphe nucleus have also been shown to stimulate VTA DA release (Morales & Margolis, 2017; Yoo et al., 2017). Maintaining proper glutamate homeostasis in the VTA is imperative given that it is in large part responsible for proper mesolimbic functioning and has been known for some time to be the driver for drug liking and drug seeking behaviours after prolonged use of psychostimulants such as cocaine, amphetamine, and methamphetamine (Fischer et al., 2021; Niedzielska-Andres et al., 2021). Lastly, GABAergic projections from the RMTg and the NAc regulate DA neurons by acting as their primary off switch (Morales & Margolis, 2017). Inhibition of VTA DA neurons is important for modulating circuits involved in reward prediction error as well as learning between appetitive and aversive stimuli (Kim et al., 2012; Lammel et al., 2012; Weitz et al., 2021). In addition, alterations in GABA signaling onto DA neurons in the VTA leads to disastrous consequences evidenced by the drug seeking behaviours which occur due to downregulation of inhibitory inputs, catalyzed by repeated used of substances such as cocaine which hijack the VTA reward system (Weitz et al, 2021).

1.3 Synapses & their neurotransmitters

In 1949, Hebb summarized the cellular mechanisms of learning into what is now most likely the most recognizable statement amongst neuroscientists – neurons that fire together, wire together (Hebb, 1949). We now know that this wiring occurs both electrically and chemically, with the majority of cells in the nervous system weighing heavily on the latter. Chemical communication between neurons occurs when a pre-synaptic cell releases neurotransmitters into the synaptic cleft to either trigger or shunt a depolarization event or make ultrastructural changes to a post-synaptic cell. A great deal of research has gone into understanding the sequence of events that occurs in the post-synaptic cell when neurotransmitters bind to post-synaptic protein channels to trigger the initiation of complex molecular cascades. To highlight the length at which these channels have been studied we can look to a-amino-3-hydroxy-5-methyl-4-isoxazolepropionic acid (AMPA) receptors and N-methyl-D-aspartate (NMDA) receptors, perhaps two of the most thoroughly studied channels in the brain (Sumi & Harada, 2020). We understand how these two receptors work in tandem to induce long term potentiation through synaptic plasticity, the basis of learning and memory, and have uncovered an extensive pool of agonists and antagonists that alter their functions (Sumi & Harada, 2020).

Our understanding of synaptic events on the pre-synaptic side are murkier. The life cycle of synaptic vesicles from neurotransmitter packaging to exocytosis has yet to be fully elucidated unlike the inner workings of their post-synaptic receptor counterparts. This life cycle is called synaptic vesicle recycling, a term coined by Heuser and Reese who used electron microscopy (EM) to visualize this event occurring for the first time (Heuser & Reese, 1973). They observed trends in synaptic vesicle depletion in motor nerve terminals of frog sartorius muscles following electrical stimulation and noticed that immediately following a 10 Hz shock, there were no synaptic vesicles present in pre-synaptic terminals. However, these stores were quickly replenished after 15 minutes, showing how quickly and efficiently vesicle recycling occurs (Heuser & Reese, 1973). Despite not fully understanding the intricate balancing act between protein and membrane interactions involved in neurotransmitter release and vesicle recycling, synaptic vesicles are some of the most thoroughly studied trafficking organelles with over 80 of their membrane proteins identified (Takamori et al., 2006). Within these 80, there are five transmembrane proteins that are ubiquitous amongst all synaptic vesicles, all with which we have

various levels of knowledge concerning their roles and functions during recycling. The two that we are most familiar with are synaptobrevin, a SNARE protein required for fusion to the pre-synaptic membrane, and synaptotagmin, a calcium sensor that triggers exocytosis (Chapman, 2002; Rizzoli & Betz, 2004). The two that we still haven't fully understood are SV2, which is believed to play a role in neurotransmitter release, and synaptophysin which may interact with lipids important in this process (Rizzoli & Betz, 2004; Takamori et al., 2006; Wan et al., 2010). Last but not least, each synaptic vesicle requires neurotransmitter transporters to, as the name suggests, transport neurotransmitters into the vesicle (Rizzoli & Betz, 2004). Although the title of "neurotransmitter transporter" seems relatively self-explanatory, they do not always act as the sole mechanism behind neurotransmitter packaging. Instead, they work in tandem with a vacuolar ATPase (V-ATPase), a proton pump which acidifies the lumen of the vesicle, triggering the translocation of neurotransmitters from the cytosol into the vesicle (T. Nishi & Forgac, 2002; Varoqui et al., 1996; Abbas et al., 2020).

In 1966, Werman laid out certain criteria that a molecule is required to meet in order to be classified as a neurotransmitter: First, it needs to be present in the pre-synaptic neuron. Second, it needs to elicit an effect on a post-synaptic neuron when released into the synaptic cleft. Third, these effects still occur when applied exogenously. Lastly, its effects can be blocked or enhanced by the presence of antagonists or agonists (Avoli & Krnjević, 2015; Werman, 1966). DA neurons of the SNc and VTA are primarily regulated by three molecules that meet these criteria - glutamate, ACh, and GABA (Kitai et al., 1999; Misgeld, 2004; Tepper & Lee, 2007; Morales & Margolis, 2017; Yoo et al., 2017). Each of these neurotransmitters exert distinct effects on the midbrain, and maintaining a fine balance of their combined influences is necessary for normal functioning.

1.3.1 Glutamate

The first evidence of glutamate acting as a neurotransmitter was documented in the 1970's and has since been found ubiquitously throughout the mammalian CNS (Özkan et al., 1997). Acting as the chief excitatory molecule in the brain, glutamate plays invaluable roles in perception, cognition, and perhaps most notably, learning and memory by acting as the trigger for the opening of AMPA and NMDA receptors (Dong et al., 2009). Because this small molecule

has a myriad of effects in all areas of the brain, it is imperative that its extracellular concentration be tightly regulated. If left uncontrolled, rogue glutamate due to insufficient reuptake from astrocytes or the presynaptic cell can induce excitotoxicity, a phenomenon caused by overstimulation of glutamate receptors leading to neuronal dysfunction and cell death (Dong et al., 2009; Zhou & Danbolt, 2014). Disturbances in this system have also been implicated in the pathophysiology of psychiatric disturbances such as anxiety, post-traumatic stress disorder (PTSD), depression, and schizophrenia (Dong et al., 2009; Nasir et al., 2020)

Glutamate is at the crossroads of two molecular synthesis pathways, glutamine, a non-essential amino acid, and GABA, the main inhibitory neurotransmitter in the CNS. Glutamate is shuttled into vesicles via vesicular glutamate transporters (VGLUT), of which there are three isoforms: VGLUT1, which is localized on neurons in the cortex and hippocampus, VGLUT2, which are more routinely found on neurons in the brainstem and diencephalon (Eriksen et al., 2020; Herzog et al., 2001), and VGLUT3, which is perhaps the least studied of three due to its more recent discovery. Despite this, intriguing research has shown that this third isoform is commonly localized on the soma of central serotonergic neurons and increases the presence of ACh and cholinergic transmission in the striatum (Amilhon et al., 2010; Herzog et al., 2001; Takamori et al., 2002). In the past, it was originally thought that glutamate was simply released into the synaptic cleft from the cytosol, bypassing the need to be packaged into vesicles (De Belleroche & Bradford, 1977), however it wasn't until 1983 that Naito and Ueda were able to isolate glutamatergic synaptic vesicles in the bovine cortex (Naito & Ttetsufumi Ueda, 1983). We now know that mechanistically the packaging of glutamate into vesicles very closely resembles that of other fast-acting neurotransmitters by utilizing the electrochemical gradient produced via a V-ATPase. A unique feature of glutamate packaging however is its reliance on the presence of a very specific range of chloride concentrations in the cytosol (Eriksen et al., 2020). Rather unexpectedly, the relationship between chloride concentration and vesicular uptake of glutamate is biphasic, with low concentrations (1-5 mM) promoting uptake, and high concentrations (above 20 mM) inhibiting the process (Özkan et al., 1997).

With the heterogeneity of glutamatergic projections in the brain, it comes as no surprise that DA centers are heavily influenced by this system. Interestingly, glutamate seems to play a neuroprotective role in the context of Parkinsonian degeneration in DA neurons (Buck et al., 2022). There are several hypotheses as to why this selective immunity occurs, however the most

promising research suggests that higher expression of VGLUT2 on these select DA cells may be somehow neuroprotective (Steinkellner et al., 2022). DA neurons in the VTA have been shown to express high levels of VGLUT2 for example and are less susceptible to Parkinsonian degeneration compared to neurons in the neighbouring SNc (Bimpisidis & Wallén-Mackenzie, 2019; Sulzer & Surmeier, 2013; Yamaguchi et al., 2015). Expression of VGLUT1 and VGLUT2 is also abnormal in non-DA midbrain regions as seen in post-mortem samples of human PD patient brains – levels were elevated in the putamen and drastically decreased in the prefrontal and temporal cortices (Kashani et al., 2007). The variations in VGLUT presence throughout the brain in mouse and human forms of PD supports the theory that glutamate is likely involved in PD pathogenesis in some capacity.

1.3.2 Acetylcholine

It is no question that ACh is an important molecule in both the CNS and peripheral nervous system (PNS). ACh is the oldest recorded neurotransmitter, first being characterized in the CNS in 1921 (Loewi, 1924). In the periphery, it plays important roles in the autonomic nervous system such as regulation of cardiac contractions, stimulation of the vagus nerve, exocrine gland secretion, and contraction of skeletal muscle (Sam & Bordoni, 2022). In the CNS, cholinergic projections arise from the brainstem nuclei, medial habenula, basal forebrain, and medial septum and is involved in complex processes such hippocampal synaptic plasticity, addiction, reward, and attention (Picciotto et al., 2012). The major cholinergic inputs to the basal ganglia and the VTA originate from the PPT and LDT, with the human PPT housing between 10 000 - 15 000 cholinergic neurons (Pahapill & Lozano, 2000). ACh acts via two different types of post-synaptic receptors, muscarinic receptors (mAChRs) which are slow, inhibitory G protein-coupled receptors, and nicotinic receptors (nAChRs) which are fast, excitatory cation channels. These receptors are found all on neurons all throughout the brain, however DA neurons in the SNc possess one of the highest densities of nAChRs (Nashmi et al, 2007) which emphasizes the significant influence ACh has on the midbrain.

For ACh to first enter the synapse and act on these post-synaptic receptors, it first needs to be packed into vesicles in the pre-synaptic terminal. Vesicular acetylcholine transporter (VAChT) is the synaptic vesicle membrane protein that shuttles ACh from the cytoplasm of the

pre-synaptic cell into vesicles (Varoqui et al., 1996). For each molecule of acetylcholine brought into the vesicle, two protons need to be shuttled out against their electrochemical gradient by the previously described V-ATPase (Bravo & Parsons, 2002; Nguyen et al., 1998). Abnormal expression of VAChT has been found to lead to a variety of behavioural and physiological disturbances in drosophila, mouse, and post-mortem human brain studies (Martella et al., 2009; Mazere et al., 2021; Showell et al., 2020; White et al., 2020), providing insurmountable evidence that this 12 transmembrane domain protein is necessary for normal functioning. In fact, VAChT and ACh are so critical for life that VAChT knock-out mouse pups do not survive past birth due to respiratory failure (Castro et al., 2009; Prado et al., 2013). In the context of PD, cholinergic transmission may play a more influential role in movement disturbances, specifically in posture and gait, than previously suspected. Janickova and colleagues selectively deleted VAChT from cholinergic neurons in the PPT and LDT of mice and noticed that their motor behaviour mimicked that of individuals with PD (Janickova et al., 2017). Indeed, these mutant mice displayed abnormal gait patterns such as slower, smaller steps and compromised posture and balance that worsened with age (Janickova et al., 2017). Cholinergic neurons of the PPT and LDT in individuals with PD experience similar patterns of degeneration as DA neurons in the SNc (Bohnen & Albin, 2009; E. C. Hirsch et al., 1987), and have been shown to contribute to motor control deficiencies hallmark to this disease (Karachi et al., 2010; Pahapill & Lozano, 2000). So much so, that the PPT has been considered a potential candidate for DBS to quell these motor disturbances (Kenney et al., 2014; Plaha & Gill, 2005; Stefani et al., 2007). As previously discussed, DBS presents with a myriad of obstacles that prevents it from being the most common therapeutic avenue despite its almost immediate and consistent results. Therefore, more pharmacological interventions are currently being investigated, with ACh possibly being an unsuspected candidate.

1.3.3 GABA

The journey in disentangling the role of GABA within the CNS has been a turbulent one. First being recognized as metabolite in the Krebs cycle, promoted to the title of neurotransmitter in 1953, demoted back to a metabolite less than a decade after this in 1960, and finally reinstated as a neurotransmitter in 1963, GABA has earned its rank amongst the fast-acting

neurotransmitters in the CNS (Jorgensen, 2005; Agner, 2001). It was one of the earlier seminal studies that launched GABA into its first stint as a neurotransmitter that uncovered its inhibitory effects by shunting the stretch reflex in crayfish by washing bovine brain precipitates over crayfish muscle fibers (Florey & Mclennan, 1955). Since then, even though it wasn't always recognized as a neurotransmitter after this study was published, it has become wildly accepted that GABA is the primary inhibitory effector in the brain. Indeed, approximately 20-40% of cortical neurons use GABA as their primary inhibitory neurotransmitter (Petroff, 2002). The importance of proper GABA signalling becomes apparent when this system is dysregulated, as a number of neurological disturbances arise such as epilepsy, generalised anxiety disorder, Huntington's disease, and PD (Buddhala et al., 2009). Similarly, mice who lack the ability to package GABA into vesicles present with a myriad of disorders such as epilepsy, schizophrenia, anxiety, and are even at risk for peripheral disturbances such as diabetes mellitus (Al-Kuraishy et al., 2021; Bolneo et al., 2022).

GABA is a derivative of glutamate, formed by the alpha-decarboxylation of glutamate catalyzed by glutamate decarboxylase (GAD) (Petroff, 2002). There are two main GAD isoforms, GAD65 and GAD67, who share the role of GABA synthesis however display unique distributions in the brain, suggesting that they are present in different contexts (Martin & Barke, 1998; Pinal & Tobin, 1998). GAD67 is thought to be evenly scattered throughout the brain and more versatile in its functions, playing a role in synaptogenesis and neuronal protection alongside its function in neurotransmission (Buddhala et al., 2009). This wider range of distribution makes sense as studies have shown that GAD67 is responsible for ~70% of total GABA synthesis in the brain, and GAD67 knockout mice do not survive past birth due to cleft palates (Asada et al., 1997; Petroff, 2002). GAD65 is more specialized, found concentrated around nerve terminals and synthesizes the remaining 30% of GABA exclusively for vesicular release (Kaufman et al., 1991; Petroff, 2002). Once synthesized from its precursor, GABA is translocated into synaptic vesicles by vesicular GABA transporter (VGAT) and driven by the electrochemical proton gradient produced by V-ATPase (Hells et al., 1990; McIntire et al., 1997). VGAT only requires one proton to shuttle a singular GABA molecule across the vesicle membrane and relies more on the change in electrical gradient than proton gradient for its neurotransmitter packaging (Ahnet-Hilger et al., 2003).

DA neurons in the SNc and VTA receive both local and longer-range GABAergic projections from a variety of different brain areas (Omelchenko & Sesack., 2009; Barrot et al., 2012; Fallon & Loughlin., 1995). In the SNc, inhibitory influence arises from the SNr, the striatum, the STN, globus pallidus externus, and somatosensory and motor cortices (Bolam & Smith, 1990; Chang et al., 1984; Galvan et al., 2006; Watabe-Uchida et al., 2012; F. M. Zhou & Lee, 2011). The VTA also receives GABAergic afferents from the striatum in addition to the LHb, lateral orbitofrontal cortex, the ventral tegmental tail, lateral hypothalamus, periaqueductal grey, and dorsal raphe nucleus (Morales & Margolis, 2017; Watabe-Uchida et al., 2012). Low levels of GABA have been found in cerebral spinal fluid of patients with PD, suggesting that the presence of GABA in the SNc may be necessary in staving off DA neuron degeneration (de Jong et al., 1984; Manyam, 1982). This has been further demonstrated in rat models of PD where injections of GAD vectors into the STN rescued motor symptoms and lessened the severity of DA neuron loss in the SNc following 6-hydroxydopamine (6-OHDA) lesions (Luo et al., 2002).

1.4 Synapse classification

In 1906, just twelve years after the drawings of Ramon y Cajal elegantly brought neurons beyond the microscope and to the naked eye in 1894, Sherrington brought Cajal's drawings to life with physiological explanations of nervous transmission and the first proposed definition of a synapse (López-Muñoz & Alamo, 2009; Cajal, 1894; Sherrington, 1906). Because of his previous electrophysiological work investigating spinal reflex arcs and Wallerian degeneration, Sherrington was able to speculate that there was a discontinuity between neurons despite not having the resolution available to see the individual compartments of a traditional synapse (Bennett, 1994). Indeed, in his efforts in understanding the polysynaptic connections of the spinal reflex arc he noticed that there was a delay in excitation of the motor neuron from the descending primary neuron, a phenomenon which he termed "synaptic delay" (Sotelo, 2020). These segregated compartments of the synapse were then visualized for the first time in 1959, when a ground-breaking paper published by E. G. Gray laid some of the most foundational groundwork in the field of neuroscience. Using EM, he describes a pre-synaptic process which usually contained mitochondria and many synaptic vesicles opposing a post-synaptic membrane across a 250 – 350 angstrom (25 - 35 nm) gap (Gray, 1959b). He then goes on to classify two

types of synapses in the CNS - Type 1 and Type 2 (Gray, 1959a). Whether a synapse is classified as Type 1 or Type 2 is determined by the thickness of the post-synaptic density (PSD) in the post-synaptic cell. Type 1 synapses have a PSD larger than the synaptic cleft and Type 2 synapses are accompanied by a PSD similar in width (Gray, 1959a; Romaus-Sanjurjo et al., 2021) to the cleft.

As with most other biological tissues structure often relates to function, so it comes as no surprise that these two types of synapses are speculated to work in different ways. It wasn't until 1968 however, nearly a decade after Gray introduced his Type 1 and Type 2 synapse, that Colonnier identified these differences and coined the terms "asymmetric" synapses for Type 1 and "symmetric" for Type 2, the vernacular that is most commonly used today (Colonnier, 1968). It was also during this time that researchers were starting to recognize that there were patterns in the size and shape of vesicles contained within the pre-synaptic boutons which seemed correlated with the synapse type. Two morphologically distinct populations of vesicles were described – spherical or flat, which is also referred to as ellipsoidal (Bodian, 1966; Uchizono, 1965). Through several studies examining the ultrastructure of the CNS and PNS, spherical vesicles are associated with excitatory transmission (Grey's Type 1 synapse), whereas flattened vesicles are responsible for inhibitory transmission (Grey's Type 2 synapse) (Levering Price, 1968; Uchizono, 1965, 1967; Walberg, 1966). Putatively, Ach-containing vesicles are large and round, with an approximate diameter of 45-50 nm (Gray & Guillery, 1966; Heuser & Reese, 1973). Prior investigations in our laboratory into the size of ACh vesicles using diaphragm muscles of the rat show that these vesicles can also average ~60 nm. Smaller round vesicles were observed to be on average 300 – 500 angstrom (30 – 50 nm) in diameter (Gray & Guillery, 1966), and associated with a PSD which are thought to be a result of glutamatergic transmission. Inhibitory synapses take on a more ellipsoid or oval shape and are commonly between 40 -50 nm at their long axis (Chang et al., 1984; Walberg, 1966), but have also been observed to be as long as 80 nm. Studies that aimed to elucidate the difference in appearance suggest that aldehyde fixation is responsible, as flattened vesicles were absent in any electron micrographs of CNS tissue fixed with only osmium (Walberg, 1966). The exact mechanism behind this remains unclear, however it is speculated that this morphological change could be the

result of change in tonicity of the tissue during fixation (Bodian, 1970; Larramendi et al., 1967; Walberg, 1966).

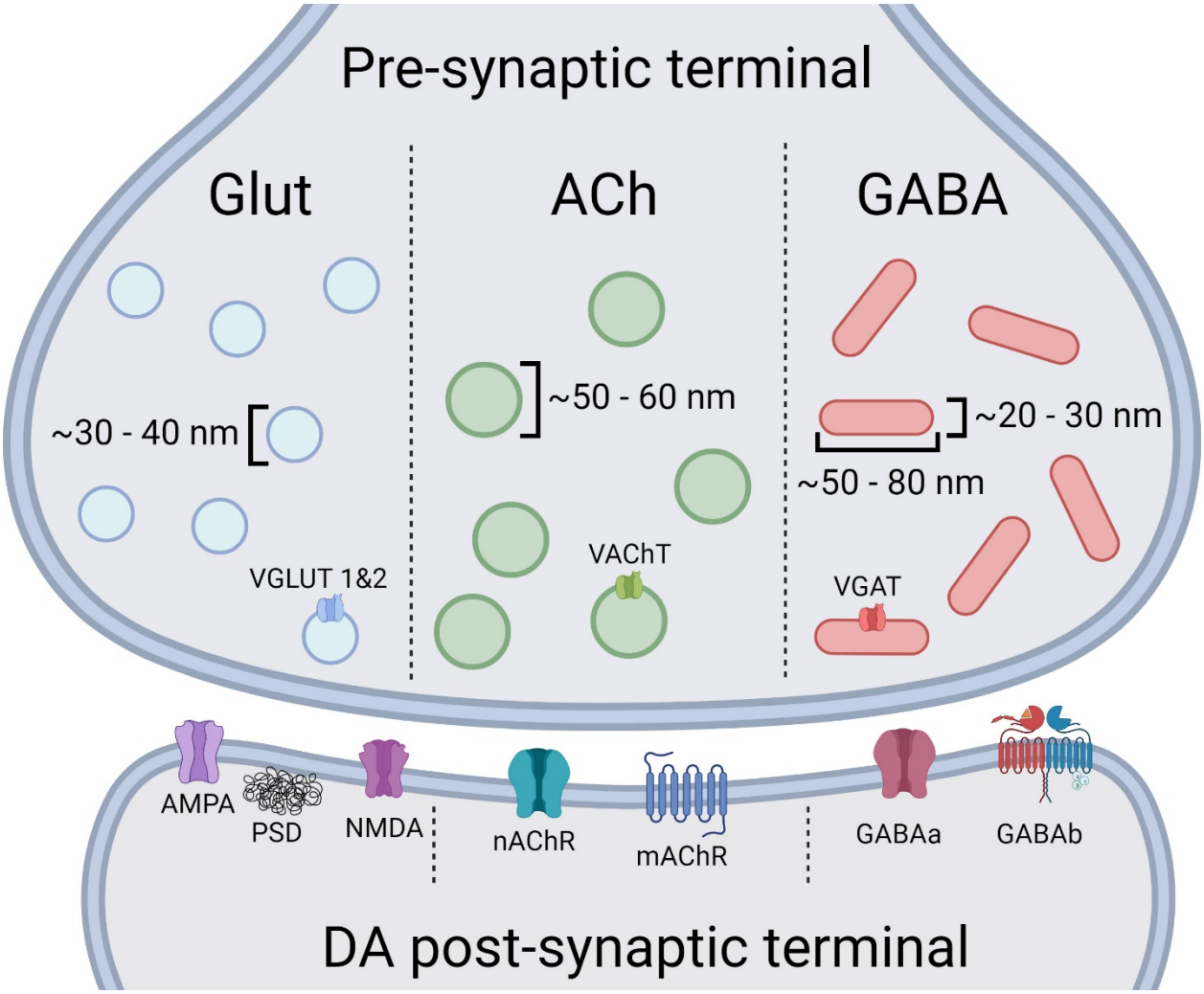

Figure 2. Schematic illustration of a variety of synapse types in the CNS based on EM ultrastructure. Glutamatergic characteristically contain round ~30-40 nm vesicles and the post-synaptic terminal contains a PSD (asymmetric synapse). Cholinergic terminals have large ~50-60 nm vesicles, whereas GABA terminals contain ellipsoid with a length of ~50-80 nm and a width of ~20-30 nm.

1.5 Co-transmission/co-localization of neurotransmitters in the CNS

During the nineteenth century a 30-year-old debate, now endearingly referred to as "the War of Soups and Sparks" was taking place between scientists who argued that communication between neurons was either purely chemical (Soups), the *cell theory*, or purely electrical (Sparks), the *syncytium theory* (Greengard., 2001; Strata & Harvey., 1999; Sotelo., 2020).

Pioneers of the field belonging to the camp of cell theory ultimately came up on top, however, unbeknownst to them, held an outdated view that a neuron had the ability to release only one neurotransmitter from their presynaptic terminals, confining it to either an excitatory or inhibitory role within the nervous system (Strata & Harvey, 1999). This school of thought is referred to as Dale's principal – "that a neuron releases a single classical neurotransmitter at all of its synapses," a dogma that earned Henry Dale and his colleague, Otto Loewi, the Nobel Prize of Physiology or Medicine in 1936 (Tritsch et al., 2016). In modern day neuroscience, we now know that neuron to neuron communication is a combination of the syncytium theory and cell theory - neurons can communicate electrically through gap junctions in addition to chemically via the release of neurotransmitters in the synaptic cleft (Kandel et al., 2000). Perhaps an even more radical discovery, one which completely uproots Dale's principal, is that pre-synaptic neurons can release more than one neurotransmitter at a time from its bouton. These findings opened the door for potentially any neuron in the CNS or PNS to be excitatory, inhibitory, or modulatory, at any given moment (Tritsch et al., 2016).

The first evidence of this phenomena was demonstrated in the PNS by Eugene Silinksy, who in 1975 showed that ACh and ATP were co-released through seminal electrophysiological experiments using rat phrenic nerves (Silinsky, 1975). Since then, an innumerable number of papers have been published reporting a slew of different combinations of co-released and co-transmitted neurotransmitters in both the CNS and PNS. Glycine and GABA for example have been shown to be co-transmitted in inhibitory interneurons of the spinal cord and co-released in rat spinal motor neurons and the mouse auditory midbrain (Jonas et al., 1998; Moore & Trussell, 2017; Triller et al., 1987). This combination is probably most intuitive, as GABA and glycine are shuttled by the same vesicular packaging machinery, vesicular inhibitory amino acid transporter (VIAAT) also known as VGAT, into vesicles (Aubrey et al., 2007; Burger et al., 1991).

Somewhat paradoxically, co-transmission/co-localization of excitatory and inhibitory neurotransmitters has also been reported. For example, glutamate and GABA co-release in several sites in the CNS such as the spinal cord, brainstem, and cerebellum (Seal & Edwards, 2006; Shabel et al., 2014; Zhang et al., 2017) have been documented. In a similar vein, Lee and colleagues discovered that ACh and GABA are co-transmitted by starburst amacrine cells onto direction-selective ganglion cells in the retina, giving rise to our ability detect image motion and direction with pinpoint accuracy (Lee et al., 2010). Studies following this demonstrated that co-

transmission of ACh and GABA also occurred in several different areas within the brain, with the majority arising from GABA localizing in the boutons of cholinergic neurons and packaged in separate vesicles (Granger et al., 2016; Saunders et al., 2015; Takács et al., 2018). There are also reports of co-transmission from midbrain DA neurons which release DA alongside either glutamate or GABA onto their output targets (Steinkellner et al., 2022). The benefits of co-transmitting an excitatory and inhibitory signal from the same synaptic ending are not fully understood and seems counterintuitive at first glance. However, several lines of evidence suggest that there is good reason for neurons in the brain to combine their on-off switches. Having extremely precise control over the balance of excitation and inhibition allows for rapid shunting of a signal, tight spatial and temporal regulation of firing patterns, and seems to play a crucial role in learning and memory (Root et al., 2014; Sloviter et al., 1996; Tritsch et al., 2016)

1.6 Objectives & Hypotheses

The objectives for this study are to categorize the types of neurotransmitters present in presynaptic terminals opposing DA neurons in the SNcM, SNcL, and the VTA, and determine the frequency at which they appear. To complete these objectives I will be using confocal microscopy to validate the claims that co-localization of ACh and GABA actually does occur, and observe the distribution patterns of ACh, Glut, and GABA in these three regions. Using EM, I will take advantage of its higher resolving power to describe the morphology of putative ACh, GABA, and Glut vesicles, which I hypothesize can appear individually, or, be co-localized in the same terminal but packaged in separate vesicles. In addition, I hypothesize that each region will have its own unique profile, both within and between one another.

Chapter 2 - Materials and Methods

2.1 Tissue processing for confocal microscopy

Wildtype 3–6-month-old male C57BL/6 mice were used and all procedures carried out in these studies have been approved by the University of Victoria Animal Care Committee and in compliance with Canadian Council for Animal Care guidelines. Mice were deeply anesthetized with isoflurane until no response was elicited to a tail or toe pinch. Once animals were sufficiently anesthetized, they were transcardially perfused with a gravity-fed perfusion device starting with heparinized 0.12 M phosphate buffered saline (PBS) (pH 7.4) until blood no longer flowed from right atrium, followed by ~80 ml of fixative composed of 4% paraformaldehyde (PFA) and 0.1% glutaraldehyde. The brain was removed from the skull and post-fixed in the same perfusion fix for up to 24 hours at 4° C. Brains were sectioned on a Leica vibratome at 50 μm intervals in PBS and collected in separate 24 well plates filled with PBS. Landmarks used to select which sections to use for further processing were the medial lemniscus to delineate the VTA from the SNc, and the third cranial nerve (oculomotor nerve) which was used to delineate the medial SNc from the lateral SNc (Fig. 18). Chemicals for tissue processing were purchased from Electron Microscopy Services (Hatfield, PA, USA).

Sections containing regions of interest were permeabilized in 0.25% Triton-X 100 (Sigma Aldrich) in PBS for 30 minutes at room temperature, followed by an hour-long incubation in blocking solution of PBS with 10% bovine serum albumin (PBS BSA) (w/v), 5% normal donkey serum (NDS), and 0.1% Triton-X-100 at 4°C. Sections were then incubated in the primary antibodies as follows: rabbit anti-tyrosine hydroxylase (1:1000, Pel-Freeze Biologicals, cat#P4010-150), goat anti-VAChT (1:1000, Sigma-Aldrich, cat#ABN100), mouse anti-VGAT (1:200, Synaptic Systems, cat#131-011), or mouse anti-VGLUT2 (1:200, abcam, cat#ab79157) diluted in 2% BSA and 0.1% Triton X-100 overnight at 4°C. After three consecutive 10 minute washes in PBS and 0.1% Triton-100, sections were incubated in the following fluorescent-tagged secondary antibodies for at least 3 hours at 4°C at a 1:400 dilution: donkey anti-rabbit Alexa Fluor 647, donkey anti-goat Alexa Fluor 488, and donkey anti-mouse Alexa Fluor 594. Sections were then washed once in PBS for 10 minutes, with then a final wash containing DAPI (blue nuclear stain) at a 1 μg/ml concentration. After three rinses, sections were mounted on glass

slides and coverslipped with Fluoro Gel with DABCO (Electron Microscopy Sciences, Hatfield, PA, USA).

2.1.1 Confocal image acquisition

Images were obtained on an Olympus Fluoview FV1000 confocal laser scanning microscope. All images were taken with a 4 µs/pixel dwell time and a 1024 x 1024 aspect ratio. Low magnification images were first obtained of each section using a 10X objective (0.41 NA) and 20X objective (0.75 NA) to create a map of each region. Regions were then imaged with a 60X oil-immersion lens (1.35 NA) at a 0.52 µm step size and both a Kalman and sequential filter enabled in order to be able to visualise puncta that correlated with individual vesicular transporters. TH labeled with Alexa Fluor 647 was excited using a 635 nm laser at below 1% max intensity, VAChT and VGLUT2 were labeled with Alexa Fluor 488 excited with a 488 nm laser at ~1.5% max intensity, and finally VGAT labeled with Alexa 594 was excited with a 561 nm laser at ~3% max intensity. Each laser line intensity and corresponding HV was set as to have as minimal saturation of pixels as possible while still maintaining a strong signal.

Analysis was performed using Fiji (ImageJ) software. Five slices of each individual channel from each stack were chosen for analysis based on strength of the signal. Slices were taken at 0.52 µm step size to create an image with a depth of 2.5 µm when merged. Merging of channels and Z-stack projection enabled us to see how many puncta on TH dendrites created a yellow pixel colour, indicating putative co-localization of VAChT and VGAT.

2.2 Tissue processing and collection for immuno-electron microscopy

Perfusion of mice (n=4) of the same sex and age for immuno-electron microscopy followed the same protocol as those used for confocal microscopy with the only difference being the fixative solution contained 4% PFA and 0.5% glutaraldehyde. Sections containing the previously described regions of interest were permeabilized with 0.1% sodium borohydride (w/v) in PBS for 30 minutes at room temperature (RT). Because of the aggressive nature of sodium borohydride, sections were rinsed once quickly in PBS to stop the reaction, then three more times at 10 minutes each. To block endogenous peroxidase activity in the tissue, sections were placed in 0.3% hydrogen peroxide (v/v) for 5 minutes at RT. Another quick wash in PBS with

three subsequent 10 minute rinses occurred at RT before an one hour-long incubation in blocking solution of 1% BSA (w/v), 5% NDS (v/v), and 0.01% Triton X-100 at 4° C. Sections then underwent an overnight incubation in a 1:1000 dilution of rabbit anti-tyrosine hydroxylase primary antibody (Pel-Freeze Biologicals, cat#P4010-150) diluted in blocking solution at 4° C. The next day, sections were rinsed three times in PBS BSA and incubated in a solution of donkey anti-rabbit horseradish peroxidase (HRP) conjugated secondary antibody (1:200, Thermo Fisher, cat#A16029) for 3 hours at 4° C with the plate covered by tin foil, followed by three rinses in PBS. TH-containing cells were visualized using a DAB (3,3'-diaminobenzidine) kit (Vector Labs, Burlingame, CA, USA) for 3-5 minutes then washed with PBS until reaction ceased. After all excess DAB solution had been rinsed, sections were transferred to a 0.15 M solution of sodium cacodylate (pH 7.4) (Electron Microscopy Sciences, Hatfield, PA, USA) at 4° C for at least one hour or until ready for further processing.

Each section containing regions of interest and adequate DAB staining were chosen for microdissection and further EM processing (Fig. 18). At least four 1 x 1 mm pieces of the medial SNc, lateral SNc, and VTA were microdissected under a dissecting microscope from the brain slices (totalling to at least 12 pieces of tissue per mouse) and transferred to labeled glass 4 ml vials with a pipette. All following steps were performed at RT on an angled rotating mixer. The sodium cacodylate buffer was carefully removed and replaced with a solution of 1% osmium tetroxide (Electron Microscopy Sciences, Hatfield, PA, USA) and 1% potassium ferrocyanide (Sigma, St. Louis, MO, USA) in 0.15 M sodium cacodylate for 3 hours. The osmium solution was then removed and tissue blocks were rinsed at three 10-minute intervals in deionized water. Tissue blocks were then stained *en bloc* with 2% aqueous uranyl acetate (Electron Microscopy Sciences, Hatfield, PA, USA) for at least 3 hours and up to overnight. After post-fixation and *en bloc* staining, sections underwent dehydration in ascending concentrations of ethanol (50%, 70%, 80%, 95%, 2 x 100%) for 10 minutes each followed by an at least a 6-hour incubation in a 1:1 mixture of 100% ethanol and Spurr's low viscosity resin (Electron Microscopy Sciences, Hatfield, PA, USA) and finally in an overnight incubation in 100% Spurr's resin. The next day, fresh Spurr's resin was replaced in the vials and mixed for at least one hour. Tissue pieces were embedded in size 3 BEEM capsules (Electron Microscopy Sciences, Hatfield, PA, USA) and polymerized in a 70°C oven overnight.

Once fully polymerized, semi-thin sections (0.5 - 1 μm thick) sections were obtained from each block on an ultramicrotome (UltraCut E, Reichert-Jung) and stained with 1% Toluidine blue (aq) at 70°C on a hotplate. Both unstained and stained sections were examined by light microscopy to ensure that there were DAB positive cells and dendrites (brown staining) within the tissue sections. Block faces were then cut into a trapezoid shape with a razor blade and ultrathin sections (60-70 nm) were obtained using a 45° diamond knife (Diatome, Hatfield, PA, USA). Five 100 hex copper mesh grids (Electron Microscopy Sciences) containing sections from each block were collected for morphometric analysis.

2.2.1 Transmission electron micrograph acquisition and analysis

Sections were observed using a JEM-1400 transmission electron microscope (TEM) (JEOL) and images captured with an Orius SC1000 digital camera (Gatan, USA). Sections were first surveyed using low magnification and once a DAB-positive dendrite with an opposing presynaptic terminal containing at least 30 vesicles was identified, an image at x80 000 magnification was taken. If the entire diameter of the dendrite was not within the x80 000 image, a lower power image was taken at x40 000 magnification. Twenty-five images were taken per block. To summarize – for each mouse, at least four pieces each of the SNcM, SNcL, and VTA were microdissected and polymerized into resin blocks from DAB-stained tissue. Each of the four blocks per region were then sectioned at 60 nm and collected on 100 hex copper mesh grids. By TEM, images of 25 different dendrites with visible synapses were taken from each block (Fig. 3). For one mouse this totals to 4 pieces of tissue per region, 4 blocks per region, 25 images per block, and therefore 100 images per region (SNcL, SNcM, VTA) for a total of 300 images per mouse. For all of the four mice, 400 images were obtained from each midbrain region adding up to a total of 1200 images across the three regions. Although 400 images per region were acquired, on average 200 were analyzed totalling 600 images for the entire experiment because of the unforeseen time-consumption of this type of analysis.

Classification of synapses, whether it be GABAergic, cholinergic, or glutamatergic, was decided based on the morphology of vesicles in the presynaptic terminal as reported in previous studies (Bodian, 1966; Uchizono, 1965; Gray & Guillery, 1966; Heuser & Reese, 1973) and from prior work done in this laboratory. A neuromuscular junction was examined from the

mouse diaphragm and was used for comparison of cholinergic vesicle sizes in the midbrain (See Fig. 28 in Appendix).

Using FIJI, vesicle shapes and sizes were measured with the "Freehand selections" and "Straight" tool respectively (Fig. 4). Using the "roundness" measurement, a value between 0 – 1 is calculated by FIJI using the equation:

$$\text{Roundness} = 4A/(\text{pi}*\text{Major Axis}^2)$$

Where A = area

A value of 1 indicates that the traced vesicle is circular in shape whereas a value less than 1 indicates an ellipsoid shape. In this study, it was decided that if a vesicle has a roundness ratio of less than 0.65 it was classified as GABAergic, and if the ratio was higher than 0.65, the diameter was used to determine if the vesicle was putatively cholinergic or glutamatergic. The "straight" tool was used on the longest axis of the traced perimeter to determine the diameter. If the average diameter was 45 nm or smaller, the synapse was considered glutamatergic, and if average diameter was more than 45 nm it was considered cholinergic. Terminals were considered mixed if there were there at least 5 oblong vesicles present in a predominately round terminal, and vice versa.

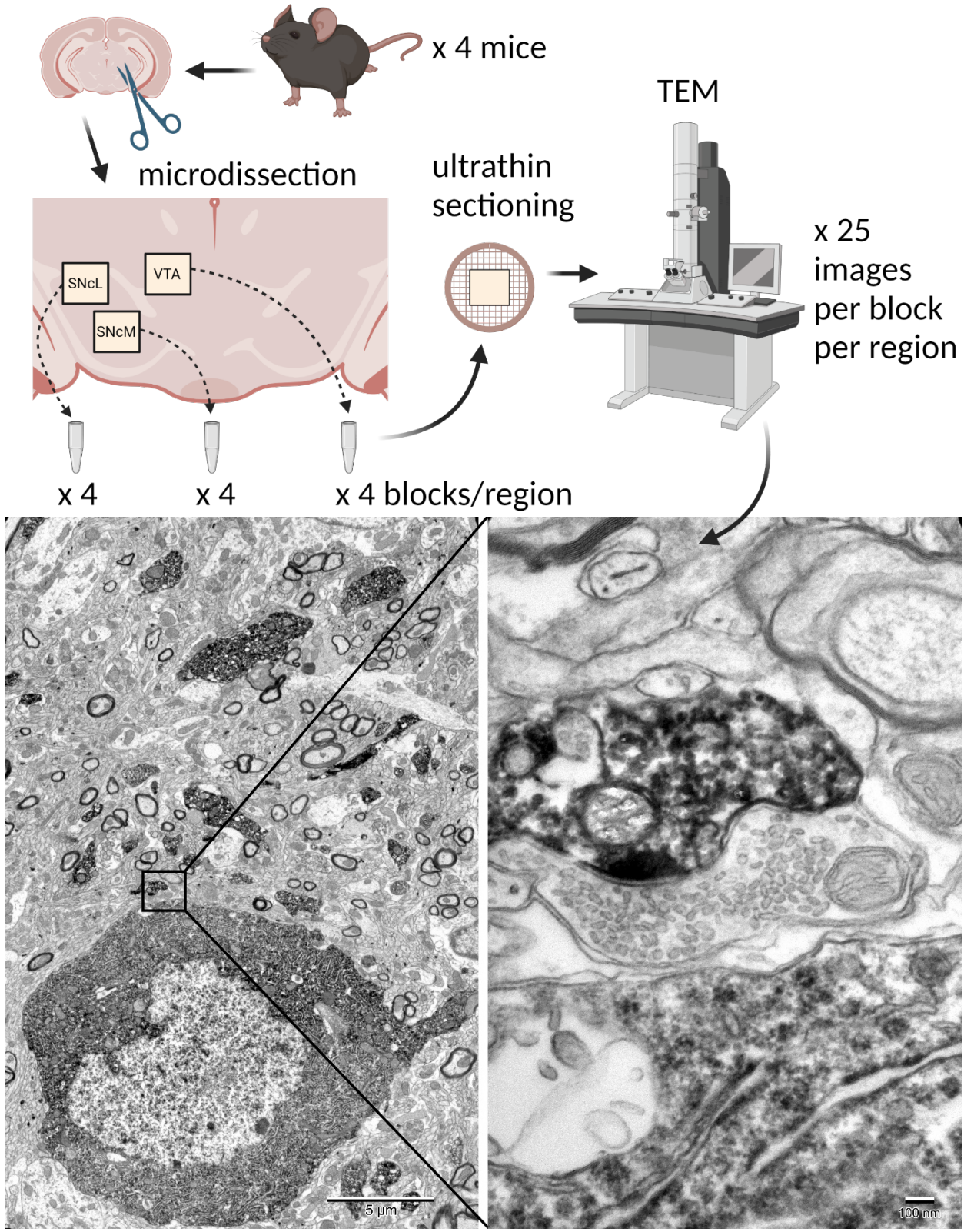

Figure 3. Flowchart for tissue collection, imaging and morphometric analysis of presynaptic terminals. From each mouse, four of SNcL, SNcM and VTA regions were microdissected from TH-DAB stained tissue, postfixed, and embedded in resin. Ultrathin sections of 60 nm thickness were cut from each block and collected on 100 hex copper grids. Twenty-five images per block per region were acquired with a JEM-1400 TEM and analysed with ImageJ.

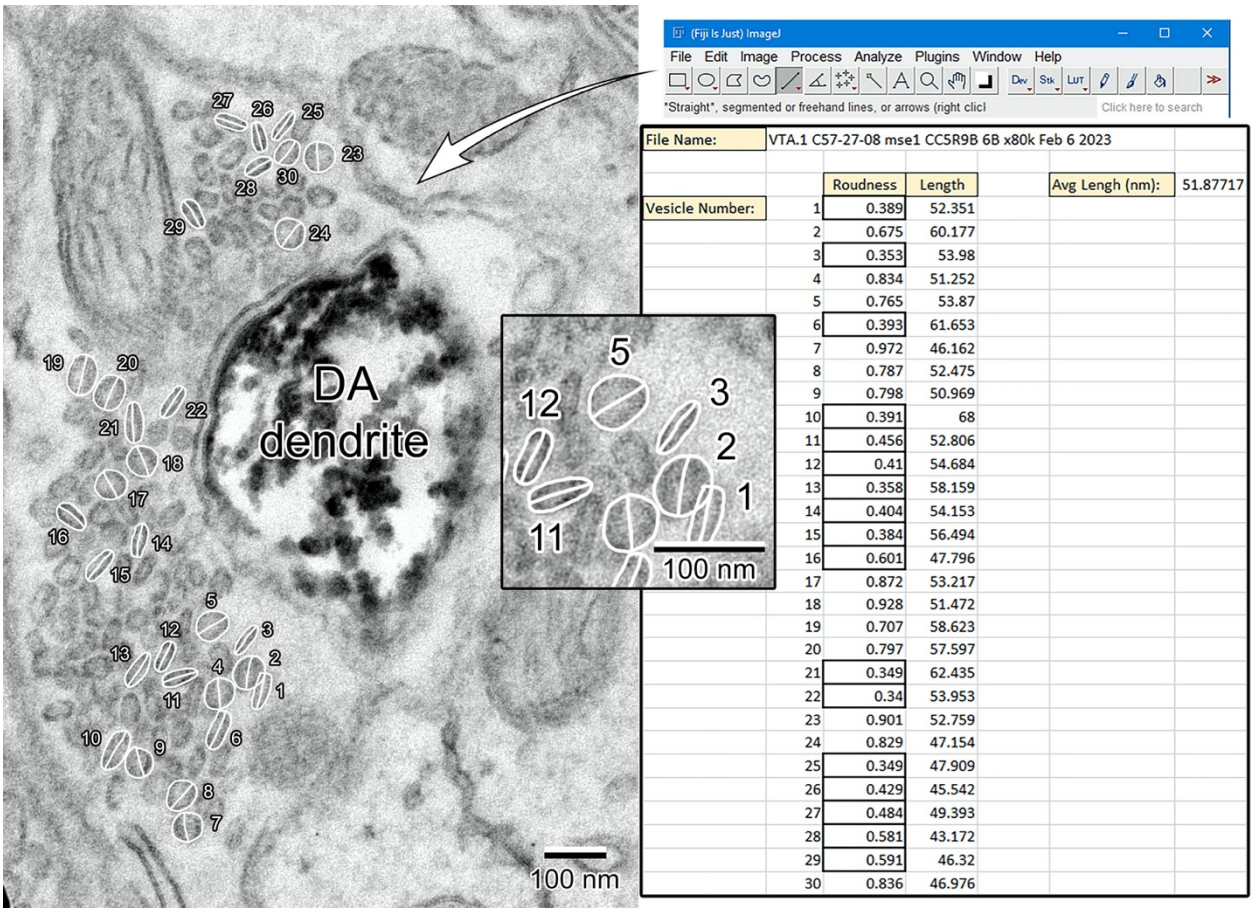

Figure 4. Morphometric analysis of vesicles within presynaptic terminals on DA dendrites using ImageJ (FIJI). Each vesicle within a terminal was outlined with the "Freehand Selection" tool to calculate the roundness value (between 0-1). A vesicle with a roundness >0.65 was classified as circular (See numbers 2, 4, and 5 in inset), whereas vesicles <0.65 were ellipsoidal (indicated by boxes on excel sheet. See numbers 1, 3, 11, and 12 in inset). The "Straightline" tool measured the greatest diameter of each vesicle. The diameters of all vesicles that scored >0.65 roundness were averaged to determine if the vesicles were cholinergic (2, 4, and 5) or glutamatergic (not shown). For examples of glutamatergic vesicles see figure 15. Total synapses from each mouse were compiled and analyzed and graphically represented with SPSS and GraphPad software.

2.2.2 3D electron-tomography

Electron tomography allows for a 3D visualization of a normally 2D electron micrograph and has been used previously to visualize synapses in the PNS and CNS (Harlow et al., 2001; Rizzoli & Betz, 2004). By adjusting the tilt of the specimen rod in the microscope, one can capture images of distinct angles within the 60 nm-thick section, allowing for visualization of the section contents from various angles. One tilt series of each synapse type (Glut, ACh, and GABA) was acquired using the same digital camera equipped TEM as previously described.

Before acquiring images, the eucentric height needed to be found to in order to orient the grid in the Z axis to reduce the severity of drift as the rod tilted. To do this, the Z axis was lowered in small increments and ± 5° tilts were done to test the intensity of the drift. After the eucentric height was found, each series had a tilted view of each image taken at ±25° with 5° increments for a total of a 50° tilt in the synapses. Images were aligned using Photoshop and saved as an animated gif in order for the 3D shape to be visualized.

2.3 Statistical analysis

Statistical analyses were carried out using SPSS (IBM, USA) and graphs were made with GraphPad Prism and SPSS. In total 613 dendrites were analysed, with n=200 in the SNcM, n=213 in the SNcL, and n=200 in the VTA. Table 1 below summarizes the total number of dendrites and vesicles counted for each presynaptic terminal in each region across 4 mice. Data did not meet assumptions of normality as was determined by a Shapiro-Wilk normality test, therefore nonparametric tests were employed for analysis. A Kruskal Wallis test was used to determine if there were any differences in NT group within and between regions, followed by Mann-Whitney U *post hoc* tests when appropriate. To determine if there was any relationship between vesicle shape and size for each NT group in each region, a correlative analysis test using Spearman's rank-order correlation was run. Results across all tests were considered significant if differences were reported at a $p<0.05$ alpha level.

Table 1. Summary of total number of terminals and vesicles contacting TH+ dendrites within each region.

n = 4 mice n = 4 blocks/region n = 25 images/region	**SNcM**		**SNcL**		**VTA**	
	Terminals	**Vesicles**	**Terminals**	**Vesicles**	**Terminals**	**Vesicles**
Glut	59	1355	64	1580	99	2208
ACh	39	691	42	793	46	856
GABA	3	111	2	60	0	0
ACh/GABA	65	1178	68	1613	33	816
Glut/GABA	34	679	37	943	22	407

Chapter 3 – Results

3.1 General histology

The SNc and VTA are two high throughput areas, receiving inputs from nearly every corner of the brain and sending DA projections, sometimes in conjunction with Glut or GABA, to highly specialized brain regions that allow us to execute smooth volitional movements and gives us motivation to engage in basic life-sustaining activities. The SNcM, SNcL, and VTA all house densely-packed DA neurons with obvious nucleoli and long branching dendrites which can be seen even with simple toluidine blue staining (Fig. 5). The DA neurons of the VTA are separated from the SNc by the heavily myelinated tracts of the medial lemniscus, and the SNc is divided into the SNcM and the SNcL by the longitudinally sectioned cranial third nerve. The neuropil encompassing these neurons is composed of a dense meshwork of interweaving axons myelinated by oligodendrocytes, discrete regions of astrocytes, and dendrites supported by surveying microglia (Fig. 6).

DA neurons themselves are relatively large cells, with cell bodies measuring regularly 10–15 μm in diameter with cytoplasm compact with free ribosomes, mitochondria, rough endoplasmic reticulum, and lysosomes (Fig 7). Their nuclei are euchromatic and often contain prominent nucleoli indicating that the cell is very active, undergoing high rates of protein translation. Not only this, but it is also not uncommon to see the nuclear envelope of DA nuclei be deeply indented (Fig. 7). A second unique feature of DA neurons is that the location of their axon initial segment (AIS) is not directly sprouting off the cell body which is the usually the case for other neurons throughout the CNS, but rather extends off primary dendrites away from the cell body (Moubarak et al., 2019). No AIS were observed in our investigations, however DA neurons with multiple long reaching dendrites were commonly present within the surrounding neuropil composed of longitudinally and cross sectioned dendrites in addition to heavily myelinated axons. Pre-synaptic terminals containing vesicles of varying shapes and sizes were found along these dendrites which we characterised as cholinergic, glutamatergic, or GABAergic based on their size and shape. Putative cholinergic vesicles are round with a diameter of ~50 – 60 nm, small round putative glutamatergic vesicles have a diameter of ~30 – 45 nm and are accompanied by a PSD on the post-synaptic terminal, the hallmark sign of an asymmetric synapse, and ellipsoidal shaped putative GABAergic vesicles had a wide range of diameters, reaching ~50 – 80 nm on their longest axis and ~20 – 30 nm on their smallest (Fig. 8). An

example of a glutamatergic synapse containing small, round vesicles in their pre-synaptic terminal and PSD on the post-synaptic cell can be seen synapsing onto a large DA dendrite in the SNcL in figure 8. A putative cholinergic terminal with large vesicles is situated below, very clearly showing the difference in size between them.

We documented the frequency of these various neurotransmitter types (ACh, Glut, GABA, ACh/GABA, and Glut/GABA) using the aforementioned vesicle morphology in the SNcM, the SNcL, and the VTA (Fig. 9), which will be discussed further in section 3.4. To substantiate the claims that ACh and Glut vesicles were indeed round and oval GABAergic vesicles were flat, 3D EM tomography was carried out for each ACh, Glut, and GABA vesicle types. At either end of the 50° tilt (-25° and +25°), the round ACh and Glut vesicles did not undergo any profound conformational change, suggesting that they take on a spherical shape in a 3D space. GABA vesicles either flatten or retain their oblong profile, indicating that they are ellipsoidal in a 3D space (Fig. 10). The animated gifs further demonstrate that putative ACh and Glut vesicles appear spherical, whereas putative GABA vesicles take on a more flattened, disc shape. Mitochondria could be seen in many of the larger pre-synaptic terminals, showing that events that take place in the boutons such as neurotransmitter vesicle packaging and vesicle fusion to the pre-synaptic membrane require an abundance of energy to be successfully carried out (Fig. 8, Fig. 9).

The structural integrity of DA neurons and the surrounding neuropil are maintained by the various support cells of the CNS such as satellite cells, which can be seen in close contact to cell bodies (Fig 7). Wandering microglia cells work as the support and clean-up crew, degrading any waste from surrounding synapses and packaging the debris into lysosomes, which under the EM appear extremely electron dense due to the amount of material compacted into the lysosomes (Fig. 11). Astrocytes were unsurprisingly found near capillaries, which on average spanned 5 µm in diameter with prominent endothelial cells lining the lumen (Fig. 12). Astrocytes can be distinguished from other support cells by their pale staining mitochondria and ability to contort into sharp angles to infiltrate every nook and cranny of the neuropil (Nahirney & Tremblay, 2021). They are also commonly found supporting the synapse, wrapping around the entire structure providing nutrients to the pre- and post-synaptic cells (Fig. 8).

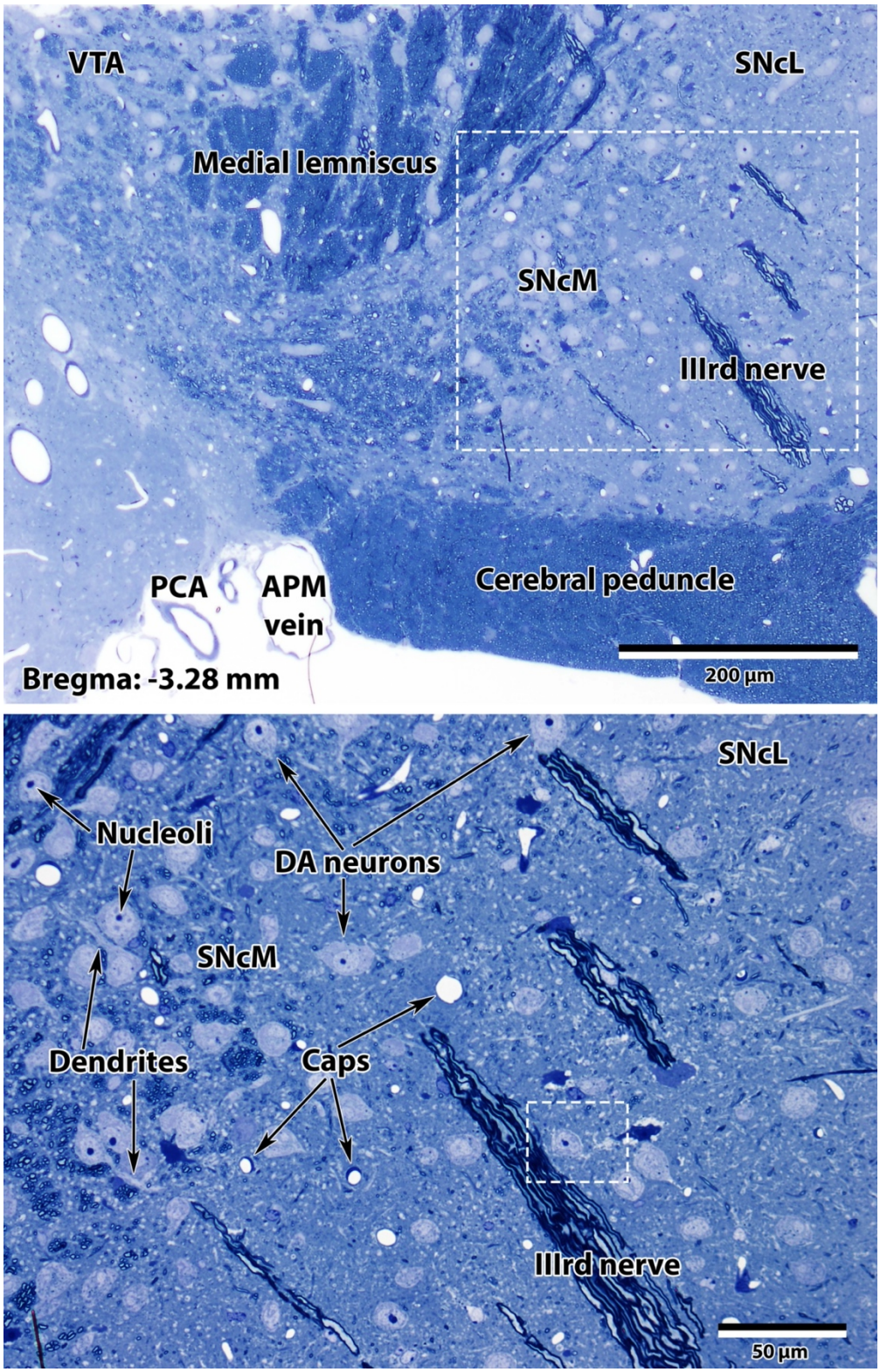

Figure 5. Low (above) and high (below) magnification LM views of a toluidine blue-stained coronal section of the mouse midbrain. Within the midrain are collections of DA neurons that are surrounded by the cerebral peduncle, medial lemniscus, and the IIIrd nerve (oculomotor) which stain dark blue due to the myelin content in axons. The large DA neurons have euchromatic nuclei with prominent nucleoli and show dendritic branches emanating from their cell bodies. Caps, Capillaries; PCA, Posterior cerebral artery; APM, anterior pontomesencephalic vein.

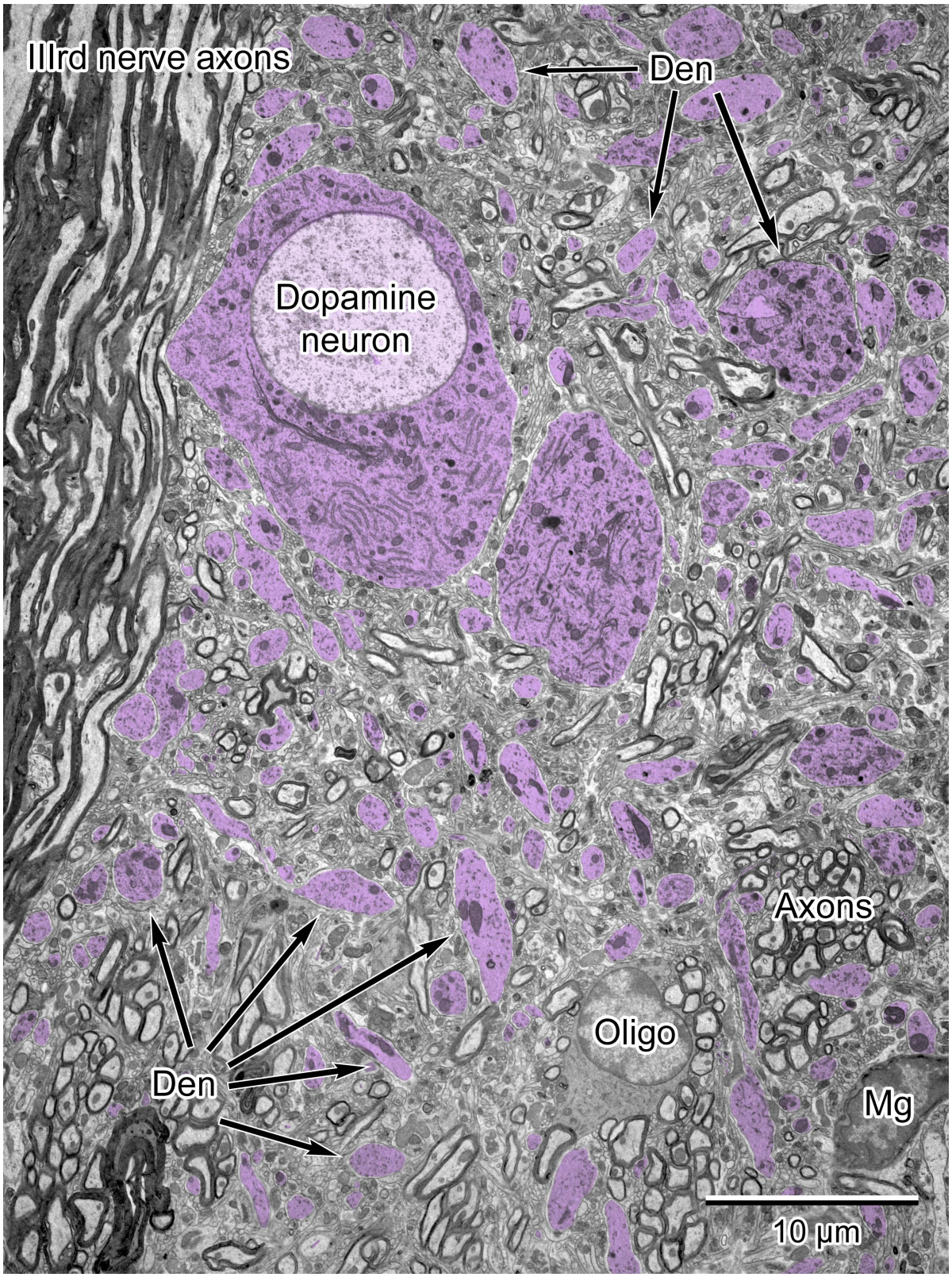

Figure 6. Low magnification EM of the SNcL in proximity to the IIIrd nerve. A large DA neuron cell body and its surrounding dendrites (Den) are pseudocolored magenta. The surrounding neuropil contains a dense array of synaptic contacts terminating onto dendrites of varying sizes not seen at this magnification. Oligo, Oligodendrocyte; Mg, microglia.

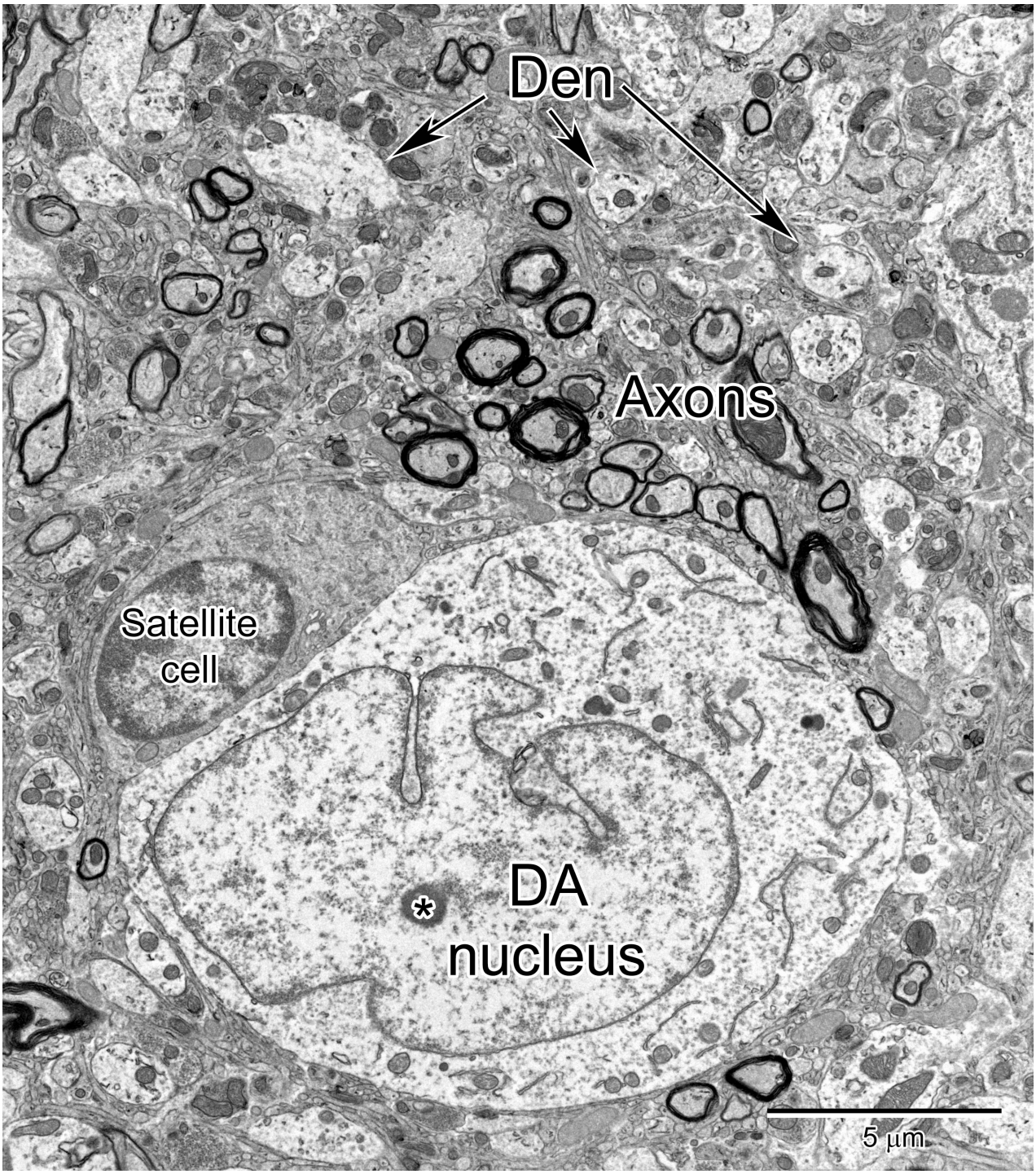

Figure 7. Medium magnification EM view of a DA neuron and surrounding neuropil in the SNcL. The euchromatic DA neuron nucleus shows elaborate nuclear envelope infolding and a prominent, centrally-located nucleolus (*). The cytoplasm is replete with free ribosomes, rough endoplasmic reticulum, lysosomes, and mitochondria. Closely opposed to the DA neuron is a supportive satellite cell. A collection of myelinated axons above and numerous dendrites (Den) occupy the surrounding neuropil

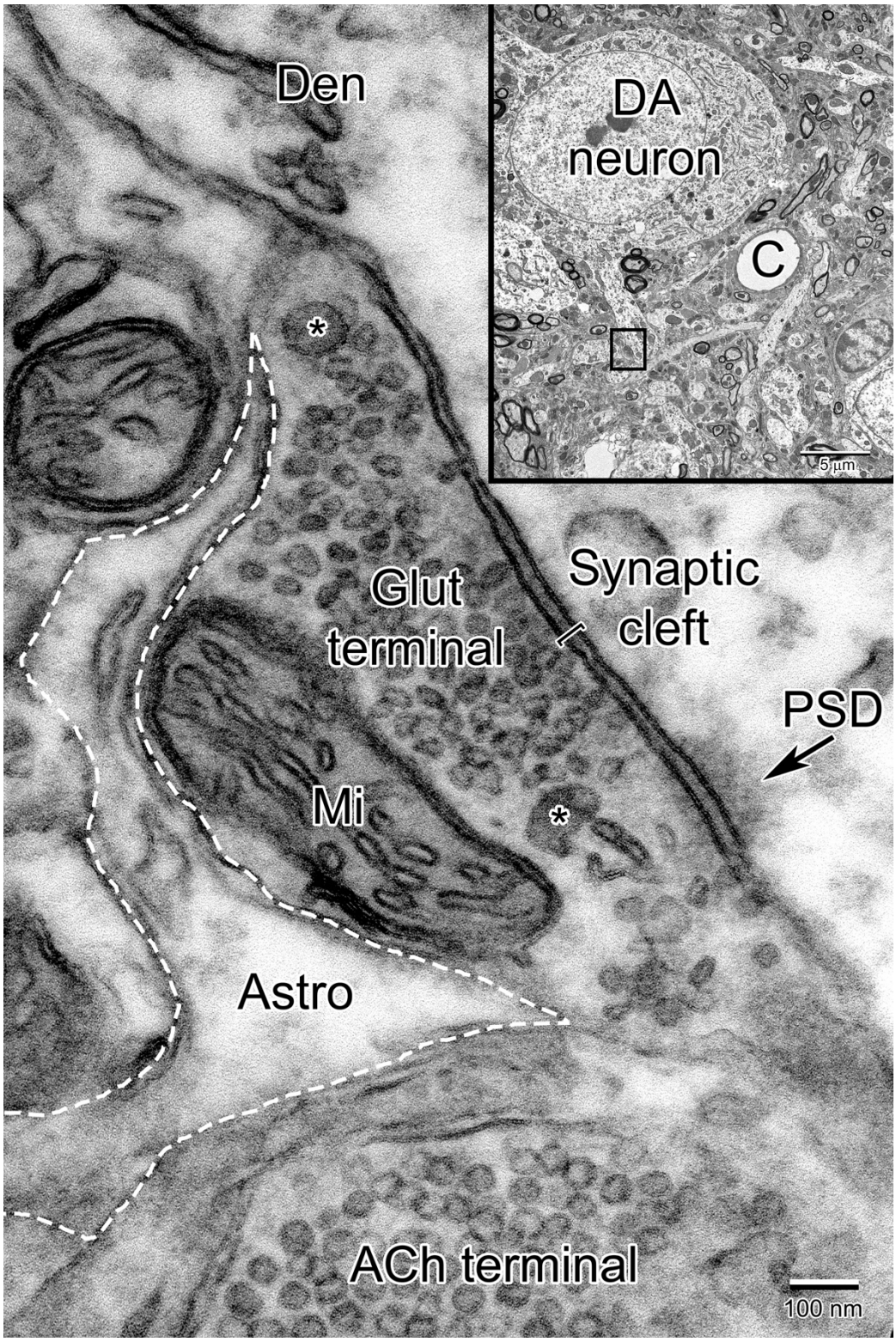

Figure 8. Detailed view of a glutamatergic synapse on a proximal DA neuron dendrite in the SNcM The rounded vesicles measure ~30 – 40 nm in diameter and a prominent PSD is present on the dendritic membrane. For comparison, an ACh terminal is below showing larger vesicles (~50-60 nm). A large mitochondria (Mi) is present within the terminal. The ~20 nm sized cleft contains amorphous. DA neuron and its neighbouring capillarity (C) can be seen at low magnification. The lateral aspects of the synapse contain enlarged endocytotic type vesicles that likely represent recycling vesicles (*). Astro, Astrocyte.

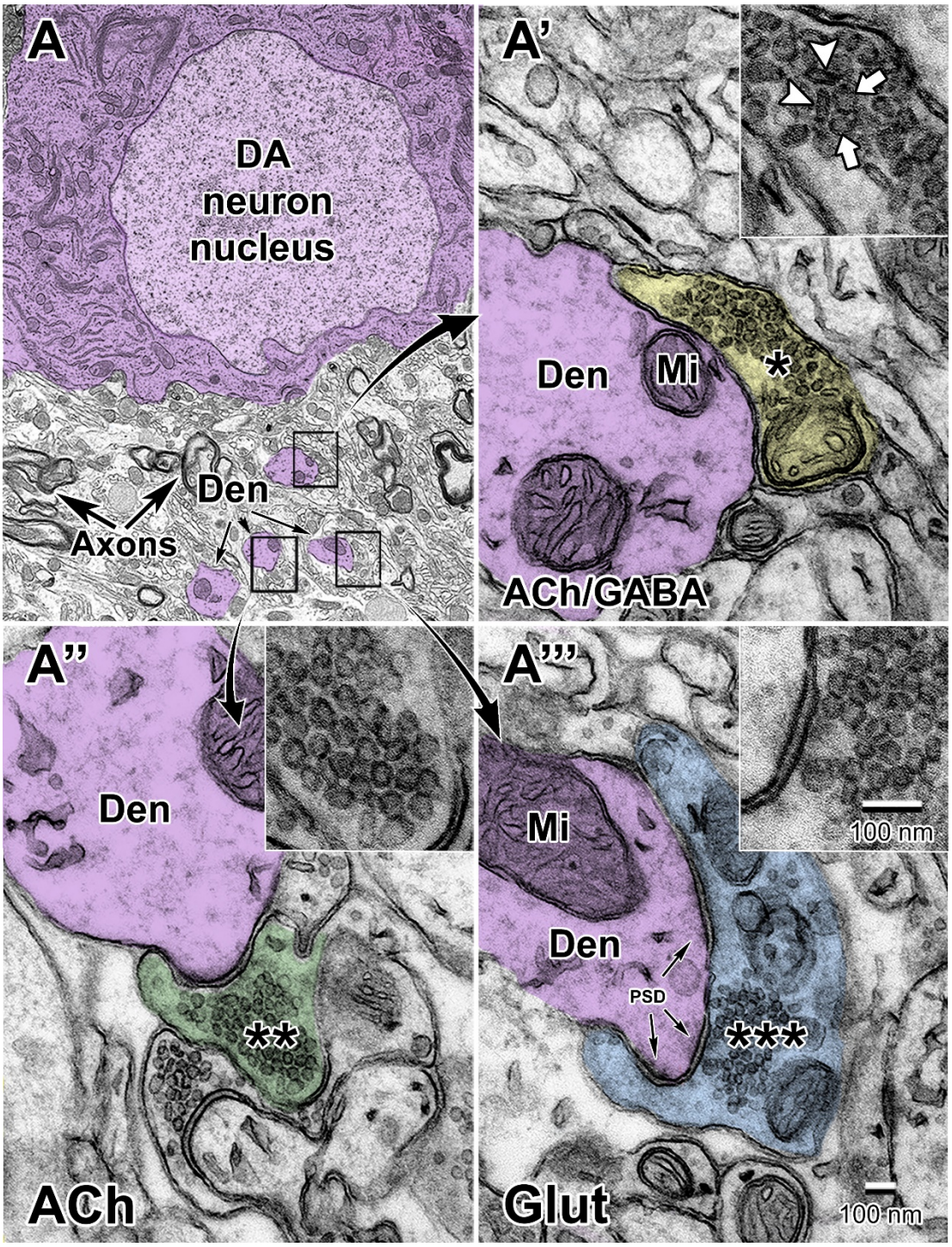

Figure 9. Examples of ACh, mixed ACh/GABA, and Glut terminals in the SNcM. Low (A) and high (A', A", A''') magnification views of a dopamine neuron and surrounding synapses in the SNcM. A large dopamine neuron (magenta) is surrounded by neuropil filled with dendrites (Den), myelinated axons (Ax), and synaptic contacts on dendrites (A', A", and A'''). Three distinct types of synapses are seen in this region. A putative cholinergic synapse (A'", green) on a dendrite is filled with large uniform-sized round vesicles ~50-60 nm (***) in diameter (shown at high magnification in inset). Another type of synapse (A', yellow) exhibits a mixture (*) of small oblong vesicles ~50 nm in diameter (arrowheads in inset) corresponding to putative GABA-type vesicles and large cholinergic-type round vesicles (arrows in inset). A third type of synapse is putative glutamate (A'', blue) with small vesicles ~35-45 nm (***) in diameter. Mi, mitochondria. Figure adapted from images I obtained for the Le Gratiet et al., 2022 paper.

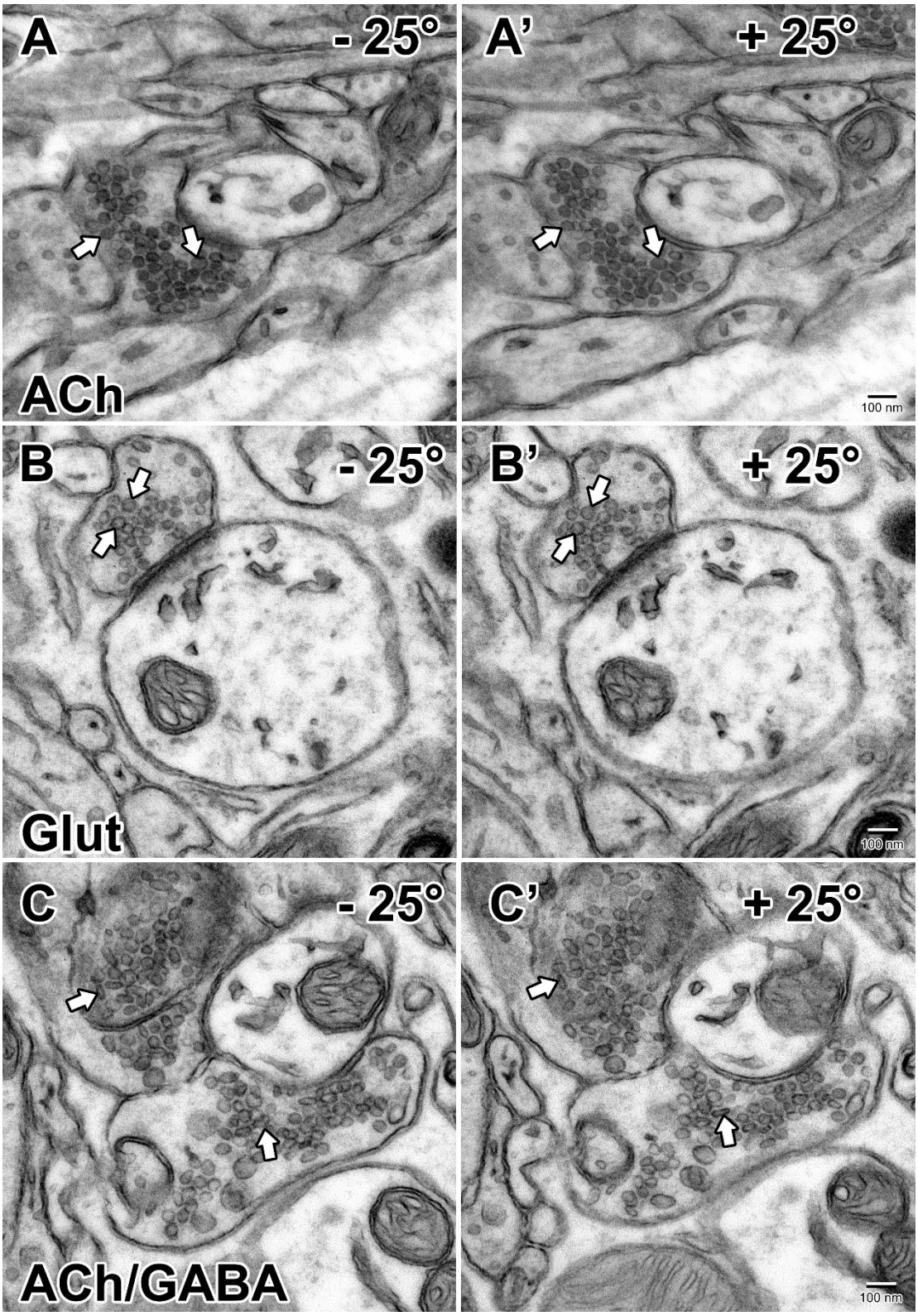

Figure 10. Fifty degree tilts of ACh, Glut, and ACh/GABA terminals. Images show each neurotransmitter vesicle type at opposite ends of 50° tilts. Putative ACh and Glut terminals remain circular at both -25° and +25°, showing that they are spherical in shape. Putative GABA vesicles either stay oval shape or seem to flatten as the section is tilted, indicating that they are morphologically different than ACh or Glut vesicles

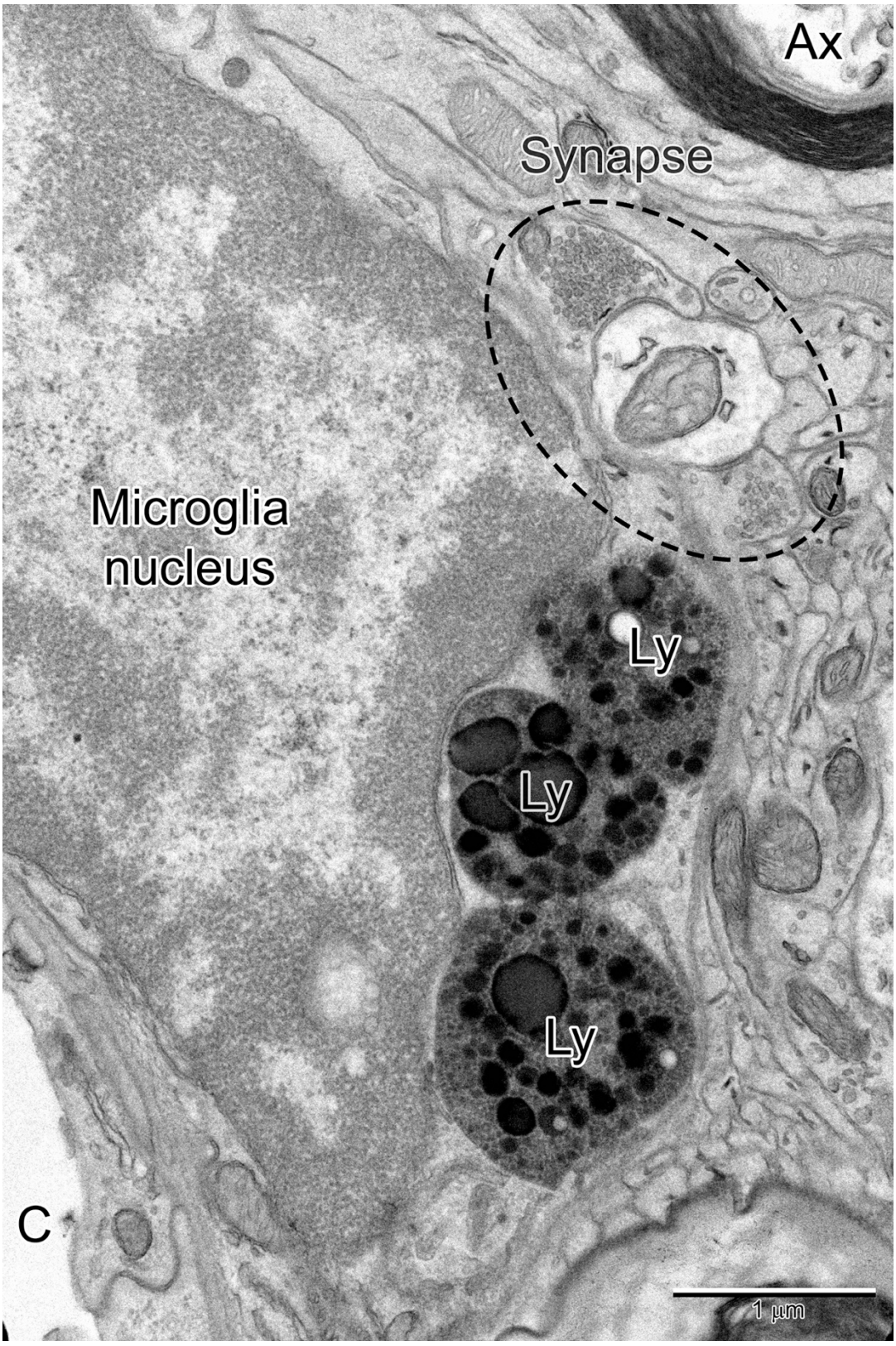

Figure 11. Other cellular constituents are also present within the midbrain neuropil. Here, a perivascular microglia with prominent lysosomes (Ly) is in close contact with a synapse suggesting that they play a role in synaptic homeostasis. C, Capillary; Ax, Axon

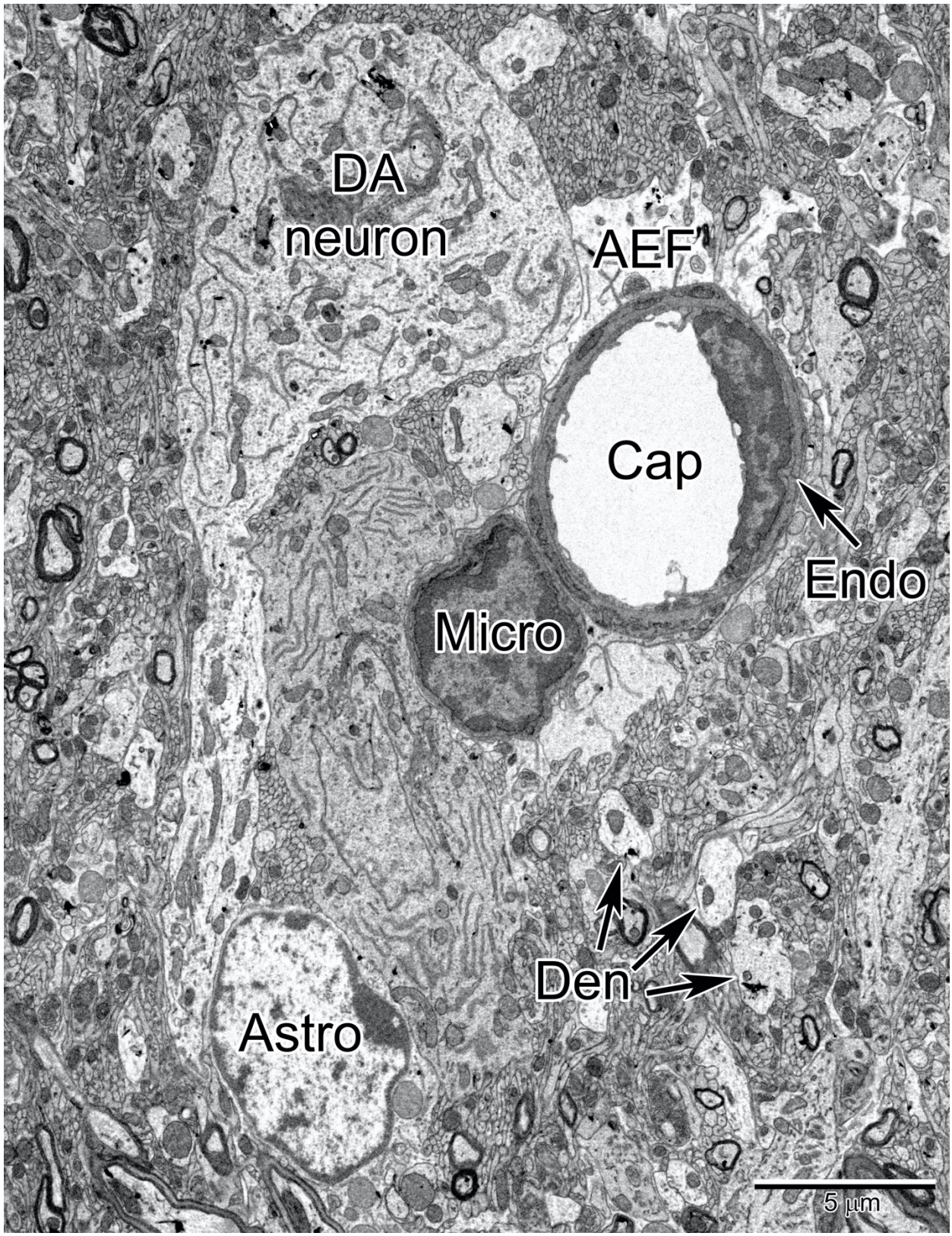

Figure 12. Low mag survey view of the SNc showing a portion of a DA neuron and its dendrite abutting a capillary (Cap) and astrocytic end feet (AEF) near the capillary. The astrocytic nucleus is seen below along with a perivascular microglial cell. Den, Dendrites; Mico, Microglia; Endo, Endothelial cell; Cap, Capillary

3.2 Confocal microscopy

Confocal microscopy was used to visualise the pattern of VGLUT2, VAChT, and VGAT terminals along DA dendrites and to validate the claims that there is indeed co-localization of ACh and GABA in synaptic terminals in the SNcM, SNcL, and VTA. Using TH (magenta) as a marker of DA neurons and tagging the appropriate vesicular transporters for each neurotransmitter, VAChT (green) for cholinergic vesicles, VGAT (red) for GABAergic vesicles, and VGLUT 2 (cyan) for Glutamatergic vesicles, the distribution of each synapse type along DA dendrites in the midbrain were observed. At low magnifications (Fig. 13, Fig. 15), DA neurons stained brightly with relatively large cell bodies and long processes than span up to tens of microns before disappearing into the dense network of intertwining dendrites. In sagittal sections, long DA projections extended anteriorly to their target regions. These include either the striatum, mPFC, or NAc depending if the origins of their cell bodies stemmed from the SNc or VTA, respectively. VGLUT2 labeling was present in the SNc and VTA, which was to be expected seeing as previous studies have shown that this vesicular transporter localizes predominantly in the midbrain (Eriksen et al., 2020). Despite this, individual puncta could not be resolved at low magnifications. In coronal sections, landmarks used to compartmentalize DA neurons to their separate regions were present. The medial lemniscus severs the VTA from the SNc, whereas the third cranial nerve separates the SNcM from the SNcL. VGAT staining was diffuse and extended past the SNc into the SNr. This comes as no surprise, as the SNr receives inhibitory input from the striatum and is a main GABA output center for the basal ganglia. VAChT puncta are mostly non-existent at these higher magnifications, being drowned out by the stronger TH and VGAT signals.

At high magnification (Fig. 14, Fig. 16, Fig. 17. Fig. 26 in appendix), individual DA neuron cell bodies and dendrites can be seen with more pronounced VGLUT2, VAChT, and VGAT puncta abutting their processes. DA neuron cell bodies measure roughly 10 – 15 µm in diameter with nuclei ~5 µm in size and branching dendrites projecting broadly through the section. Similarly to at low magnification VGLUT2 and VGAT staining is diffuse, however puncta can now be seen directly opposing DA dendrites. VAChT puncta can also be located in clusters, however appear much less frequently than VGLUT2 and VGAT. There is also a small population of mixed VAChT and VGAT terminals which appear in all three brain areas although

much less frequently than pure VGAT or VAChT terminals, a trend that does not continue when moving to EM analysis.

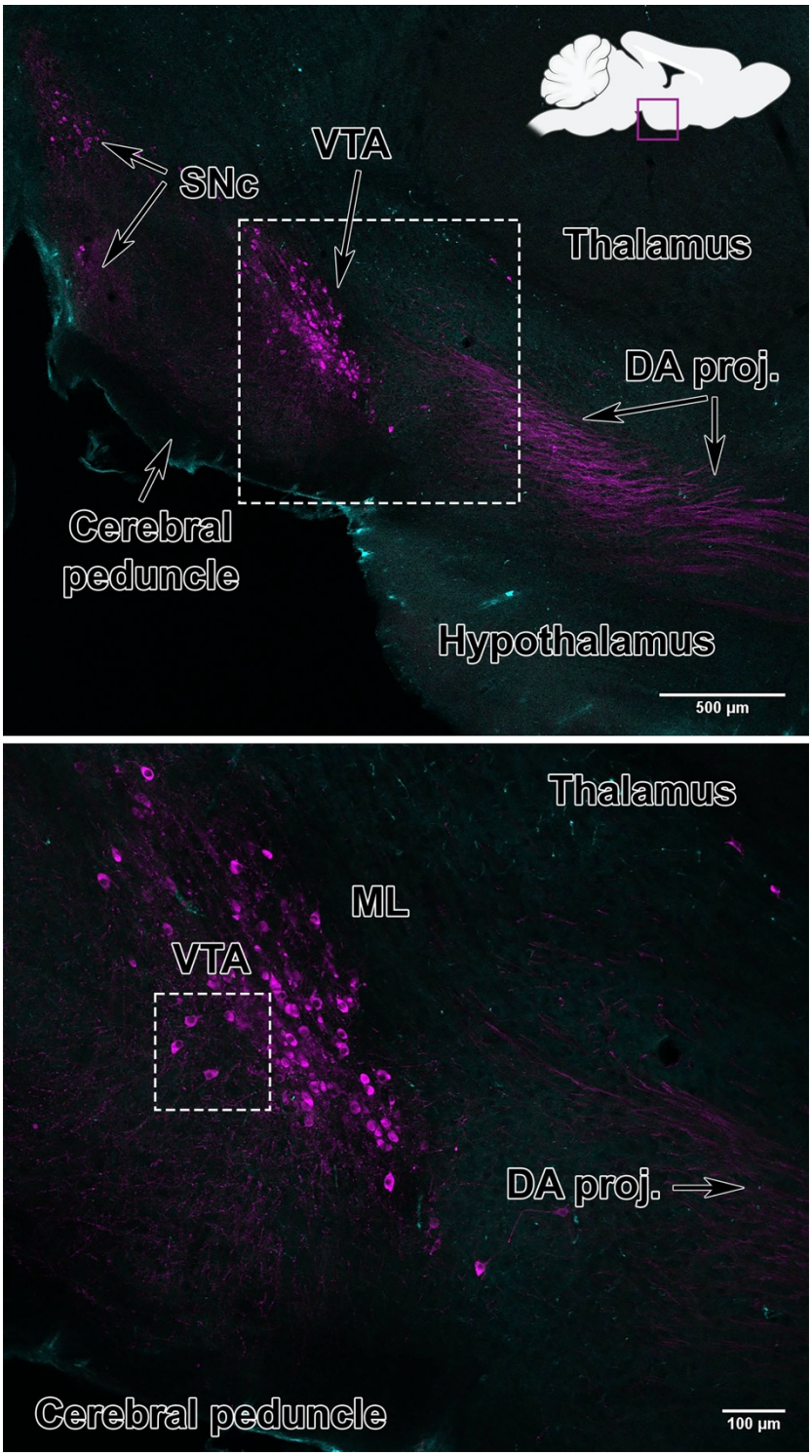

Figure 13. Low magnification confocal images of TH (magenta) and VGLUT2 (cyan) labeling in a sagittal section of the mouse midbrain. DA neurons (magenta) are clustered into the SNc and VTA which have deep branching dendrites and send long range projections anteriorly. VGLUT2 stains ubiquitously throughout the section. VTA, ventral tegmental area; SNc, medial substantia nigra pars compacta.

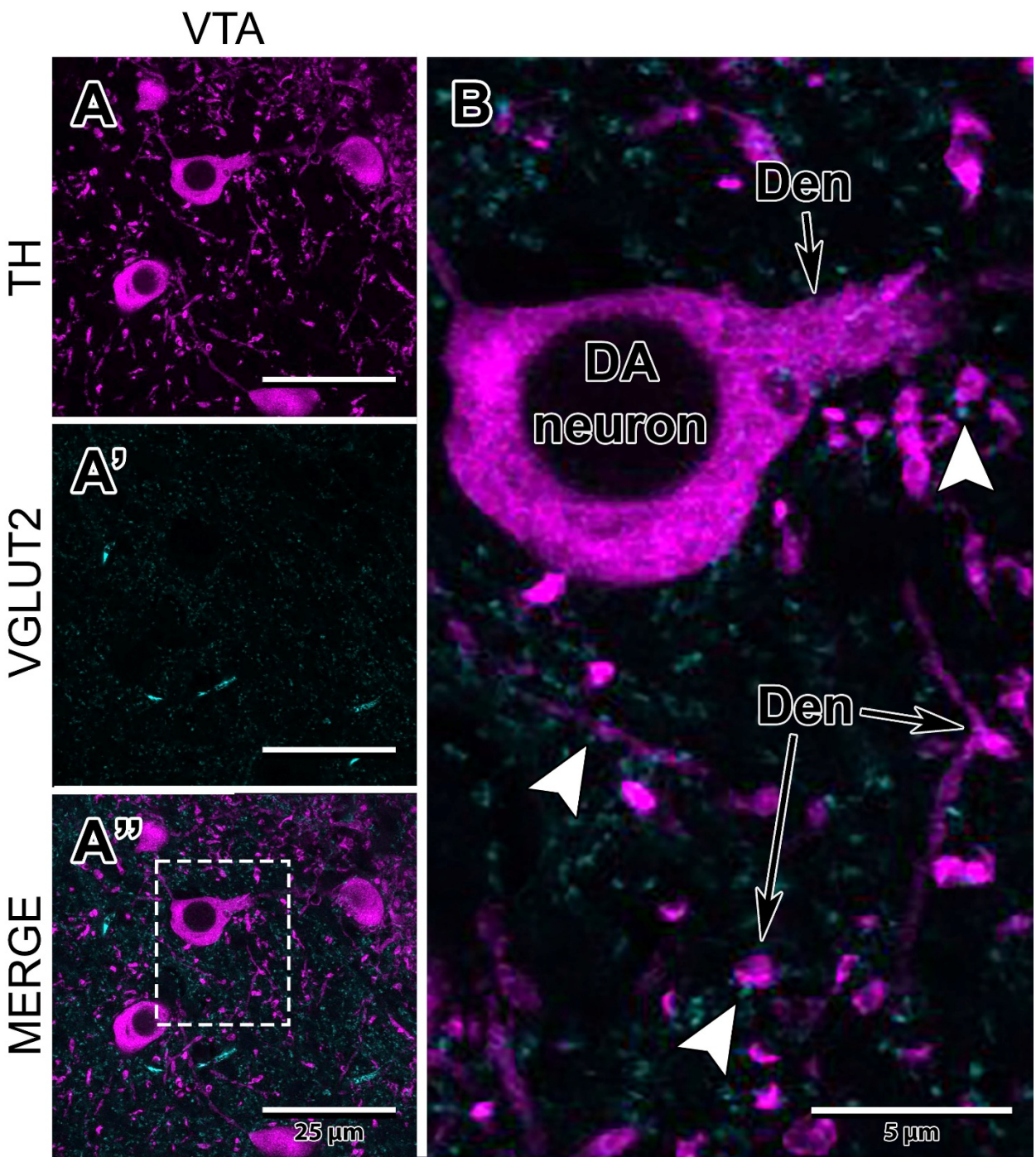

Figure 14. High magnification confocal images of TH (magenta) and VGLUT2 (cyan) labeling in the VTA. VGLUT2 puncta (white arrowheads) are present are along DA dendrites (Den). Each image is a projection image of a 5 image z-stack (0.52 µm step size) to create an image with a depth of 2.5 µm.

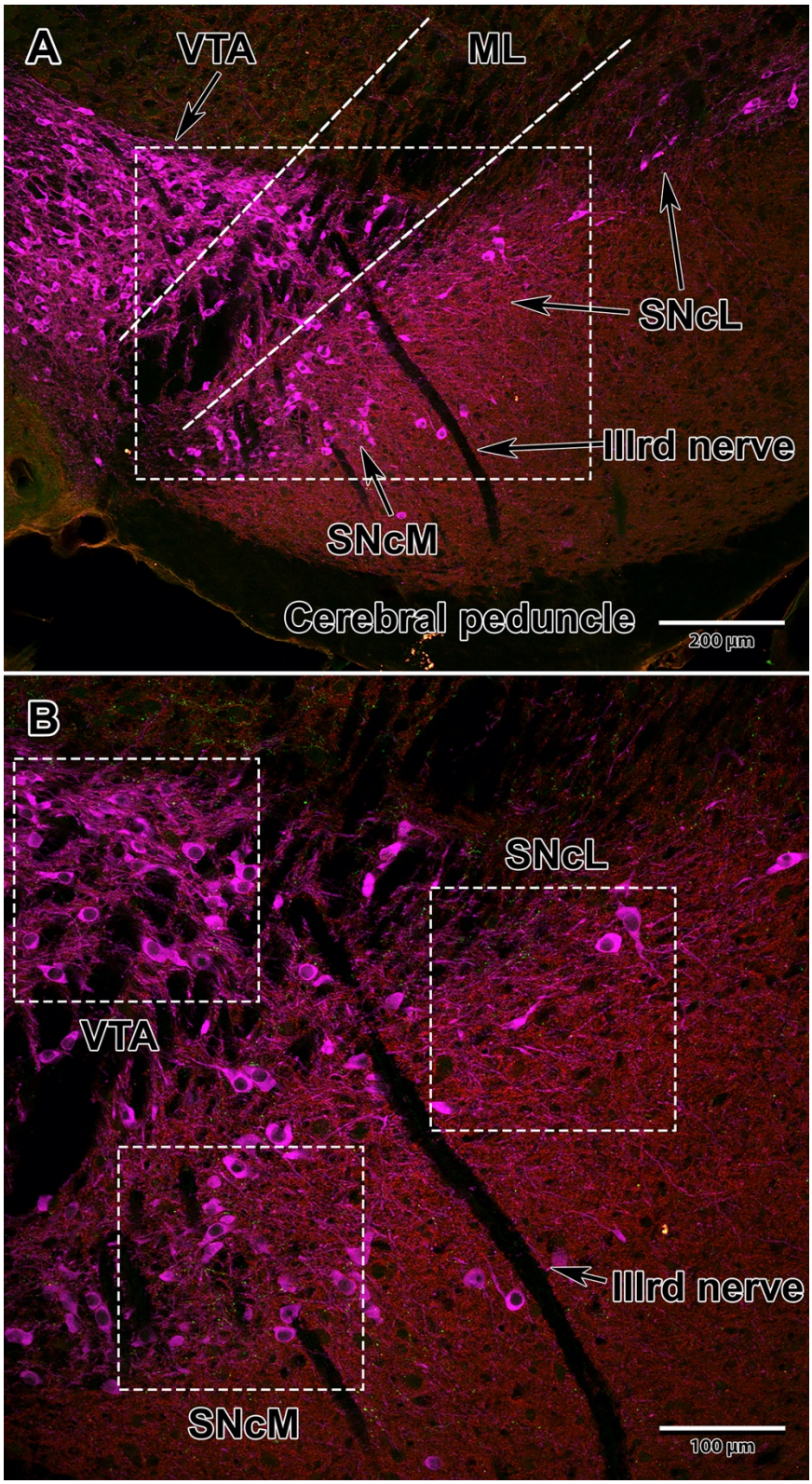

Figure 15. Confocal images of TH, VGAT, and VAChT labeling in a coronal section of the midbrain. DA neurons (magenta) can be seen clustered in three separate regions: the VTA, SNcM, and SNcL (divided by the IIIrd nerve. VGAT (red) stains diffusely while VAChT (green) puncta are scattered more discretely. VTA, ventral tegmental area; ML, medial lemniscus; SNcM, medial substantia nigra pars compacta; SNcL, lateral substantia nigra pars compacta.

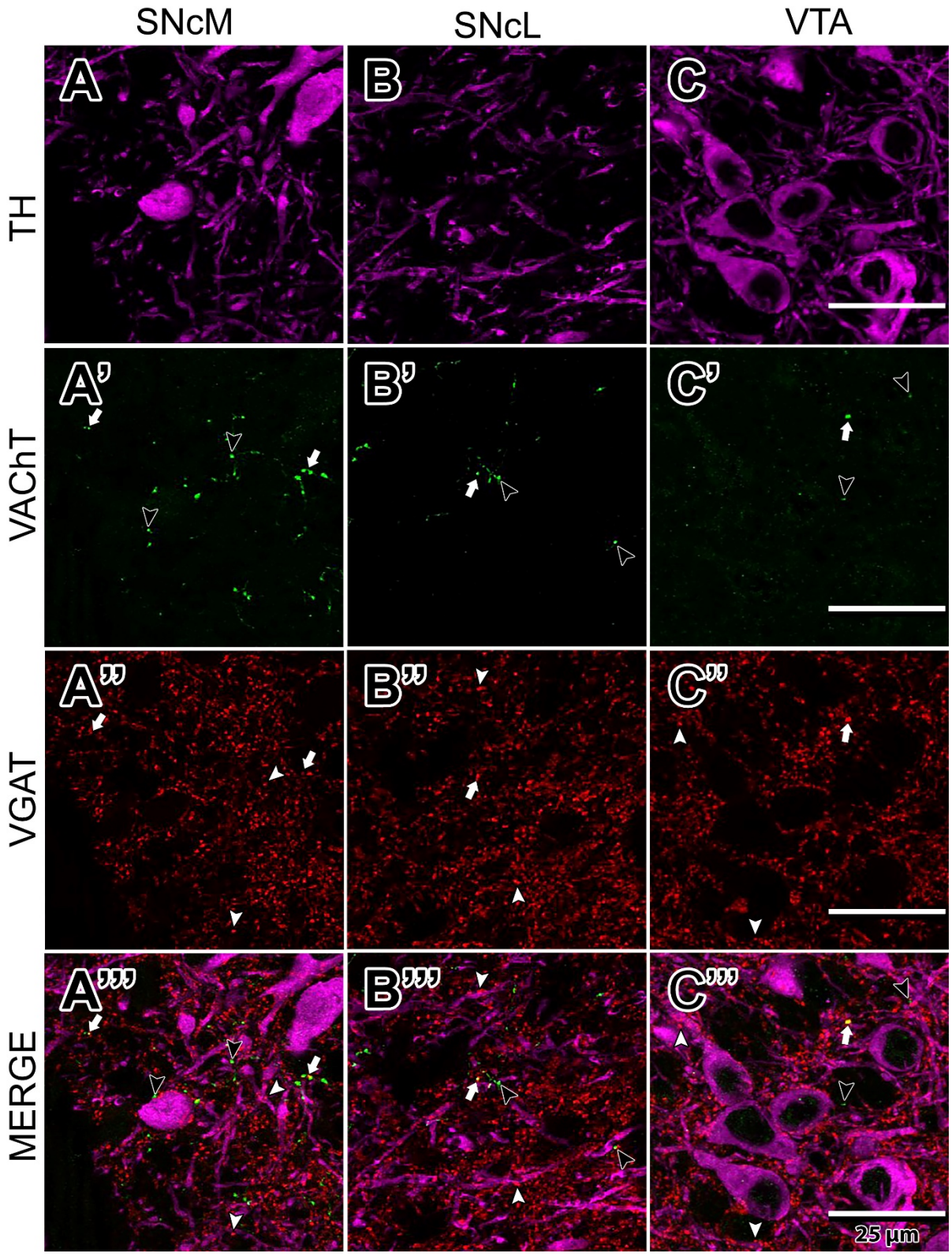

Figure 16. High magnification confocal views of VAChT (green) and VGAT (red) labeling in the SNcM, SNcL and VTA. TH+ DA neurons are magenta. Mixed terminals (white arrows) are seen in all three regions. Each image is a projection image of a 5 image z-stack (0.52 µm step size) to create an image with a depth of 2.5 µm.

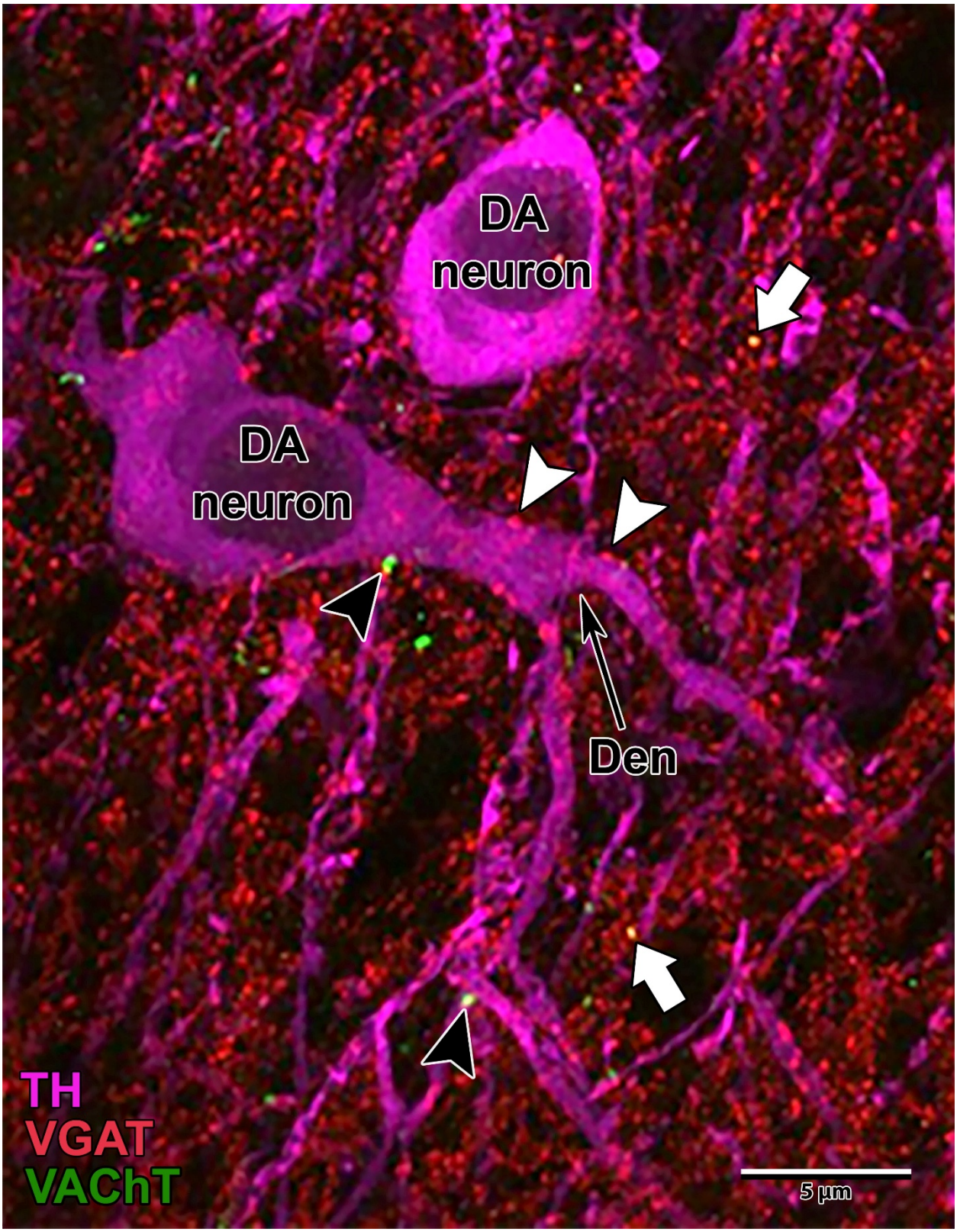

Figure 17. High magnification triple labeling of TH (magenta), VAChT (green), VGAT (red) in the SNcL. A mixture of cholinergic terminals (black arrowheads) and GABA terminals (white arrowheads) abut DA dendrites. In some cases they appear colocalized (white arrows).

3.3 Qualitative assessment of TH-DAB stained sections

DAB immunohistological staining for TH was implemented as a way to visualize DA cell bodies and dendrites at the light microscope level (Fig. 18). Despite light microscopy not having the resolution to visualise synapses, some subtle differences in DA neuron distribution between regions which mirrored immunofluorescent staining patterns seen on the confocal was observed. First, the VTA often had very similar levels of TH staining, if not more, than the SNc. In certain sections, it looked as though dendrites in the most medial aspects of the VTA crossed the midline to connect the region on the contralateral side. Additionally, stray DA neurons could sometimes be found climbing up the midline towards the aqueduct. There were many dark staining cell bodies in the VTA, however they did not appear to be as densely packed as ones located in the medial SNc. Within the SNc itself, the medial portion had many, very compact and dark staining cell bodies with diffuse dendrites that traveled deep into the SNr. There were also instances where it looked as though the VTA and SNc were connected by DA neurons crossing the medial lemniscus, which could be the case as some researchers believe that the PBP of the VTA is an extension of the anterior SNc (Palmiter, 2018; Zaborszky & Vadasz, 2001). Across the border of the third nerve, the lateral SNc had markedly fewer dark staining cell bodies and more confined dendrites. Cell bodies and dendrites got more and more scarce moving laterally through the section.

Once all of the stained tissue was microdissected, processed, and cured into resin blocks, it was necessary to ensure that the section destined for EM analysis actually contained DAB positive cells and dendrites. To do this, semi thin sections were cut on the ultramicrotome and examined qualitatively at the light microscope level. If dark brown precipitate could be visualised under the microscope without toluidine blue staining, the block was trimmed into a trapezoid shape using a razor blade and ultrathin sectioning was done. At the EM level, coronal and longitudinally sectioned dendrites and cell bodies were identified by the presence of black DAB precipitate in their cytoplasm, making them easily distinguishable from the otherwise grey neuropil (Fig. 19).

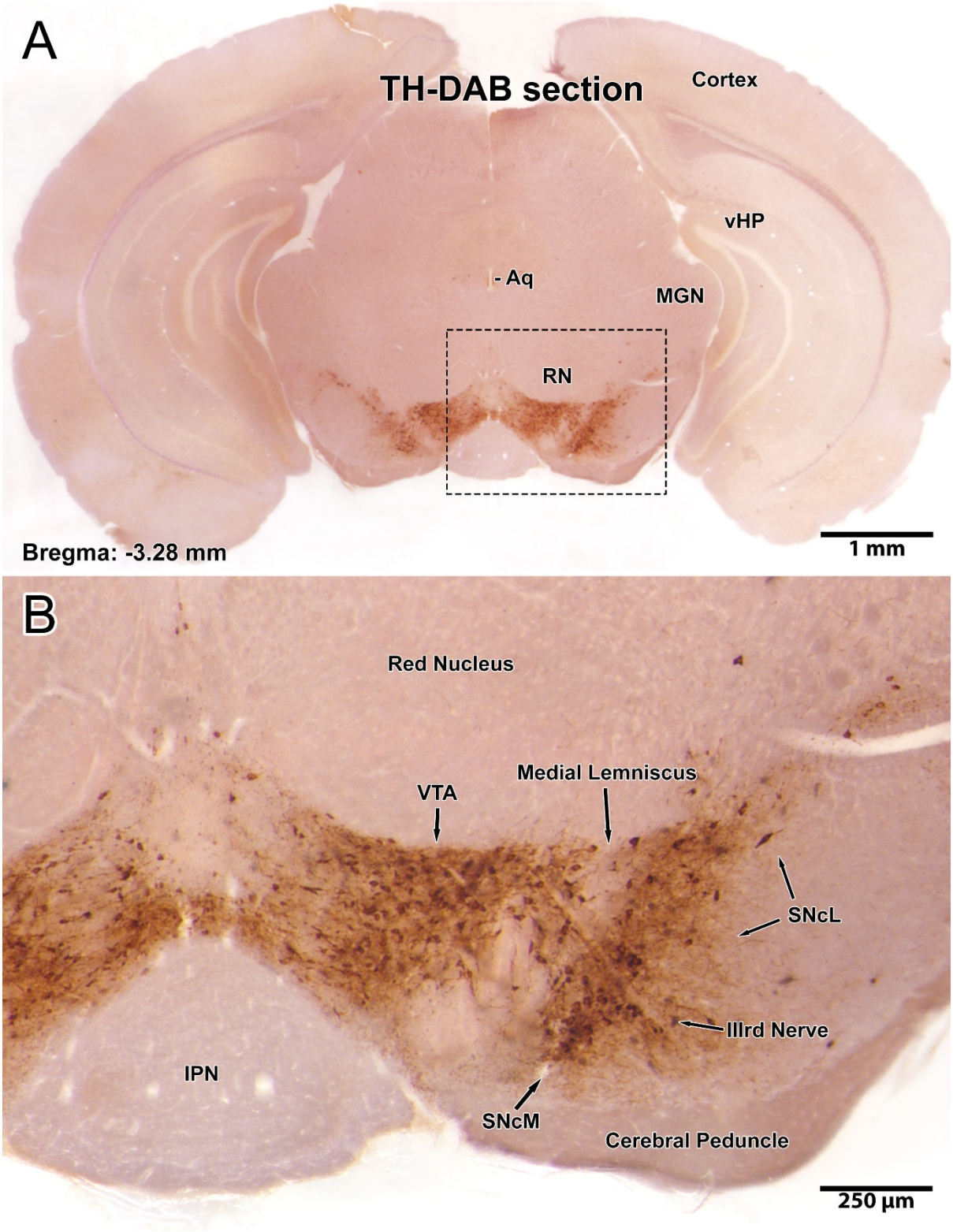

Figure 18. Low and high magnification brightfield images of TH expression in the mouse midbrain. All three regions of interest, the SNcM, SNcL, and VTA, in addition to landmarks used as guides during microdissection are present. The VTA is delineated from the SNc by the medial lemniscus, and the medial and lateral segments of the SNc are separated by cranial nerve III (oculomotor nerve). IPN, interpeduncular nucleus; vHP, ventral hippocampus; RN, red nucleus; MGN, medial geniculate nucleus; Aq, aqueduct

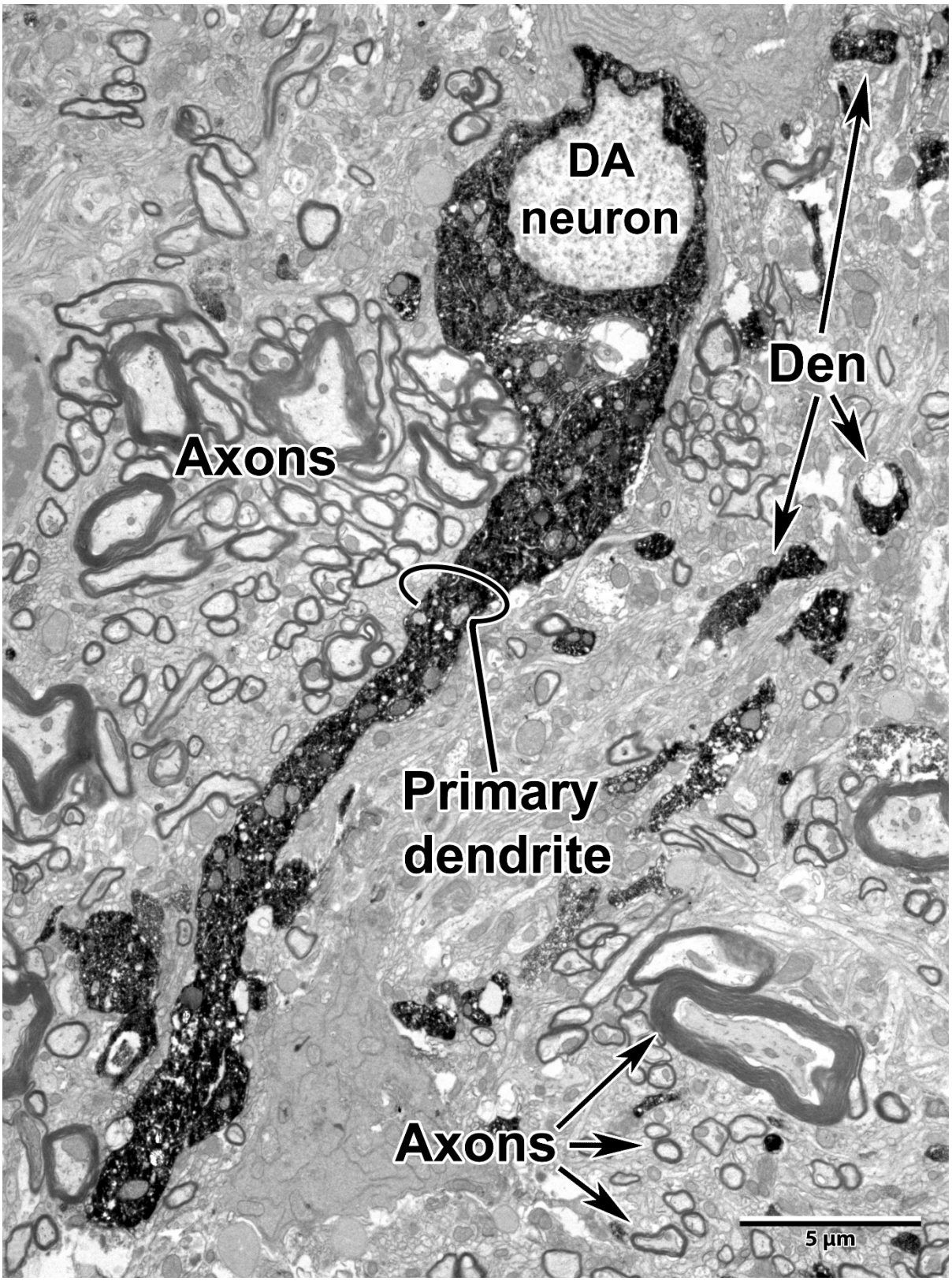

Figure 19. Immuno-EM of a TH-positive neuron labeled with DAB (dark precipitate). The signal is distributed throughout the cytoplasm and its dendrites but is not present in the nucleus. Neighbouring DA dendritic branches (Den) can be seen in the surrounding neuropil.

3.4 Heterogeneous neurotransmitter distribution between and within regions

Synapse type was determined by the size and shape of vesicles that resided in the pre-synaptic bouton opposing a TH-DAB positive dendrite. Within each region, 200 dendrites were imaged for a total of 613 dendrites and 13 290 vesicles analysed (see Table 1 for full summary). Terminals in the SNcM, SNcL, and VTA contained large round putative cholinergic vesicles of ~50 – 60 nm, small round putative glutamatergic vesicles with a diameter of ~30 – 45 nm, and ellipsoidal shaped putative GABAergic vesicles with a wide range of diameters, reaching anywhere from ~50 – 80 nm on their longest axis and ~20 -30 nm in width (Fig. 20). As analysis took place, a synaptic input kept appearing that had a mix of oval and round vesicles that did not align with the approximate 50 nm size of cholinergic vesicles. Instead, a mix of oval, putatively GABA vesicles and small, round vesicles with an average diameter of ~30 – 45 nm was observed throughout all three regions. Due to the shape and size of these vesicles being consistent with the glutamatergic vesicle criteria and there being reports of co-transmitted Glut and GABA from brain regions projecting to midbrain DA neurons, these synapses were categorized as a mixed Glut/GABA terminal.

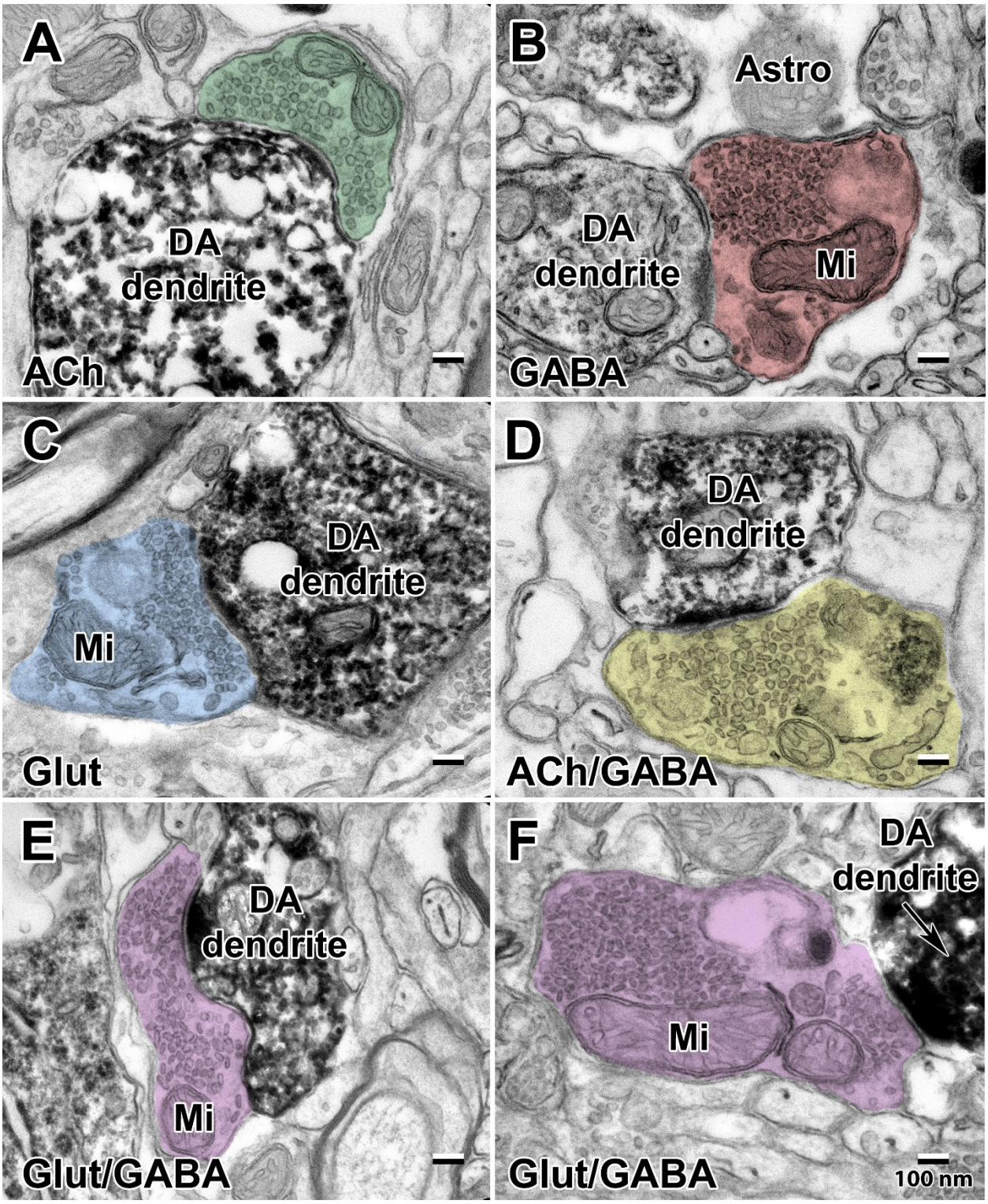

Figure 20. Examples of each terminal type opposing TH-DAB dendrites. Terminal type was determined by the vesicles found within them. ACh vesicles (green) are round with a diameter of ~50 – 60 nm. Similarly, Glut vesicles (cyan) are round and are smaller, ~30 – 40 nm in diameter. GABAergic vesicles (red) come in a variety of sizes but are usually ~50 – 80 nm on their longest axis. There are also terminals which contain a mixture of ACh and GABA vesicles (yellow), and Glut and GABA vesicles (purple).

First, it was determined how often each NT group was present within a region and if there were any significant differences in the frequency of their appearance (Fig. 21) In the SNcM, cholinergic inputs accounted for approximately ~19%, GABAergic ~1%, Glutamatergic ~30%, ACh/GABA ~33% and Glut/GABA ~17% of terminals analysed. Within the region, only Glutamatergic (p=0.002) and ACh/GABA (p=0.001) terminals significantly outnumbered pure GABA terminals. The distribution of synapses is similar in the neighbouring SNcL. Cholinergic terminals are responsible for approximately ~20%, GABAergic ~1%, Glutamatergic ~30%, ACh/GABA ~32%, and Glut/GABA ~17% of observed terminals. In the case of the SNcL, all neurotransmitter groups were present significantly more often than pure GABAergic (ACh p=0.009; Glut p=0.000; Ach/GABA p=0.000; Glut/GABA p=0.029). In the VTA, pure Glutamatergic terminals dominate the synaptic landscape, accounting for ~49% of terminals in the region. The second most prevalent neurotransmitter type in this region is cholinergic with ~23%, followed by ACh/GABA at ~17%, Glut/GABA at ~11%, and finally pure GABAergic which was not seen at all throughout this region. It is no surprise then that the frequency of observed GABAergic terminals is significantly lower from all other terminal types (ACh p=0.000; Glut p=0.000; ACh/GABA p=0.014), whereas instance of pure Glutamatergic (p=0.000) is significantly higher than all other synapse types in the VTA.

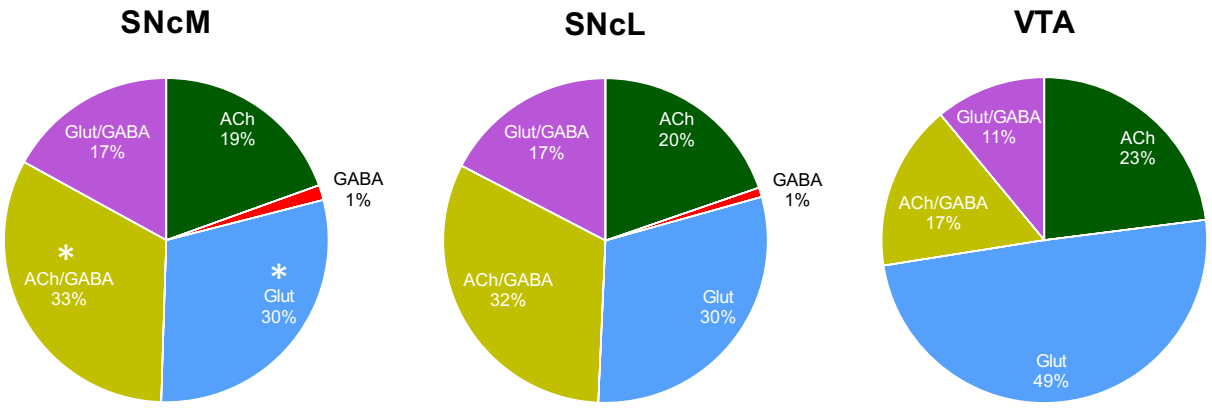

Figure 21. Percentage of each neurotransmitter groups within the SNcM, SNcL, and VTA. Each pie chart represents one region divided how often each NT group was present. n = 5 mice, n = 200 dendrites in the SNcM, n = 213 dendrites in the SNcL, and n = 200 dendrites in the VTA. Absolute values for each NT group per region are summarized in Table 1. *p < 0.05.

Next, a Kruskal-Wallis H test was used to determine if there were any differences in frequency of NT type between regions (Fig. 22), which revealed that there was only a significant difference in the number of ACh/GABA inputs (p=0.019). *Post-hoc* analysis determined that this difference existed between the VTA and lateral SNc (p=0.006), but not between the VTA and medial SNc (p=0.66), or the medial and lateral SNc (p=0.36). Despite Glut not being statistically significant between regions (p=0.051), *post hoc* analysis was conducted due to the extreme proximity to significance. Test results indicated that there is a difference in Glutamatergic transmission between the VTA and the medial SNc (p=0.18), but not between the VTA and lateral SNc (p=0.66), or the medial and lateral SNc (p=0.36).

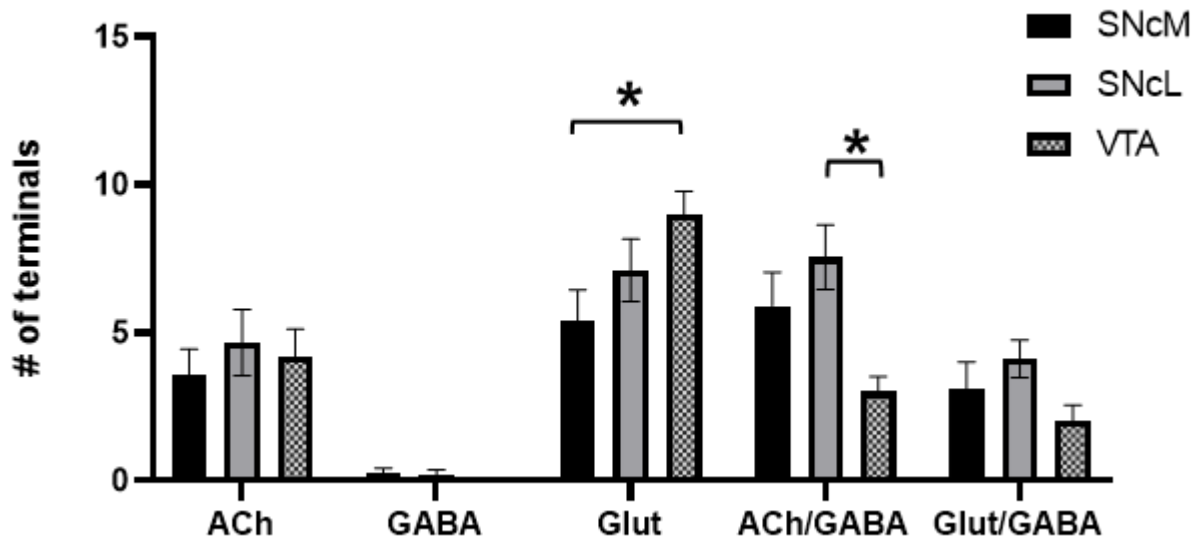

Figure 24. Differences in neurotransmitter groups between regions. Average number of times each NT group was observed in terminals between each region. The lateral SNc has a significantly higher incidence of mixed ACh/GABA terminals compared to the VTA, whereas the VTA has significantly higher number of Glut terminals compared to the medial SNc. *p < 0.05. Data are shown as mean ± SEM.

3.5 Correlation between vesicle shape and size

A correlational analysis was conducted in order to portray the relationship between vesicle size and shape for each NT group in each region. Each NT group was analyzed separately using Spearman's rank-order correlation test which revealed that there was significant negative correlation between the size and shape of vesicles for all NT groups in all regions (Table 2; Figures 23, 24, 25).

Table 2. Results from correlation tests comparing vesicle roundness and diameter length

	SNcM			SNcL			VTA		
	r	**p**	**n**	**r**	**p**	**n**	**r**	**p**	**n**
ACh	-0.3285	<0.0001	691	-0.3320	<0.0001	793	-0.3344	<0.0001	856
GABA	-0.5595	<0.0001	111	-0.7312	<0.0001	60	-	-	-
Glut	-0.3879	<0.0001	1355	-0.2373	<0.0001	1580	-0.2724	<0.0001	2208
ACh/GABA	-0.5837	<0.0001	1178	-0.5316	<0.0001	1613	-0.5746	<0.0001	816
Glut/GABA	-0.5759	<0.001	679	-0.5847	<0.0001	943	-0.6040	<0.0001	407

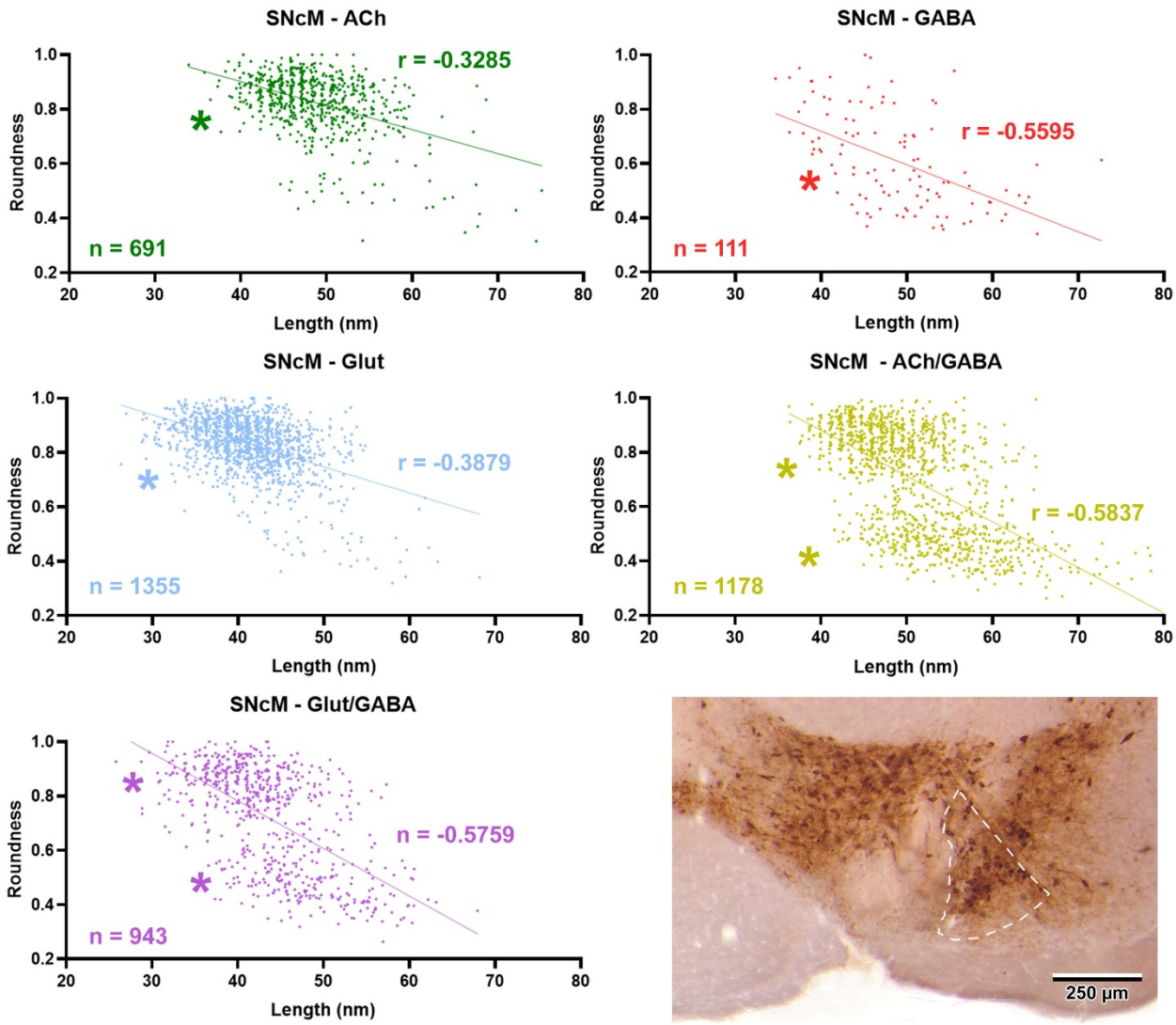

Figure 27. Correlations between vesicle size and shape of each neurotransmitter group in the SNcM. Significant negative correlations were observed in all neurotransmitter groups. Note the clustering of two groups in mixed ACh/GABA (yellow asterisks) and Glut/GABA (purple asterisks) type terminals, indicating that there are two distinct populations present in the terminal. Each vesicle is one data point and the n numbers are indicated on each graph. *$p < 0.05$.

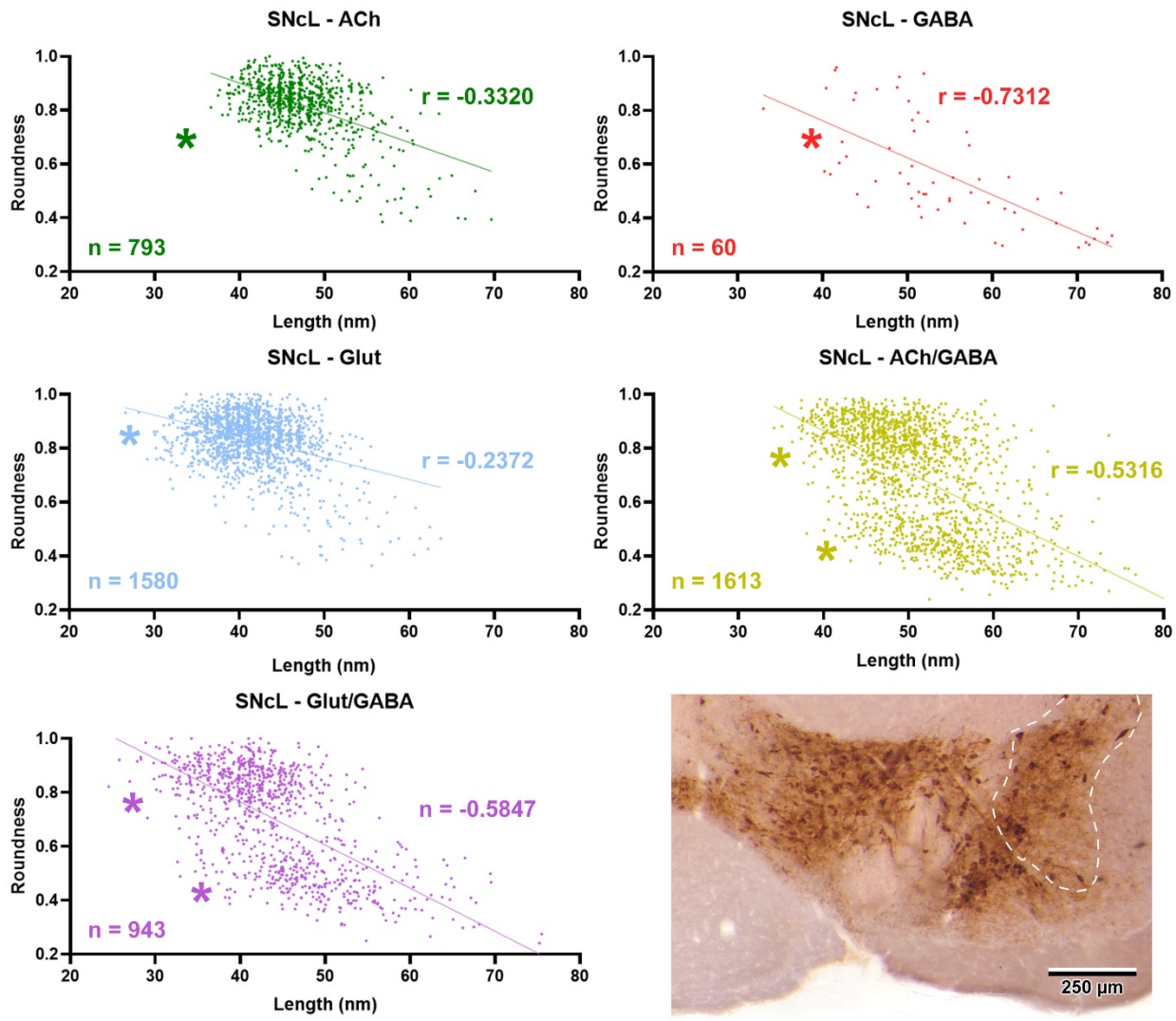

Figure 28.Correlations between size and shape of vesicles of each neurotransmitter group in the SNcL. Significant negative correlations were observed in all neurotransmitter groups. Note the clustering of two groups in mixed ACh/GABA (yellow asterisks) and Glut/GABA (purple asterisks) type terminals, indicating that there are two distinct populations present in the terminal. Each vesicle is one data point and the n numbers are indicated on each graph. *$p < 0.05$.

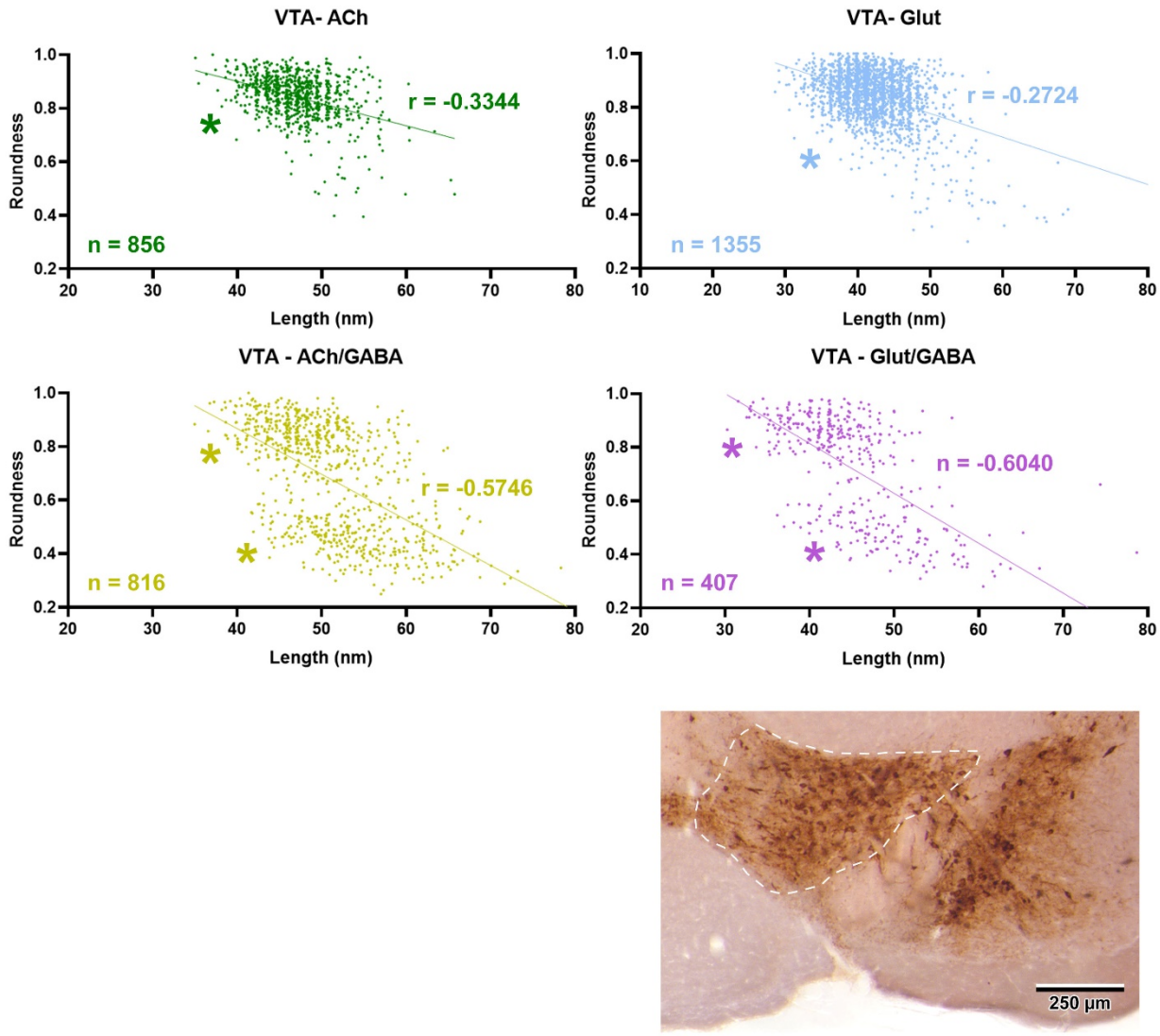

Figure 31. Correlations between size and shape of each neurotransmitter group in the VTA. Significant negative correlations were observed in all neurotransmitter groups. Note the clustering of two groups in mixed ACh/GABA (yellow asterisks) and Glut/GABA (purple asterisks) type terminals, indicating that there are two distinct populations present in the terminal. Each vesicle is one data point and the n numbers are indicated on each graph. No pure GABA terminals were seen in this region. *$p < 0.05$.

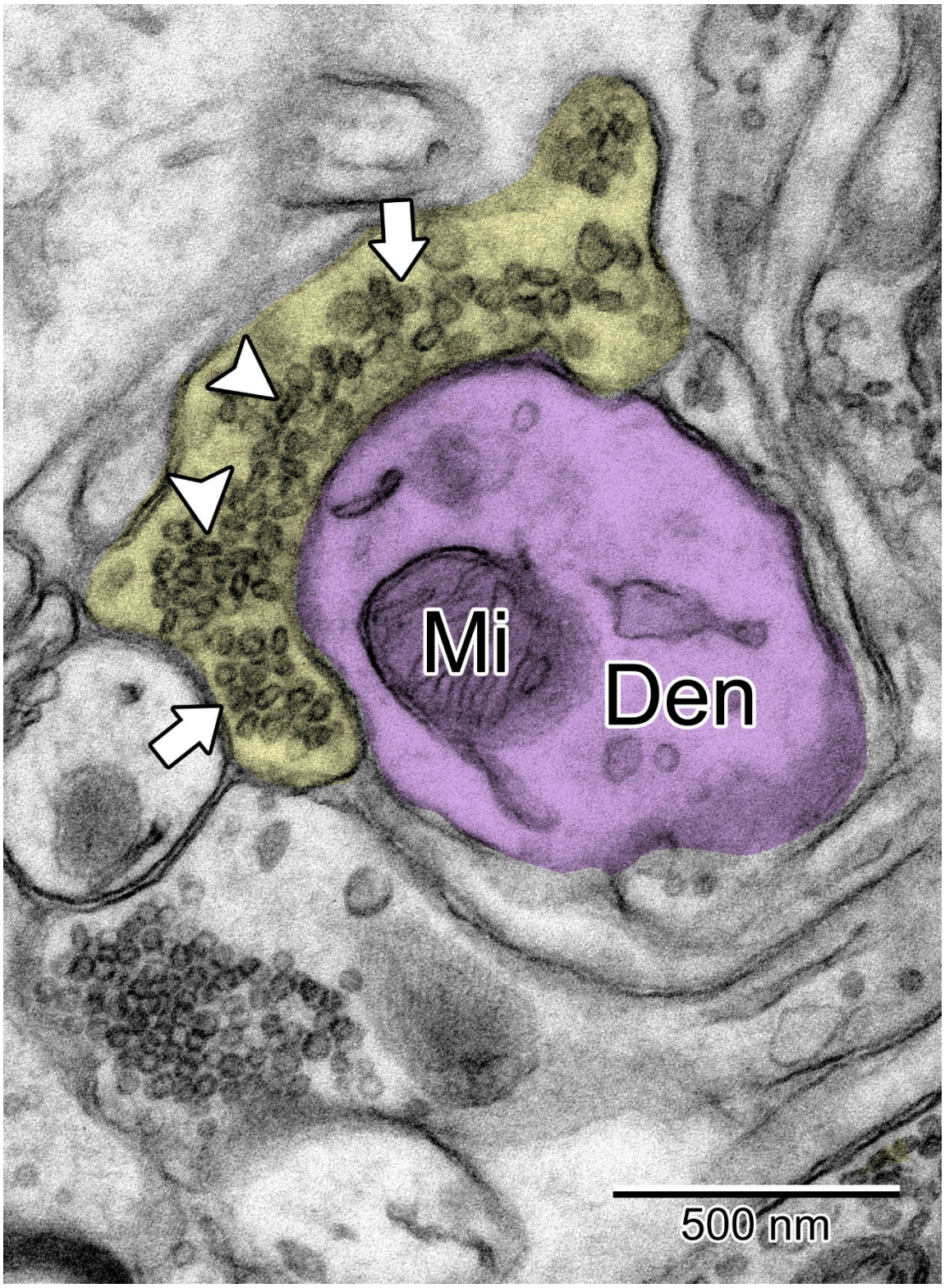

Figure 32. High magnification EM of a mixed ACh/GABA terminal (yellow) on a DA dendrite (magenta) in the SNcM. Populations of oblong vesicles (arrowheads) and large, round vesicles (arrows) are co-localized in the pre-synaptic cell, suggesting that the terminal contains a mixture of ACh and GABA.

Chapter 4 – Discussion

4.1 General discussion

At first glance, the SNc and VTA seem as though they could be easily combined into a single nucleus in the midbrain – not only are they physically close together, but they are also the two major DA output centers of the brain. However, the SNc and VTA are segmented into morphologically and functionally distinct regions and can even be divided into subregions within themselves. Despite this, it has been well documented that these brain areas receive glutamatergic, cholinergic, and GABAergic signals from a variety of outputs, as well as terminals carrying a mix of excitatory and inhibitory neurotransmitters such as ACh and GABA, and from our observations, Glut and GABA. After acknowledging that there is profound heterogeneity between both segments of the SNc and the VTA, it would then be unreasonable to speculate that the frequency of transmission of these different neurotransmitter types is consistent between each region. The present study aimed to map out the synaptic landscape of the SNcM, SNcL, and the VTA in order to better understand how DA neurons in either region are afferently regulated. With a combination of confocal and EM I categorized the frequency at which each neurotransmitter group appears in order to determine if there are any differences within and between regions. By using TH to identify DA neurons within the monochromatic neuropil, populations of glutamate, ACh, GABA, ACh/GABA, and Glut/GABA terminals were observed and documented.

First, I determined the composition of each region individually. Understanding how an area of the brain is modulated during normal, healthy functioning is an important frame of reference to have when trying to restore it from a diseased state. In the SNcM, the incidence of each neurotransmitter type was similar except for the increased frequency of appearance of ACh/GABA and pure Glut terminals compared to GABA terminals. Similarly, the SNcL had significantly fewer pure GABA terminals than all other neurotransmitter groups. The VTA saw a comparable trend wherein pure GABA terminals were completely absent from the region and was significantly lower than all neurotransmitter groups, except for Glut/GABA. Interestingly, pure Glut was the prevailing neurotransmitter in the VTA with nearly half the region's DA adjacent presynaptic terminals being composed of small, round vesicles. Next I wanted to determine if there were any differences in how often each neurotransmitter group appeared

between each region. Asking whether two brain areas receive different inputs seems redundant, seeing as it probably evident that each region would need to receive their own individual pattern of afferents due to their unique neuronal properties and output functions. The SNc and VTA are somewhat unique in that sense, as both of their most abundant neuronal population is the same and as previously mentioned, some studies suggest that the VTA and the SNc are continuations of each other (Palmiter, 2018). Despite having their morphology seem extremely similar, DA neurons in the VTA have some sort of selective resistance to PD degeneration whose mechanism we don't yet fully understand. Figuring out how these neurons differ from ones residing in the SNc can hopefully provide some insight into this phenomenon and open new doors for future PD therapeutics. Somewhat surprisingly there were no significant differences in the rate of appearance of different neurotransmitter groups between the medial and lateral SNc. This finding was unexpected seeing as there have been a number of different studies describing heterogeneity in inputs between both subregions (le Gratiet et al., 2022; Estakher et al., 2017). There were differences however between both regions of the SNc and the VTA. The SNcL has a significantly higher incidence of mixed ACh/GABA compared to the VTA, whereas the VTA has more Glutamatergic transmission than the SNcM.

We also determined that there is a negative correlation between vesicles size and shape for all neurotransmitter vesicle types, meaning that as the roundness value decreases (becomes more oval), the length of the diameter of vesicles increases. This is in line with our observations that ovoid vesicles associated with inhibitory GABAergic transduction would often appear longer in diameter on their longest axis than their round cholinergic or glutamatergic counterparts. The strongest correlations were seen in mixed neurotransmitter groups across all three regions, which makes sense seeing as there is clustering of two very different populations. As previously discussed, the reason behind the morphological differences between neurotransmitter vesicles is still up for debate, however researchers have suggested that it may be due to the change in tonicity of the tissue as a result aldehyde fixation. Future studies investigating synaptic architecture at the EM level should compare vesicular morphology in tissue fixed with a variety of aldehydes at various concentrations to observe changes in vesicle ultrastructure. This way it can be determined if it is in fact aldehydes in fixative that are the catalysts for this change, and it can be observed how vesicle size and shape changes in response to different types of fixes.

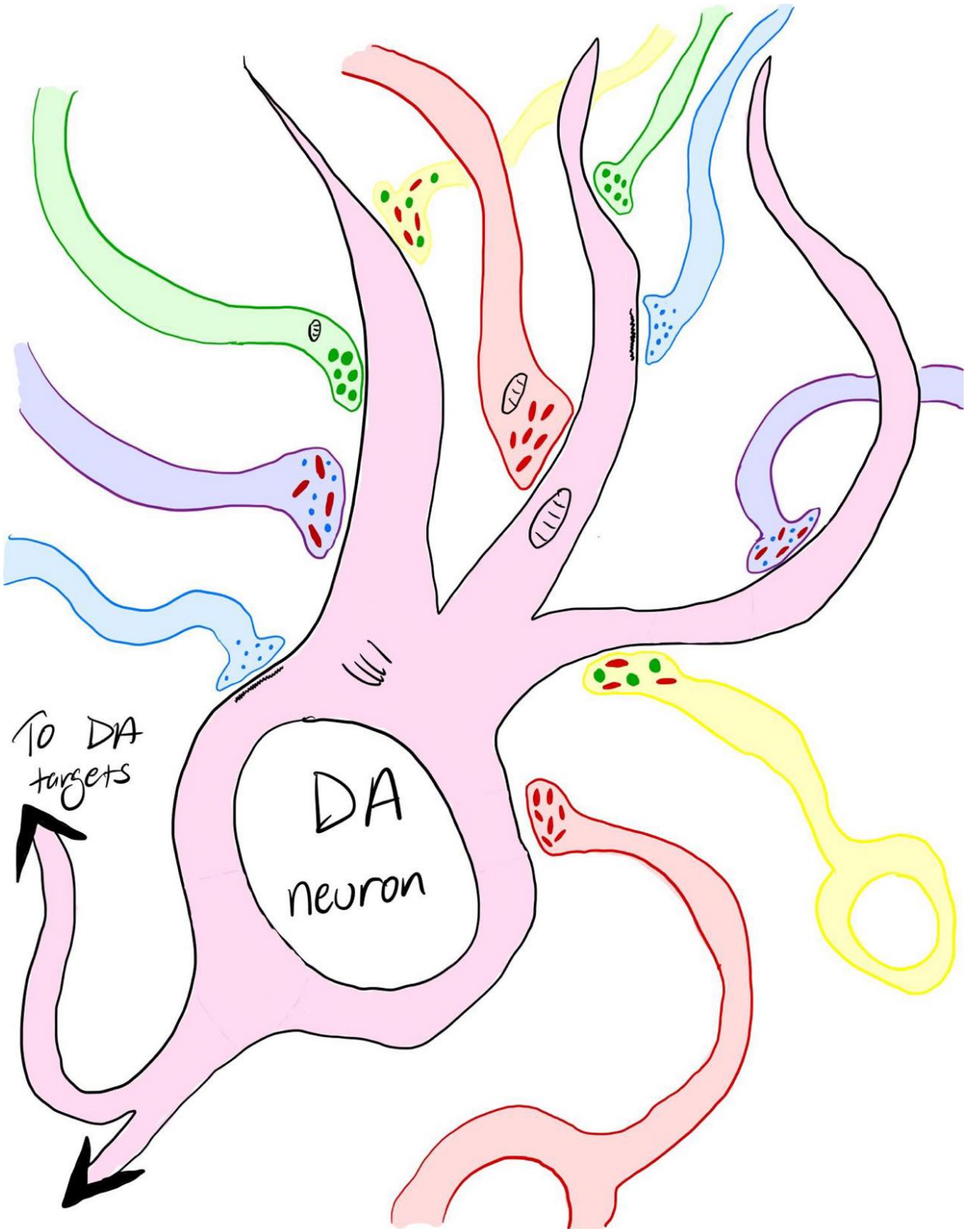

Figure 33. Visual summary. This body of work is an investigation into how DA neurons are modulated by using the morphology of vesicles in pre-synaptic terminals opposing their dendrites. We found there to be 5 distinct neurotransmitter groups, ACh (green), Glut (cyan), GABA (red), mixed ACh/GABA (yellow), and mixed Glut/GABA (purple). By documenting and categorizing the frequency of these terminals, we broaden our understanding of how these essential neurons are modulated.

4.2 The SNcL receives more co-localization than the VTA

The ability for neurons to send out excitatory and inhibitory signals from the same terminal sounds counterintuitive at best. It has been well described that for neurons to depolarize they require a certain threshold of excitatory signals from the pre-synaptic cell in order to trigger an action potential. Therefore, releasing a neurotransmitter that shunts excitation while trying to stimulate a post-synaptic neuron seems redundant. Despite this, instances of co-transmission and co-release of neurotransmitters with opposing functions have been well documented throughout the brain. We show that in the midbrain in particular there are populations of terminals that co-localize ACh and GABA, and Glut and GABA onto DA dendrites. Our results indicate that there is with seemingly little difference in the frequency of appearance of ACh/GABA or Glut/GABA terminals between either regions of the SNc, however there is significantly more ACh/GABA co-localization in the SNcL compared to the VTA.

The ability to co-transmit neurotransmitters with antagonist functions allows neurons to have more precise control over their firing patterns. This may be advantageous for fine tuning simple movements, a well-known output function of the SNc, such as tapping fingers together or opening and closing a fist, two motor tests which are used to measure the severity of bradykinesia in PD exams (Stanford Med). In contrast, the VTA is involved in more primitive functions, whose DA neurons are responsible for the feeling of reward after food, water, and sex, and positive and negative reinforcement (Morales & Margolis, 2017). The pleasurable feelings associated with completing these fundamental tasks are strongly mediated by glutamatergic transmission, which induces burst firing in tonically activated DA neurons. Perhaps these functions do not require complex firing patterns seeing as they are basic responses to the environment rather than the execution a movement in which different muscle groups are required to be activated or inhibited in a coordinate manner. Because co-transmission of excitatory and inhibitory neurotransmitters onto DA midbrain neurons is a somewhat recent discovery, further research is necessary to fully understand how they mediate DA neuronal outputs and the behavioural responses that arise as a result.

4.3 Increased glutamatergic transmission to the VTA

Glutamate is an extremely important molecule in the VTA, playing an important role in modulating the strength and spontaneity of burst firing of residing DA neurons (Paladini & Roeper, 2014). This type of firing manifests as life affirming behaviours such as feelings of reward after food, drink, and sex, and the avoidance of aversive stimuli (Alcaro et al., 2007; Barbano et al., 2020; Feltenstein et al., 2021). Glutamatergic transmission to the VTA arrives from several regions within the brain, however it has been somewhat recently discovered that the VTA has its own population of Glutamatergic neurons (~1-3% of total neurons) which have not been studied as thoroughly as the DA neurons they share the region with. Their popularity is rising amongst research groups however, as mounting evidence suggests that these Glutamatergic neurons are involved in modulating DA release by synapsing locally onto DA VTA neurons (Dobi et al., 2010). It is possible that this local synaptic input in addition to outside sources could be the reason for the increased presence of Glut in the region

The advantage of having an abundance of Glutamate transmission onto DA neurons in the VTA is not known. Glutamate is the trigger for AMPA and NMDA receptor opening, suggesting that high rates of synaptic plasticity may occur within the region. One hypothesis could be that it is advantageous for the VTA to undergo high rates of circuit remodeling seeing as DA neurons in this region are highly involved in reward learning and survival. Being able to quickly determine whether something should be sought out or avoided in a new environment, or figuring out what makes us feel good or bad, would greatly increase our likelihood of flourishing in our surroundings. In addition, greater synaptic plasticity of VTA DA neurons could help prevent repeated behaviours eventually morphing into bad-habits. Drug liking, which more often than not leads to drug addiction, arises when substances such as cocaine hijacks VTA circuits involved in feelings of reward (Mameli et al, 2009). Being able to efficiently disconnect these positive feeling from a substance or transferring the feelings of pleasure to alternative sources could greatly reduce the risk of dependency or make it easier for an individual to overcome their addiction.

Lastly, increased prevalence of Glutamate in the VTA within the region and compared to the SNcM could point to the reason as to why the VTA does not experience DA neuron loss during the progression of PD. Recent studies that have aimed to decipher the mechanism behind

the selective immunity of VTA DA neurons in PD have found that the population of DA neurons that co-transmit Glut in specific remain unscathed (Bimpisidis & Wallén-Mackenzie, 2019). It could be mere coincidence that there is significantly more Glutamatergic input onto DA neurons in the VTA than the SNc, and that DA neurons that co-transmit DA and Glut are not as likely to degenerate during PD, however further research needs to be conducted in order to determine if there is a link between the presence of Glutamatergic inputs and neuronal immunity to PD.

4.4 Limitations & Future Directions

One major limitation of this study is the reliability of using vesicle morphology as the sole determiner of neurotransmitter type. Early EM studies that pioneered this avenue of research distinguished excitatory from inhibitory neurotransmitter containing vesicles by using their morphology, specifically their shape and size, to decipher their contents. However, there is considerable variability in reported vesicle morphology across studies. Many believe that this shape conformation is the result of aldehyde fixation. The type and concentration of aldehydes used in fixation in of itself is inconsistent across different research groups, making it difficult to accurately say whether a vesicle is one hundred percent excitatory or inhibitory using their physical shape alone. Therefore, future research that delve into the neuronal wiring within these regions should utilize more robust immuno-EM techniques such as tagging vesicular transporters with varying sized gold particles alongside TH-DAB staining to confirm that specific neurotransmitters are present in the synapse.

A second limitation is the usage of 2D images taken on a TEM to describe 3D structures. Because each synapse was visualised on one section, it is hard to say whether I was observing a grazing section, only looking at the top of round vesicles therefore making their diameter appear smaller, or, looking through the middle of the synapse at a more accurate representation of the vesicle size. This would also be the case when looking at mixed vesicles, where the angle at which ellipsoid vesicles are sectioned could potentially make them seem round. This could potentially trick the observer into thinking that the terminal is mixed, where in reality it is a pure GABA terminal. One way to rectify this would be to take serial sections when cutting a block on the ultramicrotome in order to visualize structures at different levels throughout the section. Because it was imperative that an adequate number of synapses were analysed, approximately

200 per region, the timeframe needed for image acquisition, image stack rendering, and analysis for that large of a quantity of images would be beyond the scope of a master's degree.

Lastly, it would be beneficial to be more mindful of where microdissections were taken within the SNc and VTA, as each region can be split into multiple sub-regions with varying morphological and electrophysiological characteristics. As it is likely that the SNc and VTA differ in their synaptic inputs, there is a good chance that each sub-region is also unique. Future studies implementing more complex immuno-EM, correlated light and electron microscopy (CLEM), and 3D rendering techniques of entire synapses would greatly expand the breadth of knowledge that we currently have on synaptic structures and DA neurons in the midbrain.

References

Alcaro, A., Huber, R., & Panksepp, J. (2007). Behavioral Functions of the Mesolimbic Dopaminergic System: an Affective Neuroethological Perspective. *Brain Research Reviews*, *56*(2), 283. https://doi.org/10.1016/J.BRAINRESREV.2007.07.014

Al-Kuraishy, H., Hussian, N., Al-Naimi, M., Al-Gareeb, A., Al-Mamorri, F., & Al-Buhadily, A. (2021). The Potential Role of Pancreatic γ-Aminobutyric Acid (GABA) in Diabetes Mellitus: A Critical Reappraisal. *International Journal of Preventive Medicine*, *12*(1). https://doi.org/10.4103/IJPVM.IJPVM_278_19

Amilhon, B., Lepicard, È., Renoir, T., Mongeau, R., Popa, D., Poirel, O., Miot, S., Gras, C., Gardier, A. M., Gallego, J., Hamon, M., Lanfumey, L., Gasnier, B., Giros, B., & El Mestikawy, S. (2010). VGLUT3 (Vesicular Glutamate Transporter Type 3) Contribution to the Regulation of Serotonergic Transmission and Anxiety. *The Journal of Neuroscience*, *30*(6), 2198. https://doi.org/10.1523/JNEUROSCI.5196-09.2010

Asada, H., Kawamura, Y., Maruyama, K., Kume, H., Ding, R. G., Kanbara, N., Kuzume, H., Sanbo, M., Yagi, T., & Obata, K. (1997). Cleft palate and decreased brain γ-aminobutyric acid in mice lacking the 67-kDa isoform of glutamic acid decarboxylase. *Proceedings of the National Academy of Sciences of the United States of America*, *94*(12), 6496. https://doi.org/10.1073/PNAS.94.12.6496

Aubrey, K. R., Rossi, F. M., Ruivo, R., Alboni, S., Bellenchi, G. C., Le Goff, A., Gasnier, B., & Supplisson, S. (2007). The Transporters GlyT2 and VIAAT Cooperate to Determine the Vesicular Glycinergic Phenotype. *The Journal of Neuroscience*, *27*(23), 6273. https://doi.org/10.1523/JNEUROSCI.1024-07.2007

Avoli, M., & Krnjević, K. (2015). The Long and Winding Road to Gamma-Amino-Butyric Acid as Neurotransmitter. *Can J Neurol Sci*, *43*, 219–226. https://doi.org/10.1017/cjn.2015.333

Baik, J. H. (2013). Dopamine signaling in reward-related behaviors. *Frontiers in Neural Circuits*, *7*(OCT), 152. https://doi.org/10.3389/FNCIR.2013.00152/BIBTEX

Baik, J. H. (2020). Stress and the dopaminergic reward system. *Experimental & Molecular Medicine 2020 52:12*, *52*(12), 1879–1890. https://doi.org/10.1038/s12276-020-00532-4

Barbano, M. F., Wang, H. L., Zhang, S., Miranda-Barrientos, J., Estrin, D. J., Figueroa-González, A., Liu, B., Barker, D. J., & Morales, M. (2020). VTA glutamatergic neurons mediate innate defensive behaviors. *Neuron*, *107*(2), 368. https://doi.org/10.1016/J.NEURON.2020.04.024

Bennett, M. R. (1994). The concept of neurotransmitter release. *Advances in Second Messenger and Phosphoprotein Research*, *29*(C), 1–29. https://doi.org/10.1016/S1040-7952(06)80004-2

Bimpisidis, Z., & Wallén-Mackenzie, Å. (2019). Neurocircuitry of Reward and Addiction: Potential Impact of Dopamine–Glutamate Co-release as Future Target in Substance Use Disorder. *Journal of Clinical Medicine*, *8*(11). https://doi.org/10.3390/JCM8111887

Björklund, A., & Dunnett, S. B. (2007). Dopamine neuron systems in the brain: an update. *Trends in Neurosciences*, *30*(5), 194–202. https://doi.org/10.1016/J.TINS.2007.03.006

Bodian, D. (1966). Electron microscopy: two major synaptic types on spinal motoneurons. *Science (New York, N.Y.)*, *151*(3714), 1093–1094. https://doi.org/10.1126/SCIENCE.151.3714.1093

Bodian, D. (1970). AN ELECTRON MICROSCOPIC CHARACTERIZATION OF CLASSES OF SYNAPTIC VESICLES BY MEANS OF CONTROLLED ALDEHYDE FIXATION. *The Journal of Cell Biology*, *44*(1), 115. https://doi.org/10.1083/JCB.44.1.115

Bohnen, N. I., & Albin, R. L. (2009). Cholinergic denervation occurs early in Parkinson disease. *Neurology*, *73*(4), 256–257. https://doi.org/10.1212/WNL.0B013E3181B0BD3D

Bolam, J. P., & Smith, Y. (1990). The GABA and substance P input to dopaminergic neurones in the substantia nigra of the rat. *Brain Research*, *529*(1–2), 57–78. https://doi.org/10.1016/0006-8993(90)90811-O

Bolneo, E., Chau, P. Y. S., Noakes, P. G., & Bellingham, M. C. (2022). Investigating the Role of GABA in Neural Development and Disease Using Mice Lacking GAD67 or VGAT Genes. *International Journal of Molecular Sciences*, *23*(14). https://doi.org/10.3390/IJMS23147965

Bourdy, R., & Barrot, M. (2012). A new control center for dopaminergic systems: pulling the VTA by the tail. *Trends in Neurosciences*, *35*(11), 681–690. https://doi.org/10.1016/J.TINS.2012.06.007

Bravo, D., & Parsons, S. M. (2002). Microscopic kinetics and structure–function analysis in the vesicular acetylcholine transporter. *Neurochemistry International*, *41*(5), 285–289. https://doi.org/10.1016/S0197-0186(02)00058-X

Bronstein, J. M., Tagliati, M., Alterman, R. L., Lozano, A. M., Volkmann, J., Stefani, A., Horak, F. B., Okun, M. S., Foote, K. D., Krack, P., Pahwa, R., Henderson, J. M., Hariz, M. I., Bakay, R. A., Rezai, A., Marks, W. J., Moro, E., Vitek, J. L., Weaver, F. M., … DeLong, M. R. (2011). Deep Brain Stimulation for Parkinson Disease: An Expert Consensus and Review of Key Issues. *Archives of Neurology*, *68*(2), 165–165. https://doi.org/10.1001/ARCHNEUROL.2010.260

Buck, S. A., Erickson-Oberg, M. Q., Bhatte, S. H., McKellar, C. D., Ramanathan, V. P., Rubin, S. A., & Freyberg, Z. (2022). Roles of VGLUT2 and Dopamine/Glutamate Co-Transmission in Selective Vulnerability to Dopamine Neurodegeneration. *ACS Chemical Neuroscience*, *13*(2), 187. https://doi.org/10.1021/ACSCHEMNEURO.1C00741

Buddhala, C., Hsu, C. C., & Wu, J. Y. (2009). A novel mechanism for GABA synthesis and packaging into synaptic vesicles. *Neurochemistry International*, *55*(1–3), 9–12. https://doi.org/10.1016/J.NEUINT.2009.01.020

Burger, P. M., Hell, J., Mehl, E., Krasel, C., Lottspeich, F., & Jahn, R. (1991). GABA and glycine in synaptic vesicles: storage and transport characteristics. *Neuron*, *7*(2), 287–293. https://doi.org/10.1016/0896-6273(91)90267-4

Cabrera, L. Y., Goudreau, J., & Sidiropoulos, C. (2018). Critical appraisal of the recent US FDA approval for earlier DBS intervention. *Neurology*, *91*(3), 133–136. https://doi.org/10.1212/WNL.0000000000005829

Calabresi, P., Picconi, B., Tozzi, A., & Di Filippo, M. (2007). Dopamine-mediated regulation of corticostriatal synaptic plasticity. *Trends in Neurosciences*, *30*(5), 211–219. https://doi.org/10.1016/J.TINS.2007.03.001

Castro, B. M. de, Jaeger, X. De, Martins-Silva, C., Lima, R. D. F., Amaral, E., Menezes, C., Lima, P., Neves, C. M. L., Pires, R. G., Gould, T. W., Welch, I., Kushmerick, C., Guatimosim, C., Izquierdo, I., Cammarota, M., Rylett, R. J., Gomez, M. V., Caron, M. G., Oppenheim, R. W., … Prado, V. F. (2009). The Vesicular Acetylcholine Transporter Is Required for Neuromuscular Development and Function. *Molecular and Cellular Biology*, *29*(19), 5238. https://doi.org/10.1128/MCB.00245-09

Chang, H. T., Kita, H., & Kitai, S. T. (1984). The ultrastructural morphology of the subthalamic-nigral axon terminals intracellularly labeled with horseradish peroxidase. *Brain Research*, *299*(1), 182–185. https://doi.org/10.1016/0006-8993(84)90805-9

Chapman, E. R. (2002). Synaptotagmin: A Ca2+ sensor that triggers exocytosis? *Nature Reviews Molecular Cell Biology 2002 3:7*, *3*(7), 498–508. https://doi.org/10.1038/nrm855

Chinta, S. J., & Andersen, J. K. (2005). Dopaminergic neurons. *The International Journal of Biochemistry & Cell Biology*, *37*(5), 942–946. https://doi.org/10.1016/J.BIOCEL.2004.09.009

Dautan, D., Souza, A. S., Huerta-Ocampo, I., Valencia, M., Assous, M., Witten, I. B., Deisseroth, K., Tepper, J. M., Bolam, J. P., Gerdjikov, T. V., & Mena-Segovia, J. (2016). Segregated cholinergic transmission modulates dopamine neurons integrated in distinct functional circuits. *Nature Neuroscience 2016 19:8*, *19*(8), 1025–1033. https://doi.org/10.1038/nn.4335

De Belleroche, J. S., & Bradford, H. F. (1977). ON THE SITE OF ORIGIN OF TRANSMITTER AMINO ACIDS RELEASED BY DEPOLARIZATION OF NERVE TERMINALS IN VITRO. *Journal of Neurochemistry*, *29*(2), 335–343. https://doi.org/10.1111/J.1471-4159.1977.TB09627.X

de Jong, P. J., Lakke, J. P., & Teelken, A. W. (1984). CSF GABA levels in Parkinson's disease. *Advances in Neurology*, *40*, 427–430. https://europepmc.org/article/med/6695622

Deniau, J. M., Mailly, P., Maurice, N., & Charpier, S. (2007). The pars reticulata of the substantia nigra: a window to basal ganglia output. *Progress in Brain Research*, *160*, 151–172. https://doi.org/10.1016/S0079-6123(06)60009-5

Dong, X. X., Wang, Y., & Qin, Z. H. (2009). Molecular mechanisms of excitotoxicity and their relevance to pathogenesis of neurodegenerative diseases. *Acta Pharmacologica Sinica 2009 30:4*, *30*(4), 379–387. https://doi.org/10.1038/aps.2009.24

Eriksen, J., Li, F., & Edwards, R. H. (2020). The mechanism and regulation of vesicular glutamate transport: Coordination with the synaptic vesicle cycle. *Biochimica et Biophysica Acta (BBA) - Biomembranes*, *1862*(12), 183259. https://doi.org/10.1016/J.BBAMEM.2020.183259

Estakhr, J., Abazari, D., Frisby, K., McIntosh, J. M., & Nashmi, R. (2017). Differential Control of Dopaminergic Excitability and Locomotion by Cholinergic Inputs in Mouse Substantia Nigra. *Current Biology*, *27*(13), 1900-1914.e4. https://doi.org/10.1016/j.cub.2017.05.084

Feltenstein, M. W., See, R. E., & Fuchs, R. A. (2021). Neural Substrates and Circuits of Drug Addiction. *Cold Spring Harbor Perspectives in Medicine*, *11*(4). https://doi.org/10.1101/CSHPERSPECT.A039628

Fischer, K. D., Knackstedt, L. A., & Rosenberg, P. A. (2021). Glutamate homeostasis and dopamine signaling: implications for psychostimulant addiction behavior. *Neurochemistry International*, *144*, 104896. https://doi.org/10.1016/J.NEUINT.2020.104896

Florey, E., & Mclennan, H. (n.d.). THE RELEASE OF AN INHIBITORY SUBSTANCE FROM MAMMALIAN BRAIN, AND ITS EFFECT ON PERIPHERAL SYNAPTIC TRANSMISSION. *J. Physiol. (I955)*, *29*, 384–392.

Fu, Y. H., Paxinos, G., Watson, C., & Halliday, G. M. (2016). The substantia nigra and ventral tegmental dopaminergic neurons from development to degeneration. *Journal of Chemical Neuroanatomy*, *76*, 98–107. https://doi.org/10.1016/J.JCHEMNEU.2016.02.001

Fu, Y. H., Yuan, Y., Halliday, G., Rusznák, Z., Watson, C., & Paxinos, G. (2012). A cytoarchitectonic and chemoarchitectonic analysis of the dopamine cell groups in the

substantia nigra, ventral tegmental area, and retrorubral field in the mouse. *Brain Structure and Function*, *217*(2), 591–612. https://doi.org/10.1007/S00429-011-0349-2/FIGURES/9
Galtieri, D. J., Estep, C. M., Wokosin, D. L., Traynelis, S., & Surmeier, D. J. (2017). Pedunculopontine glutamatergic neurons control spike patterning in substantia nigra dopaminergic neurons. *ELife*, *6*. https://doi.org/10.7554/ELIFE.30352
Galvan, A., Kuwajima, M., & Smith, Y. (2006). Glutamate and GABA receptors and transporters in the basal ganglia: What does their subsynaptic localization reveal about their function? *Neuroscience*, *143*(2), 351. https://doi.org/10.1016/J.NEUROSCIENCE.2006.09.019
Gantz, S. C., Ford, C. P., Morikawa, H., & Williams, J. T. (2018). The Evolving Understanding of Dopamine Neurons in the Substantia Nigra and Ventral Tegmental Area. *Https://Doi.Org/10.1146/Annurev-Physiol-021317-121615*, *80*, 219–241. https://doi.org/10.1146/ANNUREV-PHYSIOL-021317-121615
Grace, A. A., & Bunney, B. S. (1984a). The control of firing pattern in nigral dopamine neurons: burst firing. *The Journal of Neuroscience : The Official Journal of the Society for Neuroscience*, *4*(11), 2877–2890. https://doi.org/10.1523/JNEUROSCI.04-11-02877.1984
Grace, A. A., & Bunney, B. S. (1984b). The control of firing pattern in nigral dopamine neurons: single spike firing. *The Journal of Neuroscience*, *4*(11), 2866. https://doi.org/10.1523/JNEUROSCI.04-11-02866.1984
Granger, A. J., Mulder, N., Saunders, A., & Sabatini, B. L. (2016). Cotransmission of acetylcholine and GABA. In *Neuropharmacology* (Vol. 100, pp. 40–46). Elsevier Ltd. https://doi.org/10.1016/j.neuropharm.2015.07.031
Gratiet, K. L. Le, Anderson, C. K., Puente, N., Grandes, P., Copas, C., Nahirney, P. C., Delaney, K. R., & Nashmi, R. (2022). Differential Subcellular Distribution and Release Dynamics of Cotransmitted Cholinergic and GABAergic Synaptic Inputs Modify Dopaminergic Neuronal Excitability. *Journal of Neuroscience*, *42*(46), 8670–8693. https://doi.org/10.1523/JNEUROSCI.2514-21.2022
Gray, E. G. (1959a). Axo-somatic and axo-dendritic synapses of the cerebral cortex: An electron microscope study. *Journal of Anatomy*, *93*(Pt 4), 420. https://www.ncbi.nlm.nih.gov/pmc/articles/PMC1244535/
Gray, E. G. (1959b). Electron Microscopy of Synaptic Contacts on Dendrite Spines of the Cerebral Cortex. *Nature 1959 183:4675*, *183*(4675), 1592–1593. https://doi.org/10.1038/1831592a0
Gray, E. G., & Guillery, R. W. (1966). Synaptic Morphology in the Normal and Degenerating Nervous System. *International Review of Cytology*, *19*(C), 111–182. https://doi.org/10.1016/S0074-7696(08)60566-5
Grillner, S., & Robertson, B. (2016). The Basal Ganglia Over 500 Million Years. *Current Biology*, *26*(20), R1088–R1100. https://doi.org/10.1016/J.CUB.2016.06.041
Guatteo, E., Cucchiaroni, M. L., & Mercuri, N. B. (2009). Substantia nigra control of basal ganglia nuclei. In *Journal of Neural Transmission, Supplementa* (Issue 73, pp. 91–101). Springer-Verlag Wien. https://doi.org/10.1007/978-3-211-92660-4_7
Harlow, M. L., Ress, D., Stoschek, A., Marshall, R. M., & McMahan, U. J. (2001). The architecture of active zone material at the frog's neuromuscular junction. *Nature 2001 409:6819*, *409*(6819), 479–484. https://doi.org/10.1038/35054000
Hauser, T. U., Eldar, E., & Dolan, R. J. (2017). Separate mesocortical and mesolimbic pathways encode effort and reward learning signals. *Proceedings of the National Academy of Sciences*

of the United States of America, *114*(35), E7395–E7404. https://doi.org/10.1073/PNAS.1705643114/SUPPL_FILE/PNAS.1705643114.SAPP.PDF

Hells, J. W., Maycox, P. R., & Jahn, R. (1990). THE JOURNAL OF BIOLOOICA~ CHEMISTRY Energy Dependence and Functional Reconstitution of the y-Aminobutyric Acid Carrier from Synaptic Vesicles*. *Journal of Biological Chemistry*, *265*(4), 2111–2117. https://doi.org/10.1016/S0021-9258(19)39947-8

Herzog, E., Bellenchi, G. C., Gras, C., Ronique Bernard, V., Ravassard, P., Cile Bedet, C., Gasnier, B., Giros, B., & Mestikawy, S. El. (2001). *The Existence of a Second Vesicular Glutamate Transporter Specifies Subpopulations of Glutamatergic Neurons*. http://www.jneurosci.org/cgi/content/full/5807

Heuser, E., & Reese, T. S. (1973). EVIDENCE FOR RECYCLING OF SYNAPTIC VESICLE MEMBRANE DURING TRANSMITTER RELEASE AT THE FROG NEUROMUSCULAR JUNCTION. *THE JOURNAL OF CELL BIOLOGY*, *57*, 15–344.

Hirsch, E. C., Graybiel, A. M., Duyckaerts, C., & Javoy-Agid, F. (1987). Neuronal loss in the pedunculopontine tegmental nucleus in Parkinson disease and in progressive supranuclear palsy. *Proceedings of the National Academy of Sciences of the United States of America*, *84*(16), 5976–5980. https://doi.org/10.1073/PNAS.84.16.5976

Hirsch, E., Graybiel, A. M., & Agid, Y. A. (1988). Melanized dopaminergic neurons are differentially susceptible to degeneration in Parkinson's disease. *Nature 1988 334:6180*, *334*(6180), 345–348. https://doi.org/10.1038/334345a0

Holly, E. N., & Miczek, K. A. (2015). Ventral tegmental area dopamine revisited: effects of acute and repeated stress. *Psychopharmacology 2015 233:2*, *233*(2), 163–186. https://doi.org/10.1007/S00213-015-4151-3

Hong, S., & Hikosaka, O. (2014). Pedunculopontine tegmental nucleus neurons provide reward, sensorimotor, and alerting signals to midbrain dopamine neurons. *Neuroscience*, *282*, 139–155. https://doi.org/10.1016/J.NEUROSCIENCE.2014.07.002

Ikemoto, S. (2007). Dopamine reward circuitry: Two projection systems from the ventral midbrain to the nucleus accumbens–olfactory tubercle complex. *Brain Research Reviews*, *56*(1), 27–78. https://doi.org/10.1016/J.BRAINRESREV.2007.05.004

Janickova, H., Rosborough, K., Al-Onaizi, M., Kljakic, O., Guzman, M. S., Gros, R., Prado, M. A. M., & Prado, V. F. (2017). Deletion of the vesicular acetylcholine transporter from pedunculopontine/laterodorsal tegmental neurons modifies gait. *Journal of Neurochemistry*, *140*(5), 787–798. https://doi.org/10.1111/JNC.13910

Jonas, P., Bischofberger, J., & Sandkühler, J. (1998). Corelease of Two Fast Neurotransmitters at a Central Synapse. *Science*, *281*(5375), 419–424. https://doi.org/10.1126/SCIENCE.281.5375.419

Juárez Olguín, H., Calderón Guzmán, D., Hernández García, E., & Barragán Mejía, G. (2016). The Role of Dopamine and Its Dysfunction as a Consequence of Oxidative Stress. *Oxidative Medicine and Cellular Longevity*, *2016*. https://doi.org/10.1155/2016/9730467

Karachi, C., Grabli, D., Bernard, F. A., Tandé, D., Wattiez, N., Belaid, H., Bardinet, E., Prigent, A., Nothacker, H. P., Hunot, S., Hartmann, A., Lehéricy, S., Hirsch, E. C., & François, C. (2010). Cholinergic mesencephalic neurons are involved in gait and postural disorders in Parkinson disease. *The Journal of Clinical Investigation*, *120*(8), 2745–2754. https://doi.org/10.1172/JCI42642

Kashani, A., Betancur, C., Giros, B., Hirsch, E., & Mestikawy, S. El. (2007). Altered expression of vesicular glutamate transporters VGLUT1 and VGLUT2 in Parkinson disease.

Neurobiology of Aging, *28*(4), 568. https://doi.org/10.1016/J.NEUROBIOLAGING.2006.02.010

Kaufman, D. L., Houser, C. R., & Tobin, A. J. (1991). Two Forms of the γ-Aminobutyric Acid Synthetic Enzyme Glutamate Decarboxylase Have Distinct Intraneuronal Distributions and Cofactor Interactions. *Journal of Neurochemistry*, *56*(2), 720. https://doi.org/10.1111/J.1471-4159.1991.TB08211.X

Kenney, C., Fernandez, H. H., & Okun, M. S. (2014). Role of deep brain stimulation targeted to the pedunculopontine nucleus in Parkinson's disease. *Http://Dx.Doi.Org/10.1586/14737175.7.6.585*, *7*(6), 585–589. https://doi.org/10.1586/14737175.7.6.585

Kim, Y., Wood, J., & Moghaddam, B. (2012). Coordinated Activity of Ventral Tegmental Neurons Adapts to Appetitive and Aversive Learning. *PLoS ONE*, *7*(1), 29766. https://doi.org/10.1371/JOURNAL.PONE.0029766

Kitai, S. T., Shepard, P. D., Callaway, J. C., & Scroggs, R. (1999). Afferent modulation of dopamine neuron firing patterns. *Current Opinion in Neurobiology*, *9*(6), 690–697. https://doi.org/10.1016/S0959-4388(99)00040-9

Lammel, S., Hetzel, A., Häckel, O., Jones, I., Liss, B., & Roeper, J. (2008). Unique properties of mesoprefrontal neurons within a dual mesocorticolimbic dopamine system. *Neuron*, *57*(5), 760–773. https://doi.org/10.1016/J.NEURON.2008.01.022

Lammel, S., Ion, D. I., Roeper, J., & Malenka, R. C. (2011). Projection-Specific Modulation of Dopamine Neuron Synapses by Aversive and Rewarding Stimuli. *Neuron*, *70*(5), 855–862. https://doi.org/10.1016/J.NEURON.2011.03.025

Lammel, S., Lim, B. K., Ran, C., Huang, K. W., Betley, M. J., Tye, K. M., Deisseroth, K., & Malenka, R. C. (2012). Input-specific control of reward and aversion in the ventral tegmental area. *Nature*, *491*(7423), 212. https://doi.org/10.1038/NATURE11527

Larramendi, L. M. H., Fickenscher, L., & Lemkey-Johnston, N. (1967). Synaptic Vesicles of Inhibitory and Excitatory Terminals in the Cerebellum. *Science*, *156*(3777), 967–969. https://doi.org/10.1126/SCIENCE.156.3777.967

Lee, C. R., & Tepper, J. M. (2007). Morphological and physiological properties of parvalbumin- and calretinin-containing γ-aminobutyric acidergic neurons in the substantia nigra. *Journal of Comparative Neurology*, *500*(5), 958–972. https://doi.org/10.1002/CNE.21220

Lee, S., Kim, K., & Zhou, Z. J. (2010). Role of ACh-GABA Cotransmission in Detecting Image Motion and Motion Direction. *Neuron*, *68*(6), 1159–1172. https://doi.org/10.1016/J.NEURON.2010.11.031

Lerner, T. N., Shilyansky, C., Davidson, T. J., Evans, K. E., Beier, K. T., Zalocusky, K. A., Crow, A. K., Malenka, R. C., Luo, L., Tomer, R., & Deisseroth, K. (2015). Intact-Brain Analyses Reveal Distinct Information Carried by SNc Dopamine Subcircuits. *Cell*, *162*(3), 635–647. https://doi.org/10.1016/J.CELL.2015.07.014

Levering Price, J. (1968). The synaptic vesicles of the reciprocal synapse of the olfactory bulb. *Brain Research*, *11*(3), 697–700. https://doi.org/10.1016/0006-8993(68)90161-3

Lewitt, P. A. (2015). Levodopa therapy for Parkinson's disease: Pharmacokinetics and pharmacodynamics. *Movement Disorders*, *30*(1), 64–72. https://doi.org/10.1002/MDS.26082

Li, H. quan, & Spitzer, N. C. (2020). Exercise enhances motor skill learning by neurotransmitter switching in the adult midbrain. *Nature Communications 2020 11:1*, *11*(1), 1–13. https://doi.org/10.1038/s41467-020-16053-7

Limousin, P., & Foltynie, T. (2019). Long-term outcomes of deep brain stimulation in Parkinson disease. *Nature Reviews Neurology*, *15*(4), 234–242. https://doi.org/10.1038/S41582-019-0145-9

Limousin, P., Krack, P., Pollak, P., Benazzouz, A., Ardouin, C., Hoffmann, D., & Benabid, A.-L. (1998). Electrical Stimulation of the Subthalamic Nucleus in Advanced Parkinson's Disease. *Https://Doi.Org/10.1056/NEJM199810153391603*, *339*(16), 1105–1111. https://doi.org/10.1056/NEJM199810153391603

Lipski, J., Nistico, R., Berretta, N., Guatteo, E., Bernardi, G., & Mercuri, N. B. (2011). L-DOPA: A scapegoat for accelerated neurodegeneration in Parkinson's disease? *Progress in Neurobiology*, *94*(4), 389–407. https://doi.org/10.1016/J.PNEUROBIO.2011.06.005

Liu, L., Zhao-Shea, R., McIntosh, J. M., Gardner, P. D., & Tapper, A. R. (2012). Nicotine Persistently Activates Ventral Tegmental Area Dopaminergic Neurons via Nicotinic Acetylcholine Receptors Containing α4 and α6 Subunits. *Molecular Pharmacology*, *81*(4), 541. https://doi.org/10.1124/MOL.111.076661

Loewi, O. (1924). Über humorale Übertragbarkeit der Herznervenwirkung - V. Mitteilung. Die Übertragbarkeit der negativ chrono- und dromotropen Vaguswirkung. *Pflügers Archiv Für Die Gesamte Physiologie Des Menschen Und Der Tiere*, *204*(1), 629–640. https://doi.org/10.1007/BF01731235

Luo, J., Kaplitt, M. G., Fitzsimons, H. L., Zuzga, D. S., Liu, Y., Oshinsky, M. L., & During, M. J. (2002). Subthalamic GAD gene therapy in a Parkinson's disease rat model. *Science*, *298*(5592), 425–429. https://doi.org/10.1126/SCIENCE.1074549

Mameli, M., Halbout, B., Creton, C., Engblom, D., Parkitna, J. R., Spanagel, R., & Lüscher, C. (2009). Cocaine-evoked synaptic plasticity: persistence in the VTA triggers adaptations in the NAc. *Nature Neuroscience*, *12*(8), 1036–1041. https://doi.org/10.1038/NN.2367

Manyam, B. V. (1982). Low CSF γ-Aminobutyric Acid Levels in Parkinson's Disease: Effect of Levodopa and Carbidopa. *Archives of Neurology*, *39*(7), 391–392. https://doi.org/10.1001/ARCHNEUR.1982.00510190009002

Mao, D., Gallagher, K., & Mcgehee, D. S. (2011). Nicotine Potentiation of Excitatory Inputs to Ventral Tegmental Area Dopamine Neurons. *The Journal of Neuroscience*, *31*(18), 6710. https://doi.org/10.1523/JNEUROSCI.5671-10.2011

Martella, G., Tassone, A., Sciamanna, G., Platania, P., Cuomo, D., Viscomi, M. T., Bonsi, P., Cacci, E., Biagioni, S., Usiello, A., Bernardi, G., Sharma, N., Standaert, D. G., & Pisani, A. (2009). Impairment of bidirectional synaptic plasticity in the striatum of a mouse model of DYT1 dystonia: role of endogenous acetylcholine. *Brain*, *132*(9), 2336–2349. https://doi.org/10.1093/BRAIN/AWP194

Martin, D., & Barke, K. (1998). Are GAD65 and GAD67 associated with specific pools of GABA in brain? *Perspectives on Developmental Neurobiology*.

Mazere, J., Dilharreguy, B., Catheline, G., Vidailhet, M., Deffains, M., Vimont, D., Ribot, B., Barse, E., Cif, L., Mazoyer, B., Langbour, N., Pisani, A., Allard, M., Lamare, F., Guehl, D., Fernandez, P., & Burbaud, P. (2021). Striatal and cerebellar vesicular acetylcholine transporter expression is disrupted in human DYT1 dystonia. *Brain : A Journal of Neurology*, *144*(3), 909–923. https://doi.org/10.1093/BRAIN/AWAA465

McGregor, M. M., & Nelson, A. B. (2019). Circuit Mechanisms of Parkinson's Disease. *Neuron*, *101*(6), 1042–1056. https://doi.org/10.1016/J.NEURON.2019.03.004

McIntire, S. L., Reimer, R. J., Schuske, K., Edwards, R. H., & Jorgensen, E. M. (1997). Identification and characterization of the vesicular GABA transporter. *Nature 1997 389:6653*, *389*(6653), 870–876. https://doi.org/10.1038/39908

Misgeld, U. (2004). Innervation of the substantia nigra. In *Cell and Tissue Research* (Vol. 318, Issue 1, pp. 107–114). Springer. https://doi.org/10.1007/s00441-004-0918-2

Moore, L. A., & Trussell, L. O. (2017). Corelease of Inhibitory Neurotransmitters in the Mouse Auditory Midbrain. *Journal of Neuroscience*, *37*(39), 9453–9464. https://doi.org/10.1523/JNEUROSCI.1125-17.2017

Morales, M., & Margolis, E. B. (2017). Ventral tegmental area: cellular heterogeneity, connectivity and behaviour. *Nature Reviews Neuroscience 2017 18:2*, *18*(2), 73–85. https://doi.org/10.1038/nrn.2016.165

Nagatsua, T., & Sawadab, M. (2009). l-dopa therapy for Parkinson's disease: Past, present, and future. *Parkinsonism and Related Disorders*, *15*(1). https://doi.org/10.1016/S1353-8020(09)70004-5

Nahirney, P. C., & Tremblay, M. E. (2021). Brain Ultrastructure: Putting the Pieces Together. *Frontiers in Cell and Developmental Biology*, *9*, 629503. https://doi.org/10.3389/FCELL.2021.629503/BIBTEX

Nair-Roberts, R. G., Chatelain-Badie, S. D., Benson, E., White-Cooper, H., Bolam, J. P., & Ungless, M. A. (2008). Stereological estimates of dopaminergic, GABAergic and glutamatergic neurons in the ventral tegmental area, substantia nigra and retrorubral field in the rat. *Neuroscience*, *152*(4–2), 1024. https://doi.org/10.1016/J.NEUROSCIENCE.2008.01.046

Naito, S., & Ttetsufumi Ueda, ". (n.d.). *Characterization of Glutamate Uptake into Synaptic Vesicles*.

Nashmi, R., Xiao, C., Deshpande, P., McKinney, S., Grady, S. R., Whiteaker, P., Huang, Q., McClure-Begley, T., Lindstrom, J. M., Labarca, C., Collins, A. C., Marks, M. J., & Lester, H. A. (2007). Chronic Nicotine Cell Specifically Upregulates Functional α4* Nicotinic Receptors: Basis for Both Tolerance in Midbrain and Enhanced Long-Term Potentiation in Perforant Path. *Journal of Neuroscience*, *27*(31), 8202–8218. https://doi.org/10.1523/JNEUROSCI.2199-07.2007

Nasir, M., Trujillo, D., Levine, J., Dwyer, J. B., Rupp, Z. W., & Bloch, M. H. (2020). Glutamate Systems in DSM-5 Anxiety Disorders: Their Role and a Review of Glutamate and GABA Psychopharmacology. *Frontiers in Psychiatry*, *11*, 548505. https://doi.org/10.3389/FPSYT.2020.548505

Nelson, E. L., Liang, C.-L., Sinton, C. M., & German, D. C. (1996). Midbrain Dopaminergic Neurons in the Mouse: Computer-Assisted Mapping. *THE JOURNAL OF COMPARATIVE NEUROLOGY*, 369–361. https://doi.org/10.1002/(SICI)1096-9861(19960603)369:3

Nguyen, M. L., Cox, G. D., & Parsons, S. M. (1998). Kinetic parameters for the vesicular acetylcholine transporter: Two protons are exchanged for one acetylcholine. *Biochemistry*, *37*(38), 13400–13410. https://doi.org/10.1021/BI9802263/SUPPL_FILE/BI13400A.PDF

Niedzielska-Andres, E., Pomierny-Chamioło, L., Andres, M., Walczak, M., Knackstedt, L. A., Filip, M., & Przegaliński, E. (2021). Cocaine use disorder: A look at metabotropic glutamate receptors and glutamate transporters. *Pharmacology & Therapeutics*, *221*, 107797. https://doi.org/10.1016/J.PHARMTHERA.2020.107797

Nishi, A., Kuroiwa, M., & Shuto, T. (2011). Mechanisms for the modulation of dopamine D 1 receptor signaling in striatal neurons. *Frontiers in Neuroanatomy*, *0*(JULY), 43. https://doi.org/10.3389/FNANA.2011.00043/BIBTEX

Nishi, T., & Forgac, M. (2002). The vacuolar (H+)-ATPases — nature's most versatile proton pumps. *Nature Reviews Molecular Cell Biology 2002 3:2*, *3*(2), 94–103. https://doi.org/10.1038/nrm729

Omelchenko, N., & Sesack, S. R. (2006). Cholinergic Axons in the Rat Ventral Tegmental Area Synapse Preferentially onto Mesoaccumbens Dopamine Neurons. *The Journal of Comparative Neurology*, *494*(6), 863. https://doi.org/10.1002/CNE.20852

Özkan, E. D., Lee, F. S., & Ueda, T. (1997). A protein factor that inhibits ATP-dependent glutamate and gamma-aminobutyric acid accumulation into synaptic vesicles: purification and initial characterization. *Proceedings of the National Academy of Sciences of the United States of America*, *94*(8), 4137–4142. https://doi.org/10.1073/PNAS.94.8.4137

Pahapill, P. A., & Lozano, A. M. (2000). The pedunculopontine nucleus and Parkinson's disease. *Brain*, *123*(9), 1767–1783. https://doi.org/10.1093/BRAIN/123.9.1767

Paladini, C. A., & Roeper, J. (2014). Generating bursts (and pauses) in the dopamine midbrain neurons. *Neuroscience*, *282*, 109–121. https://doi.org/10.1016/J.NEUROSCIENCE.2014.07.032

Paladini, C. A., & Tepper, J. M. (2016). *Chapter 17. Neurophysiology of Substantia Nigra Dopamine Neurons Modulation by GABA and Glutamate*. https://doi.org/10.1016/B978-0-12-802206-1.00017-9

Palmiter, R. D. (2018). The Parabrachial Nucleus: CGRP Neurons Function as a General Alarm. *Trends in Neurosciences*, *41*(5), 280–293. https://doi.org/10.1016/J.TINS.2018.03.007

Petroff, O. A. C. (2002). Book Review: GABA and Glutamate in the Human Brain. *Http://Dx.Doi.Org/10.1177/1073858402238515*, *8*(6), 562–573. https://doi.org/10.1177/1073858402238515

Picciotto, M. R., Higley, M. J., & Mineur, Y. S. (2012). Acetylcholine as a Neuromodulator: Cholinergic Signaling Shapes Nervous System Function and Behavior. *Neuron*, *76*(1), 116–129. https://doi.org/10.1016/J.NEURON.2012.08.036

Pinal, C., & Tobin, A. (1998). Uniqueness and redundancy in GABA production. *Perspectives on Developmental Neurobiology*.

Plaha, P., & Gill, S. S. (2005). Bilateral deep brain stimulation of the pedunculopontine nucleus for Parkinson's disease. *NeuroReport*, *16*(17), 1883–1887. https://doi.org/10.1097/01.WNR.0000187637.20771.A0

Prado, V. F., Roy, A., Kolisnyk, B., Gros, R., & Prado, M. A. M. (2013). Regulation of cholinergic activity by the vesicular acetylcholine transporter. *The Biochemical Journal*, *450*(2), 265–274. https://doi.org/10.1042/BJ20121662

Rizzoli, S. O., & Betz, W. J. (2004). The Structural Organization of the Readily Releasable Pool of Synaptic Vesicles. *Science*, *303*(5666), 2037–2039. https://doi.org/10.1126/SCIENCE.1094682/SUPPL_FILE/RIZZOLI.SOM.PDF

Romaus-Sanjurjo, D., Custodia, A., Aramburu-Núñez, M., Posado-Fernández, A., Vázquez-Vázquez, L., Camino-Castiñeiras, J., Leira, Y., Pías-Peleteiro, J. M., Aldrey, J. M., Ouro, A., & Sobrino, T. (2021). Symmetric and Asymmetric Synapses Driving Neurodegenerative Disorders. *Symmetry 2021, Vol. 13, Page 2333*, *13*(12), 2333. https://doi.org/10.3390/SYM13122333

Root, D. H., Mejias-Aponte, C. A., Zhang, S., Wang, H. L., Hoffman, A. F., Lupica, C. R., & Morales, M. (2014). Single rodent mesohabenular axons release glutamate and GABA. *Nature Neuroscience*, *17*(11), 1543. https://doi.org/10.1038/NN.3823

Salamone, J. D., Correa, M., Mingote, S., & Weber, S. M. (2003). Nucleus accumbens dopamine and the regulation of effort in food-seeking behavior: Implications for studies of natural motivation, psychiatry, and drug abuse. *Journal of Pharmacology and Experimental Therapeutics*, *305*(1), 1–8. https://doi.org/10.1124/JPET.102.035063

Sam, C., & Bordoni, B. (2022). Physiology, Acetylcholine. *StatPearls*. https://www.ncbi.nlm.nih.gov/books/NBK557825/

Sánchez-Catalán, M. J., Faivre, F., Yalcin, I., Muller, M. A., Massotte, D., Majchrzak, M., & Barrot, M. (2017). Response of the Tail of the Ventral Tegmental Area to Aversive Stimuli. *Neuropsychopharmacology*, *42*(3), 638. https://doi.org/10.1038/NPP.2016.139

Saunders, A., Granger, A. J., & Sabatini, B. L. (2015). Corelease of acetylcholine and GABA from cholinergic forebrain neurons. *ELife*, *2015*(4). https://doi.org/10.7554/ELIFE.06412

Schiemann, J., Schlaudraff, F., Klose, V., Bingmer, M., Seino, S., Magill, P. J., Zaghloul, K. A., Schneider, G., Liss, B., & Roeper, J. (2012). K-ATP channels in dopamine substantia nigra neurons control bursting and novelty-induced exploration. *Nature Neuroscience*, *15*(9), 1272. https://doi.org/10.1038/NN.3185

Schultz, W. (1998). Predictive reward signal of dopamine neurons. *Journal of Neurophysiology*, *80*(1), 1–27. https://doi.org/10.1152/JN.1998.80.1.1/ASSET/IMAGES/LARGE/JNP.JY19F12.JPEG

Seal, R. P., & Edwards, R. H. (2006). Functional implications of neurotransmitter co-release: Glutamate and GABA share the load. *Current Opinion in Pharmacology*, *6*(1 SPEC. ISS.), 114–119. https://doi.org/10.1016/J.COPH.2005.12.001

Sesack, S. R., & Grace, A. A. (2010). Cortico-Basal Ganglia reward network: microcircuitry. *Neuropsychopharmacology : Official Publication of the American College of Neuropsychopharmacology*, *35*(1), 27–47. https://doi.org/10.1038/NPP.2009.93

Shabel, S. J., Proulx, C. D., Piriz, J., & Malinow, R. (2014). GABA/glutamate co-release controls habenula output and is modified by antidepressant treatment. *Science (New York, N.Y.)*, *345*(6203), 1494. https://doi.org/10.1126/SCIENCE.1250469

Showell, S. S., Martinez, Y., Gondolfo, S., Boppana, S., & Lawal, H. O. (2020). Overexpression of the vesicular acetylcholine transporter disrupts cognitive performance and causes age-dependent locomotion decline in Drosophila. *Molecular and Cellular Neurosciences*, *105*. https://doi.org/10.1016/J.MCN.2020.103483

Silinsky, E. M. (1975). On the association between transmitter secretion and the release of adenine nucleotides from mammalian motor nerve terminals. *The Journal of Physiology*, *247*(1), 145–162. https://doi.org/10.1113/JPHYSIOL.1975.SP010925

Sloviter, R. S., Dichter, M. A., Rachinsky, T. L., Dean, E., Goodman, J. H., Sollas, A. L., & Martin, D. L. (1996). Basal Expression and Induction of Glutamate Decarboxylase and GABA in Excitatory Granule Cells of the Rat and Monkey Hippocampal Dentate Gyrus. *THE JOURNAL OF COMPARATIVE NEUROLOGY*, *373*(593). https://doi.org/10.1002/(SICI)1096-9861(19960930)373:4

Sonne, J., Reddy, V., & Beato, M. R. (2022). Neuroanatomy, Substantia Nigra. *StatPearls*. https://www.ncbi.nlm.nih.gov/books/NBK536995/

Sotelo, C. (2020). The History of the Synapse. *The Anatomical Record*, *303*(5), 1252–1279. https://doi.org/10.1002/AR.24392

Stefani, A., Lozano, A. M., Peppe, A., Stanzione, P., Galati, S., Tropepi, D., Pierantozzi, M., Brusa, L., Scarnati, E., & Mazzone, P. (2007). Bilateral deep brain stimulation of the pedunculopontine and subthalamic nuclei in severe Parkinson's disease. *Brain*, *130*(6), 1596–1607. https://doi.org/10.1093/BRAIN/AWL346

Steinkellner, T., Conrad, W. S., Kovacs, I., Rissman, R. A., Lee, E. B., Trojanowski, J. Q., Freyberg, Z., Roy, S., Luk, K. C., Lee, V. M., & Hnasko, T. S. (2022). Dopamine neurons exhibit emergent glutamatergic identity in Parkinson's disease. *Brain*, *145*(3), 879–886. https://doi.org/10.1093/BRAIN/AWAB373

Strata, P., & Harvey, R. (1999). *Dale's principle*.

Sulzer, D., & Surmeier, D. J. (2013). Neuronal vulnerability, pathogenesis, and Parkinson's disease. *Movement Disorders : Official Journal of the Movement Disorder Society*, *28*(1), 41–50. https://doi.org/10.1002/MDS.25095

Sumi, T., & Harada, K. (2020). Mechanism underlying hippocampal long-term potentiation and depression based on competition between endocytosis and exocytosis of AMPA receptors. *Scientific Reports 2020 10:1*, *10*(1), 1–14. https://doi.org/10.1038/s41598-020-71528-3

Takács, V. T., Cserép, C., Schlingloff, D., Pósfai, B., Szőnyi, A., Sos, K. E., Környei, Z., Dénes, Á., Gulyás, A. I., Freund, T. F., & Nyiri, G. (2018). Co-transmission of acetylcholine and GABA regulates hippocampal states. *Nature Communications 2018 9:1*, *9*(1), 1–15. https://doi.org/10.1038/s41467-018-05136-1

Takamori, S., Holt, M., Stenius, K., Lemke, E. A., Grønborg, M., Riedel, D., Urlaub, H., Schenck, S., Brügger, B., Ringler, P., Müller, S. A., Rammner, B., Gräter, F., Hub, J. S., De Groot, B. L., Mieskes, G., Moriyama, Y., Klingauf, J., Grubmüller, H., … Jahn, R. (2006). Molecular anatomy of a trafficking organelle. *Cell*, *127*(4), 831–846. https://doi.org/10.1016/J.CELL.2006.10.030

Takamori, S., Malherbe, P., Broger, C., & Jahn, R. (2002). Molecular cloning and functional characterization of human vesicular glutamate transporter 3. *EMBO Reports*, *3*(8), 798. https://doi.org/10.1093/EMBO-REPORTS/KVF159

Tepper, J. M., & Lee, C. R. (2007). GABAergic control of substantia nigra dopaminergic neurons. In *Progress in Brain Research* (Vol. 160, pp. 189–208). Elsevier. https://doi.org/10.1016/S0079-6123(06)60011-3

Triller, A., Cluzeaud, F., & Korn, H. (1987). Gamma-Aminobutyric Acid-containing Terminals Can Be Apposed to Glycine Receptors at Central Synapses. *The Journal of Cell Biology*, *104*, 947–956. http://rupress.org/jcb/article-pdf/104/4/947/1054454/947.pdf

Tritsch, N. X., Granger, A. J., & Sabatini, B. L. (2016). Mechanisms and functions of GABA co-release. *Nature Reviews Neuroscience 2016 17:3*, *17*(3), 139–145. https://doi.org/10.1038/nrn.2015.21

Trutti, A. C., Mulder, M. J., Hommel, B., & Forstmann, B. U. (2019). Functional neuroanatomical review of the ventral tegmental area. *NeuroImage*, *191*, 258–268. https://doi.org/10.1016/J.NEUROIMAGE.2019.01.062

Tye, K. M., Mirzabekov, J. J., Warden, M. R., Ferenczi, E. A., Tsai, H. C., Finkelstein, J., Kim, S. Y., Adhikari, A., Thompson, K. R., Andalman, A. S., Gunaydin, L. A., Witten, I. B., & Deisseroth, K. (2012). Dopamine neurons modulate neural encoding and expression of depression-related behaviour. *Nature 2012 493:7433*, *493*(7433), 537–541. https://doi.org/10.1038/nature11740

Tysnes, O. B., & Storstein, A. (2017). Epidemiology of Parkinson's disease. *Journal of Neural Transmission 2017 124:8*, *124*(8), 901–905. https://doi.org/10.1007/S00702-017-1686-Y

Uchizono, K. (1965). Characteristics of Excitatory and Inhibitory Synapses in the Central Nervous System of the Cat. *Nature 1965 207:4997*, *207*(4997), 642–643. https://doi.org/10.1038/207642a0

Uchizono, K. (1967). Synaptic organization of the Purkinje cells in the cerebellum of the cat. *Experimental Brain Research*, *4*(2), 97–113. https://doi.org/10.1007/BF00240355

van Hooijdonk, C. F. M., van der Pluijm, M., Bosch, I., van Amelsvoort, T. A. M. J., Booij, J., de Haan, L., Selten, J. P., & Giessen, E. van de. (2023). The substantia nigra in the pathology of schizophrenia: A review on post-mortem and molecular imaging findings. *European Neuropsychopharmacology*, *68*, 57–77. https://doi.org/10.1016/J.EURONEURO.2022.12.008

Varoqui, H., Meunier, F. M., Meunier, F. A., Molgo, J., Berrard, S., Cervini, R., Mallet, J., Israel, M., & Diebler, M. F. (1996). Chapter 6 Expression of the vesicular acetylcholine transporter in mammalian cells. *Progress in Brain Research*, *109*, 83–95. https://doi.org/10.1016/S0079-6123(08)62090-7

Verharen, J. P. H., Adan, R. A. H., & Vanderschuren, L. J. M. J. (2019). Differential contributions of striatal dopamine D1 and D2 receptors to component processes of value-based decision making. *Neuropsychopharmacology 2019 44:13*, *44*(13), 2195–2204. https://doi.org/10.1038/s41386-019-0454-0

Walberg, F. (1966). Elongated vesicles in terminal boutons of the central nervous system, a result of aldehyde fixation. *Cells Tissues Organs*, *65*(1–3), 224–235. https://doi.org/10.1159/000142873

Wan, Q. F., Zhou, Z. Y., Thakur, P., Vila, A., Sherry, D. M., Janz, R., & Heidelberger, R. (2010). SV2 acts via Presynaptic Calcium to Regulate Neurotransmitter Release. *Neuron*, *66*(6), 884. https://doi.org/10.1016/J.NEURON.2010.05.010

Watabe-Uchida, M., Zhu, L., Ogawa, S. K., Vamanrao, A., & Uchida, N. (2012). Whole-brain mapping of direct inputs to midbrain dopamine neurons. *Neuron*, *74*(5), 858–873. https://doi.org/10.1016/J.NEURON.2012.03.017

Welberg, L. (2008). A split (mid)brain for dopamine. *Nature Reviews Neuroscience 2008 9:5*, *9*(5), 326–326. https://doi.org/10.1038/nrn2381

Werman, R. (1966). A review — critical for idenctification of a central nervous system transmitter. *Comparative Biochemistry and Physiology*, *18*(4), 745–766. https://doi.org/10.1016/0010-406X(66)90209-X

White, D., de Sousa Abreu, R. P., Blake, A., Murphy, J., Showell, S., Kitamoto, T., & Lawal, H. O. (2020). Deficits in the vesicular acetylcholine transporter alter lifespan and behavior in adult Drosophila melanogaster. *Neurochemistry International*, *137*. https://doi.org/10.1016/J.NEUINT.2020.104744

Wise, R. A. (2009). Roles for nigrosriatal—not just mesocorticolimbic—dopamine in reward and addiction. *Trends in Neurosciences*, *32*(10), 517. https://doi.org/10.1016/J.TINS.2009.06.004

Yamaguchi, T., Qi, J., Wang, H. L., Zhang, S., & Morales, M. (2015). Glutamatergic and Dopaminergic Neurons in the Mouse Ventral Tegmental Area. *The European Journal of Neuroscience*, *41*(6), 760. https://doi.org/10.1111/EJN.12818

Yoo, J. H., Zell, V., Wu, J., Punta, C., Ramajayam, N., Shen, X., Faget, L., Lilascharoen, V., Lim, B. K., & Hnasko, T. S. (2017). Activation of Pedunculopontine Glutamate Neurons Is Reinforcing. *The Journal of Neuroscience*, *37*(1), 38. https://doi.org/10.1523/JNEUROSCI.3082-16.2016

Young, C. B., Reddy, V., & Sonne, J. (2022). Neuroanatomy, Basal Ganglia. *StatPearls*. https://www.ncbi.nlm.nih.gov/books/NBK537141/

Zaborszky, L., & Vadasz, C. (2001). The midbrain dopaminergic system: anatomy and genetic variation in dopamine neuron number of inbred mouse strains. *Behavior Genetics*, *31*(1), 47–59. https://doi.org/10.1023/A:1010257808945

Zecca, L., Tampellini, D., Gerlach, M., Riederer, P., Fariello, R. G., & Sulzer, D. (2001). Substantia nigra neuromelanin: Structure, synthesis, and molecular behaviour. In *Journal of Clinical Pathology - Molecular Pathology* (Vol. 54, Issue 6, pp. 414–418). BMJ Publishing Group. https://doi.org/10.1136/mp.54.6.414

Zhang, S., Root, D. H., Barker, D. J., & Morales, M. (2017). The Lateral Habenula Has Vesicles That Accumulate Either GABA or Glutamate. *Microscopy and Microanalysis*, *23*(S1), 1288–1289. https://doi.org/10.1017/s1431927617007103

Zhang, Y., Larcher, K. M. H., Misic, B., & Dagher, A. (2017). Anatomical and functional organization of the human substantia nigra and its connections. *ELife*, *6*. https://doi.org/10.7554/ELIFE.26653

Zhou, F. M., & Lee, C. R. (2011). Intrinsic and integrative properties of substantia nigra pars reticulata neurons. *Neuroscience*, *198*, 69. https://doi.org/10.1016/J.NEUROSCIENCE.2011.07.061

Zhou, Y., & Danbolt, N. C. (2014). Glutamate as a neurotransmitter in the healthy brain. *Journal of Neural Transmission*, *121*(8), 799. https://doi.org/10.1007/S00702-014-1180-8

Appendix

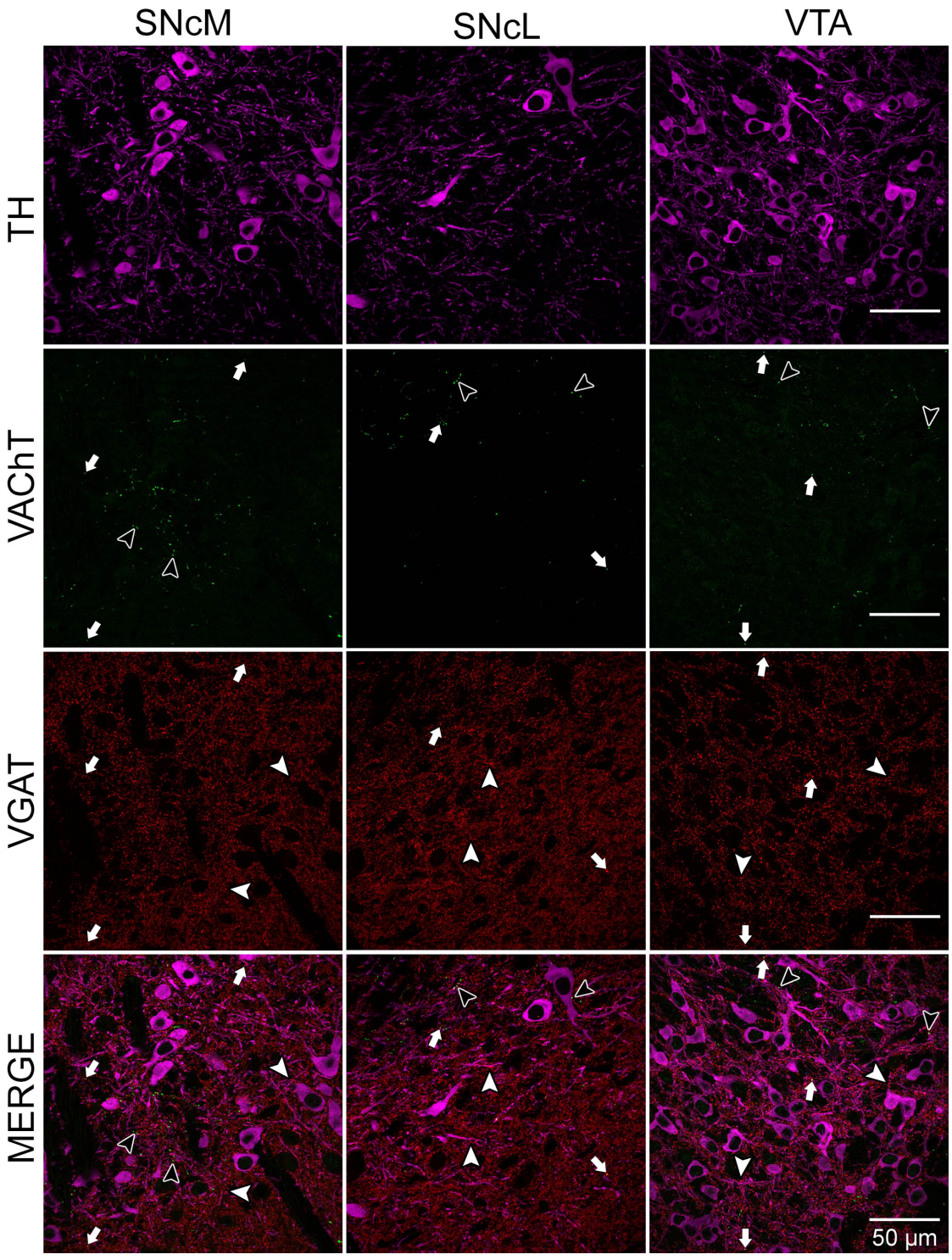

Figure 36. Lower magnification confocal images of VAChT (green) and VGAT (red) labeling in the SNcM, SNcL and VTA from figure 17. TH+ DA neurons are magenta. Mixed terminals (white arrows) are seen in all three regions. Each image is a projection image of a 5 image z-stack (0.52 µm step size) to create an image with a depth of 2.5 µm

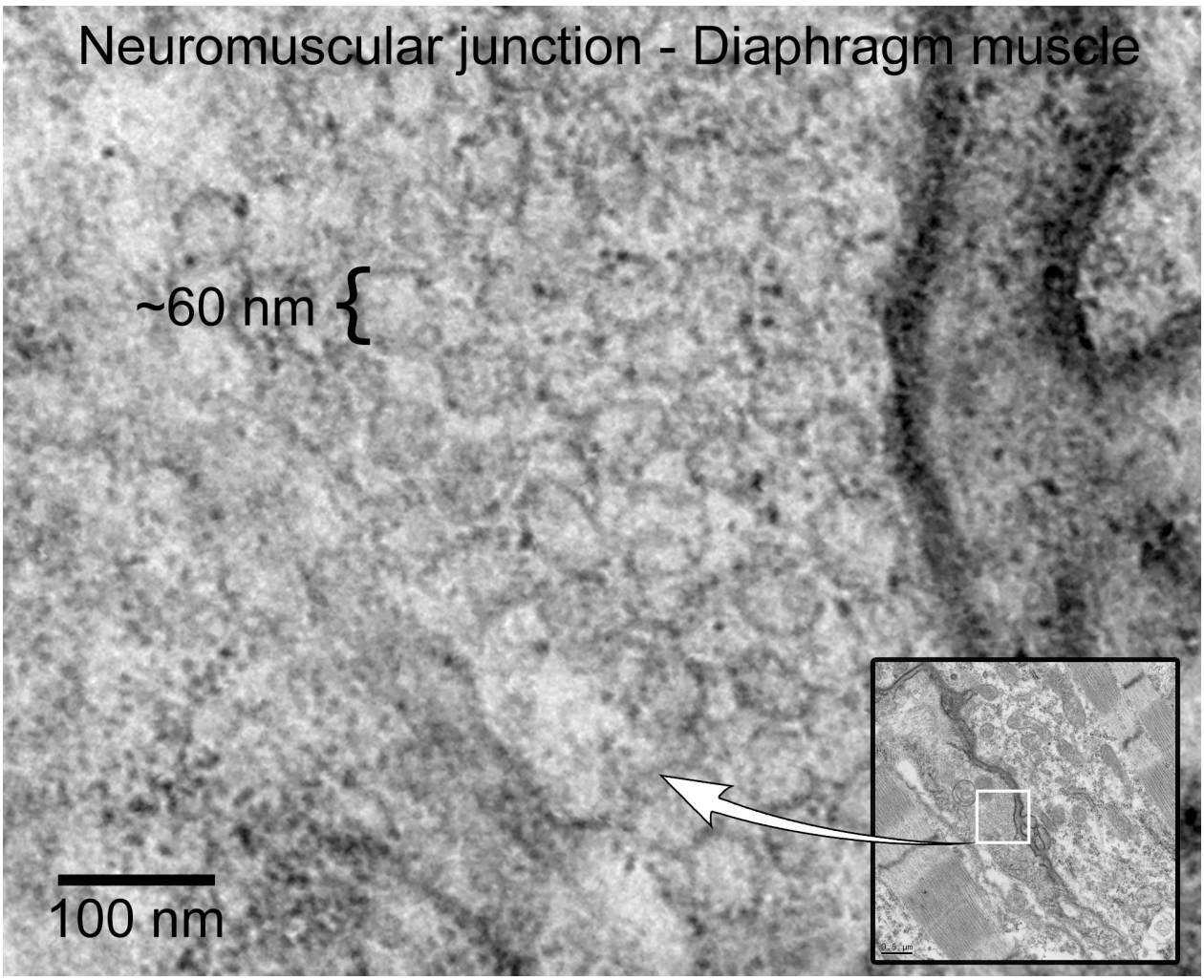

Figure 39. EM of a neuromuscular junction in a diaphragm muscle of a rat showing the size and shape of ACh vesicles. Neuromuscular junctions are famously known for exclusively using ACh as their sole excitatory neurotransmitter, making them perfect sites for measuring ACh vesicle morphology**.** Diameters measured from 11 separate vesicles were averaged to obtain a value of 60.439 nm.

Table 3. Antibody list

Antibody	Manufacturer, Catalog number	Species raised, monoclonal or polyclonal	Dilution used
Tyrosine Hydroxylase	Pel-Freeze Biologicals, P4010-150	Rabbit, polyclonal	1:1000
Vesicular Acetylcholine Transporter (VAChT)	Sigma-Aldrich, ABN100	Goat, polyclonal	1:1000
Vesicular GABA Transporter (VGAT)	Synaptic Systems, 131-011	Mouse, monoclonal	1:200
Vesicular Glutamate Transporter 1 (VGLUT2)	Abcam, ab79157	Guinea-pig, monoclonal	1:200
HRP conjugated anti-rabbit secondary	Invitrogen, A16029	Donkey	1:200
Alexa Fluor 647 conjugated anti-rabbit secondary	Invitrogen, A31573	Donkey	1:400
Alexa Fluor 597 conjugated anti-mouse secondary	Invitrogen, A21203	Donkey	1:400
Alexa Fluor 488 conjugated anti-goat secondary	Invitrogen, A11055	Donkey	1:400
Alexa Fluor 488 conjugated anti-mouse secondary	Invitrogen, A-21202	Donkey	1:400